ORGANOMETALLICS
Article
Cite This: Organometallics XXXX, XXX, XXX−XXX
pubs.acs.org/Organometallics

Asymmetric Intra- and Intermolecular Hydroamination Catalyzed by 3,3′-Bis(trisarylsilyl)- and 3,3′-Bis(arylalkylsilyl)-Substituted Binaphtholate Rare-Earth-Metal Complexes

Hiep N. Nguyen,[†] Hyeunjoo Lee,[†] Stephan Audörsch,[‡] Alexander L. Reznichenko,[†] Agnieszka J. Nawara-Hultzsch,[§] Bernd Schmidt,[‡] and Kai C. Hultzsch*[,†,§]

[†]Department of Chemistry & Chemical Biology, Rutgers, The State University of New Jersey, 610 Taylor Road, Piscataway, New Jersey 08854-8087, United States

[‡]Institut für Chemie, Organische Synthesechemie, Universität Potsdam, Karl-Liebknecht-Strasse 24-25, D-14476 Golm, Germany

[§]University of Vienna, Faculty of Chemistry, Institute of Chemical Catalysis, Währinger Strasse 38, 1090 Vienna, Austria

Supporting Information

ABSTRACT: The series of novel 3,3′-bis(trisarylsilyl)- and 3,3′-bis(arylalkylsilyl)-substituted binaphtholate rare-earth-metal complexes **2a**−**i** (SiR_3 = Si(*o*-biphenylene)Ph (**a**), $SiCyPh_2$ (**b**), Si-*t*-$BuPh_2$ (**c**), Si(*i*-Pr)$_3$ (**d**), $SiCy_2Ph$ (**e**), Si(2-tolyl)Ph_2 (**f**), Si(4-*t*-Bu-C_6H_4)$_3$ (**g**), Si(4-MeO-C_6H_4)Ph_2 (**h**), $SiBnPh_2$ (**i**)) have been prepared via arene elimination from [Ln(*o*-$C_6H_4CH_2NMe_2$)$_3$] (Ln = Y, Lu) and the corresponding 3,3′-bis(silyl)-substituted binaphthol. The complexes exhibit high catalytic activity in the hydroamination/cyclization of aminoalkenes, with activities exceeding 1000 h^{-1} for (*R*)-**2f-Ln**, (*R*)-**2g-Ln**, and (*R*)-**2h-Ln** in the cyclization of 2,2-diphenylpent-4-enylamine (**3a**) at 25 °C, while the rigid dibenzosilole-substituted complexes (*R*)-**2a-Ln** and the triisopropylsilyl-substituted complexes (*R*)-**2d-Ln** exhibited the lowest activity in the range of 150−270 h^{-1}. Catalysts (*R*)-**2b-Lu**, (*R*)-**2c-Lu**, (*R*)-**2f-Lu**, and (*R*)-**2i-Lu** provide the highest selectivities for the majority of the substrates, while the yttrium congeners are usually less selective. The highest enantioselectivities of 96% ee were observed using (*R*)-**2a-Lu** and (*R*)-**2c-Lu** in the cyclization of (4*E*)-2,2,5-triphenylpent-4-enylamine (**9**). The reactions show apparently zero-order rate dependence on substrate concentration and first-order rate dependence on catalyst concentration, with some reactions exhibiting a slightly accelerated rate at high conversion due to a shift in the equilibrium between a less active, higher coordinate catalyst species in favor of a more active, lower coordinate species as a result of weaker binding of the hydroamination product in comparison to the aminoalkene substrate. The shift in equilibrium from the higher to the lower coordinate species is also entropically favored at elevated temperatures, which results in an unusual increase in selectivity in the cyclization of 2,2-dimethylpent-4-enylamine (**3d**), presumably due to a higher selectivity of the lower coordinate catalyst species. All binaphtholate yttrium complexes, except (*R*)-**2a-Y**, are catalytically active in the intermolecular hydroamination of benzylamines with terminal alkenes. The highest selectivity of 66% ee was observed for the reaction of benzylamine with 4-phenyl-1-butene using (*R*)-**2h-Y** at 110 °C.

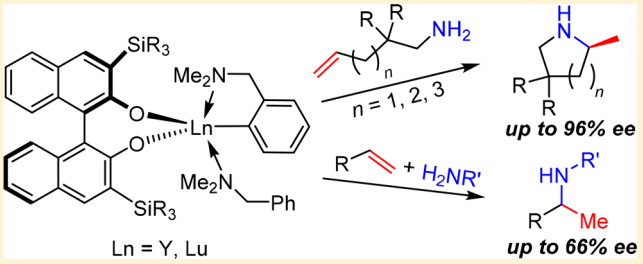

INTRODUCTION

The synthesis of nitrogen-containing molecules has drawn significant interest, because of their omnipresence in the majority of naturally occurring compounds and their relevance as biologically active substances.[1] Therefore, catalytic methods for the preparation of amines are highly desirable. The hydroamination reaction[2−7] represents a highly attractive process in which an amine N−H functionality is added to an unsaturated carbon−carbon linkage, because it is 100% atom economical without formation of any waste byproduct. As many of the targeted amine products are chiral, the development of chiral catalyst systems for asymmetric hydroamination reactions has been the focus of a large number of studies over the last two decades.[8] We[9] and others[10] have reported catalyst systems that exceed 90% ee in intramolecular hydroamination reactions of aminoalkenes.[11] However, intermolecular hydroamination reactions remain highly challenging,[2c,g,3,12] especially when they are carried out in a stereoselective manner. Most studies focused on activated or strained alkene substrates, such as vinylarenes, 1,3-dienes, and norbonene, generally applied to amines with low nucleophilicity, such as anilines, carboxamides, sulfonamides, and other protected amines.[13] Only a few systems have been reported for the hydroamination of simple, unactivated alkenes.[14,15]

Special Issue: Organometallic Complexes of Electropositive Elements for Selective Synthesis

Received: July 20, 2018

DOI: 10.1021/acs.organomet.8b00510
Organometallics XXXX, XXX, XXX−XXX

We have previously studied rare-earth-metal complexes based on biphenolate, binaphtholate, and aminodiolate ligands as catalysts for the asymmetric hydroamination of alkenes (Chart 1).[9a,14b,16] Our important finding for the biphenolate-

Chart 1

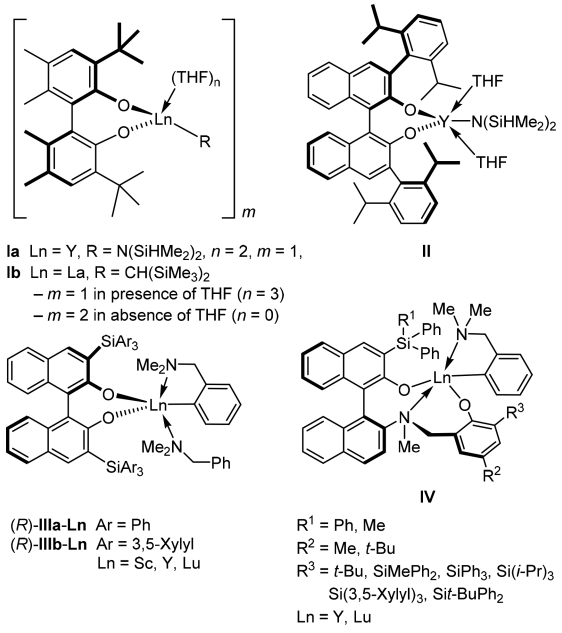

Ia Ln = Y, R = $N(SiHMe_2)_2$, n = 2, m = 1,
Ib Ln = La, R = $CH(SiMe_3)_2$
– m = 1 in presence of THF (n = 3)
– m = 2 in absence of THF (n = 0)

II

(*R*)-**IIIa-Ln** Ar = Ph
(*R*)-**IIIb-Ln** Ar = 3,5-Xylyl
Ln = Sc, Y, Lu

R^1 = Ph, Me
R^2 = Me, *t*-Bu
R^3 = *t*-Bu, $SiMePh_2$, $SiPh_3$, Si(*i*-Pr)$_3$
Si(3,5-Xylyl)$_3$, Si*t*-BuPh_2
Ln = Y, Lu

and binaphtholate-based catalysts **I**–**III** was that steric bulk at the 3- and 3′-positions of the binaphtholate ligand played a crucial role in preventing the formation of higher aggregates and in stabilizing rare-earth-metal precatalysts. More importantly, highly sterically demanding silyl substituents at these positions significantly enhance catalytic activity and/or enantioselectivities in the intramolecular hydroamination of aminoalkenes. While the highest enantioselectivity of 95% ee was observed with **IIIa-Sc**, a catalyst containing the larger yttrium, **IIIa-Y**, cyclized aminopentenes with a high turnover frequency of up to 840 h^{-1} at the expense of selectivity.[9a] Furthermore, binaphtholate complexes **III** and NOBIN-based aminodiolate complexes **IV** were active in the asymmetric hydroamination of terminal alkenes with simple primary amines, producing secondary amines with up to 61% ee.[14b,16e]

In an extension of these previous studies focusing on catalysts for asymmetric hydroamination of alkenes, we report herein the synthesis of rare-earth-metal complexes based on binaphtholate ligands bearing a variety of sterically demanding silyl substituents at the 3- and 3′-positions and their application in asymmetric intra- and intermolecular hydroamination reactions.[17]

RESULTS AND DISCUSSION

Synthesis of 3,3′-Bis(silyl)-Substituted Binaphtholate Ligands. A number of binaphtholate ligands with different sterically demanding silyl substituents at the 3- and 3′-positions are available through an established[18] two-step reaction sequence starting from (*R*)-3,3′-dibromo-1,1′-binaphthalene-2,2′-diol via the bis(silyl ethers), followed by a retro-Brook rearrangement, in 33–82% overall yield (Scheme 1). An alternative approach involving direct silylation of 3,3′-dilithiated MOM-protected binaphthol in the presence of HMPA[19] is only suitable for sterically less demanding

Scheme 1. Synthesis of 3,3′-Disilyl-Substituted Binaphthols

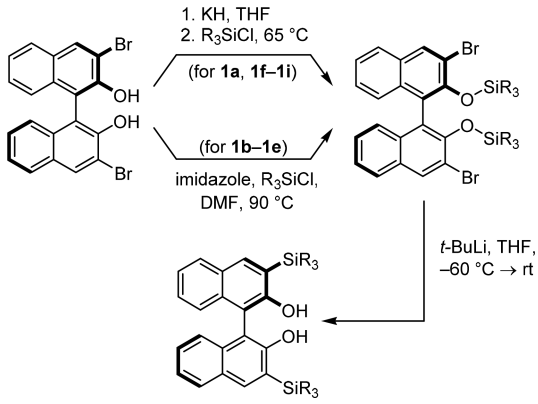

(*R*)-**1a** SiR_3 =

(*R*)-**1b** SiR_3 = $SiCyPh_2$, 82%
(*R*)-**1c** SiR_3 = Si*t*-$BuPh_2$, 71%
(*R*)-**1d** SiR_3 = Si(*i*-Pr)$_3$, 63%
(*R*)-**1e** SiR_3 = $SiCy_2Ph$, 80%
(*R*)-**1f** SiR_3 = Si(2-tolyl)Ph_2, 51%
(*R*)-**1g** SiR_3 = Si(4-*t*-Bu-C_6H_4)$_3$, 50%
(*R*)-**1h** SiR_3 = Si(4-MeO-C_6H_4)Ph_2, 69%
(*R*)-**1i** SiR_3 = $SiBnPh_2$, 47%

chlorosilanes, e.g. triphenylchlorosilane, while sterically more hindered chlorosilanes gave inferior (<15%) yields in our hands. The bis(silyl) ether intermediates were prepared from (*R*)-3,3′-dibromo-1,1′-binaphthalene-2,2′-diol either by sequential treatment with KH and a tris(aryl)chlorosilane, while sterically more congested chlorosilanes, e.g. chloro(cyclohexyl)diphenylsilane, *tert*-butylchlorodiphenylsilane, chlorotriisopropylsilane, or chlorodicyclohexyl(phenyl)silane gave better yields utilizing an optimized version of the classical silyl ether synthesis[18] involving imidazole (up to 6 equiv) and an excess of the respective chlorosilane (up to 4 equiv) in DMF.

Synthesis and Characterization of Binaphtholate Rare-Earth-Metal Complexes. Prospective rare-earth-metal complexes for efficient hydroamination catalysis generally possess at least one reactive Ln–C or Ln–N bond to allow catalyst activation via protonolysis to occur. While a number of suitable tris-amido and tris-alkyl precursors, such as $[Ln\{N(SiHMe_2)_2\}_3(THF)_2]$, $[Ln\{N(SiMe_3)_2\}_3]$, and $[Ln\{CH(SiMe_3)_2\}_3]$, may be used for the synthesis of diolate rare-earth-metal complexes through amine and alkane elimination, respectively,[9a,16a,c] the resulting diolate amido complexes suffer from inferior catalytic activity in hydroamination reactions due to incomplete catalyst activation,[9a,16a,20] while the tris-alkyl precursors $[Ln\{CH(SiMe_3)_2\}_3]$ are prepared in a rather tedious three-step synthesis.[21] In a previous study[9a] we identified the tris-aryl complexes $[Ln(o\text{-}C_6H_4CH_2NMe_2)_3]$ (Ln = Y, Lu),[22] which are available in a single-step procedure on a multigram scale, as suitable precursors for the preparation of the highly active hydroamination catalysts (*R*)-**IIIa-Ln** and (*R*)-**IIIb-Ln** (Chart 1).

Indeed, reaction of the bulky binaphthols (*R*)-**1a–i** with $[Ln(o\text{-}C_6H_4CH_2NMe_2)_3]$ (Ln = Y, Lu) resulted in clean formation of the rare-earth-metal complexes (*R*)-**2a–i** in quantitative yields (by ^{1}H NMR spectroscopy) at room temperature in less than 2 h (Scheme 2). The formation of

DOI: 10.1021/acs.organomet.8b00510
Organometallics XXXX, XXX, XXX–XXX

yttrium complexes was generally completed more quickly than that of the corresponding lutetium complexes.

Scheme 2. Synthesis of Binaphtholate Rare-Earth-Metal Complexes (*R*)-2a−i

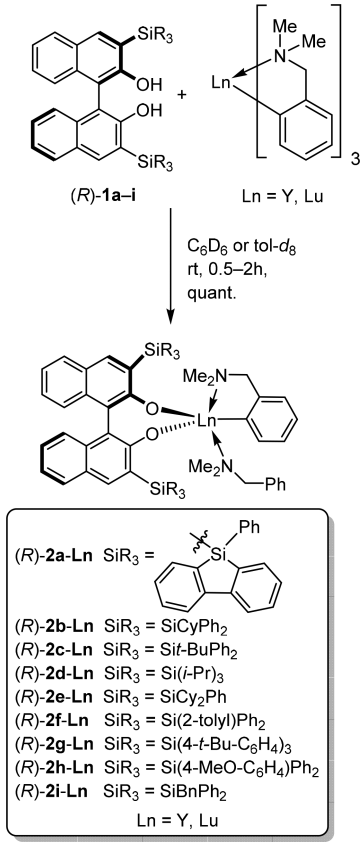

Complexes (*R*)-**2a−i** were prepared in either C_6D_6 or toluene-d_8 and stored at room temperature for 7 days without decomposition. Attempts to crystallize the complexes from toluene, hexanes/toluene, and pentane/toluene mixtures yielded finely powdered materials, which were not suitable for X-ray crystallographic analysis. After the solvents were removed under vacuum, white or pale yellow solids were generally obtained in quantitative yields. On the basis of ^{1}H and ^{13}C NMR spectra, the observation of methylene and methyl groups of *N*,*N*-dimethylbenzylamine suggests that the complexes retain 1 equiv of *N*,*N*-dimethylbenzylamine. Exchange between coordinated and free *N*,*N*-dimethylbenzylamine is slow on the NMR time scale at 6 °C, but NMR spectra collected at 25 °C tend to have broadened signals due to the onset of exchange between coordinated and free *N*,*N*-dimethylbenzylamine. The overall symmetry of the ^{1}H and ^{13}C NMR spectra is indicative of a C_1-symmetric monomeric structure in solution in accordance with observations made for the binaphtholate complexes **IIIa-Ln** and **IIIb-Ln**. The ipso carbon of the ortho-metalated *N*,*N*-dimethylbenzylamine appears as a single doublet in the ^{13}C{^{1}H} NMR spectrum of the yttrium complexes, indicating coupling to a single yttrium atom. The complexes exhibit good solubility in aromatic solvents, whereas dimeric biphenolate and binaphtholate complexes are generally much less soluble.[16a,c]

Although the complexation reactions proceeded cleanly by NMR spectroscopy, the isolated complexes retained varying trace amounts of free *N*,*N*-dimethylbenzylamine (in addition to one coordinated amine molecule), which proved to be difficult to remove. Attempts to purify the complexes further via recrystallization or washing with pentane or hexanes were unsuccessful. Therefore, the complexes were generally prepared in situ as stock solutions in C_6D_6 or toluene-d_8 that were then used directly for catalytic experiments without isolation.[23]

Asymmetric Intramolecular Hydroamination of Aminoalkenes. The binaphtholate rare-earth-metal complexes **2a−i** were evaluated with aminoalkenes for asymmetric intramolecular hydroamination/cyclization (Tables 1−5). While aminopentenes **3a−d** and aminohexene **5** were commonly cyclized smoothly at room temperature using 2 mol % catalyst loading, aminoheptene **7** required higher catalytic loadings and elevated temperatures to generate azepane **8** (Table 3). As has been commonly observed,[2,3] the hydroamination/cyclization reaction rates decreased with increasing sizes of heterocyclic rings: 5 > 6 ≫ 7. For example, the turnover frequencies in the hydroamination using (*R*)-**2b-Y** decreased in the following sequence: aminopentene **3a** (750 h^{-1} at 25 °C) > aminohexene **5** (6.5 h^{-1} at 25 °C) ≫ aminoheptene **7** (0.17 h^{-1} at 80 °C) (Table 1, entry 3; Table 3, entries 3 and 16).

The Thorpe−Ingold effect[24] of the *gem*-diaryl/-dialkyl substituents plays a significant role in enhancing the cyclization rates of the *gem*-disubstituted aminopentenes **3a**,**b**,**d** in comparison to that of the unsubstituted aminopentene **3c**. As expected, the rates of the hydroamination reactions decrease with decreasing size of the substituents in the order **3a** > **3b** > **3d** > **3c** (Tables 1 and 2). Ring closing of the *gem*-diphenyl-substituted aminopentene **3a** proceeded at room temperature using 2 mol % of the catalysts with the highest turnover frequency of >1000 h^{-1} (Table 1, entries 11, 13, 15, 17, 19, and 20) when the trisarylsilyl-substituted yttrium and lutetium catalysts (*R*)-**2f−h** were employed, whereas the unsubstituted aminopentene **3c** required either elevated reaction temperatures or higher catalytic loadings to achieve complete cyclization in a reasonable period of time in most cases (Table 1, entries 47−62).

While generally the catalytic activity decreases with decreasing ionic radius for most binaphtholate catalysts, there are notable exceptions (e.g., Table 1, entry 9 vs entry 10 and Table 3, entry 11 vs entry 12).

The enantioselectivities observed for the *gem*-diphenyl-substituted aminopentene **3a** range from 47% ee up to 95% ee (Figure 1), with the highest selectivities being obtained using the sterically demanding cyclohexyldiphenylsilyl-substituted (*R*)-**2b-Lu** (95% ee), the *tert*-butyldiphenylsilyl-substituted (*R*)-**2c-Lu** (95% ee), the diphenyl(*o*-tolyl)silyl-substituted (*R*)-**2f-Lu** (92% ee), and the benzyldiphenylsilyl-substituted (*R*)-**2i-Ln** (Ln = Lu (95% ee), Y (90% ee)), which are comparable to those for the triphenylsilyl-substituted (*R*)-**IIIa-Ln** (Ln = Sc (95% ee), Lu (93% ee))[9a] (compare Table 1, entries 4, 6, 13, 21, and 22, with entries 24 and 25). The lowest selectivities were observed for the complex (*R*)-**2a-Y** (66% ee) containing the rigid dibenzosilole moiety and the tris(4-*tert*-butylphenyl)silyl-substituted complex (*R*)-**2g-Y** (47% ee at 25 °C) (Table 1, entries 1 and 15). The selectivity of the latter catalyst increased to 62% ee when the reaction was performed at 60 °C (Table 1, entry 16). Furthermore, the selectivity of (*R*)-**2f-Y** also increased from 75% ee at 25 °C to 90% ee at 60 °C (Table 1, entries 11 and 12). Similar unusual temperature

DOI: 10.1021/acs.organomet.8b00510
Organometallics XXXX, XXX, XXX−XXX

Table 1. Asymmetric Intramolecular Hydroamination of Primary Aminopentenes Catalyzed by Binaphtholate Rare-Earth-Metal Complexes[a]

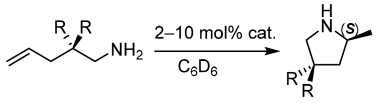

3a R = Ph
3b -R-R- = -$(CH_2)_5$-
3c R = H

4a R = Ph
4b -R-R- = -$(CH_2)_5$-
4c R = H

entry	subst	cat.	[cat.]/[subst] (%)	T (°C)	t (h)[b]	N_t (h^{-1})	ee (%)[c]
1	**3a**	(*R*)-**2a-Y**	2	25	0.27	185	66
2	**3a**	(*R*)-**2a-Lu**	2	25	0.30	167	82
3	**3a**	(*R*)-**2b-Y**	2	25	0.067	750	85
4	**3a**	(*R*)-**2b-Lu**	2	25	0.067	750	95
5	**3a**	(*R*)-**2c-Y**	2	25	0.067	750	87
6	**3a**	(*R*)-**2c-Lu**	2	25	0.071	700	95
7	**3a**	(*R*)-**2d-Y**	2	25	0.18	270	78
8	**3a**	(*R*)-**2d-Lu**	2	25	0.33	150	81
9	**3a**	(*R*)-**2e-Y**	2	25	0.158	320	77
10	**3a**	(*R*)-**2e-Lu**	2	25	0.083	600	86
11	**3a**	(*R*)-**2f-Y**	2	25	<0.05	>1000	75
12	**3a**	(*R*)-**2f-Y**	2	60	<0.05	>1000	90
13	**3a**	(*R*)-**2f-Lu**	2	25	<0.05	>1000	92
14	**3a**	(*R*)-**2f-Lu**	2	100	<0.05	>1000	92
15	**3a**	(*R*)-**2g-Y**	2	25	<0.05	>1000	47
16	**3a**	(*R*)-**2g-Y**	2	60	<0.05	>1000	62
17	**3a**	(*R*)-**2g-Lu**	2	25	<0.05	>1000	83
18	**3a**	(*R*)-**2g-Lu**	2	60	<0.05	>1000	73
19	**3a**	(*R*)-**2h-Y**	2	25	0.046	1090	73
20	**3a**	(*R*)-**2h-Lu**	2	25	0.05	1000	82
21	**3a**	(*R*)-**2i-Y**	2	25	<0.16	≥300	90
22	**3a**	(*R*)-**2i-Lu**	2	25	<0.16	≥300	95
23	**3a**	(*R*)-**IIIa-Y**	2	25	0.06	≥840	84[d]
24	**3a**	(*R*)-**IIIa-Lu**	2	25	0.25	≥180	93[d]
25	**3a**	(*R*)-**IIIa-Sc**	2	25	0.6	110	95[d]
26	**3b**	(*R*)-**2a-Y**	2	25	0.50	98	49
27	**3b**	(*R*)-**2a-Lu**	2	25	0.58	84	75
28	**3b**	(*R*)-**2b-Y**	2	25	0.083	600	80
29	**3b**	(*R*)-**2b-Lu**	2	25	0.083	590	89
30	**3b**	(*R*)-**2c-Y**	2	25	0.075	640	69
31	**3b**	(*R*)-**2c-Lu**	2	25	0.14	340	86
32	**3b**	(*R*)-**2d-Y**	2	25	0.22	220	43
33	**3b**	(*R*)-**2d-Lu**	2	25	0.50	97	59
34	**3b**	(*R*)-**2e-Y**	2	25	0.183	270	73
35	**3b**	(*R*)-**2e-Lu**	2	25	0.233	210	87
36	**3b**	(*R*)-**2f-Y**	2	25	0.15	330	80
37	**3b**	(*R*)-**2f-Y**	2	100	<0.05	>1000	84
38	**3b**	(*R*)-**2f-Lu**	2	25	0.15	330	88
39	**3b**	(*R*)-**2g-Y**	2	25	0.05	1000	45
40	**3b**	(*R*)-**2g-Lu**	2	25	0.15	330	72
41	**3b**	(*R*)-**2h-Y**	2	25	0.133	375	65
42	**3b**	(*R*)-**2h-Lu**	2	25	0.233	210	81
43	**3b**	(*R*)-**2i-Y**	2	25	<0.16	≥300	80
44	**3b**	(*R*)-**2i-Lu**	2	25	<0.16	≥300	95
45	**3b**	(*R*)-**IIIa-Lu**	2	25	0.11	460	83[d]
46	**3b**	(*R*)-**IIIa-Sc**	2	25	6	11	85[d]
47	**3c**	(*R*)-**2a-Y**	5	25	31.0	0.65	49
48	**3c**	(*R*)-**2a-Lu**	10	25	46.0	0.22	67
49	**3c**	(*R*)-**2b-Y**	2	60	1.5	32	70
50	**3c**	(*R*)-**2b-Lu**	2	60	1.58	31	87
51	**3c**	(*R*)-**2b-Lu**	5	25	27.0	0.73	83
52	**3c**	(*R*)-**2c-Y**	5	25	10.0	2.0	71
53	**3c**	(*R*)-**2c-Lu**	5	25	35.0	0.57	75
54	**3c**	(*R*)-**2d-Y**	10	25	46.0	0.22	31

DOI: 10.1021/acs.organomet.8b00510
Organometallics XXXX, XXX, XXX−XXX

Table 1. continued

entry	subst	cat.	[cat.]/[subst] (%)	T (°C)	t (h)[b]	N_t (h^{-1})	ee (%)[c]
55	**3c**	(*R*)-**2d-Lu**	10	25	140.0	0.07	46
56	**3c**	(*R*)-**2e-Y**	5	25	11.5	1.7	59
57	**3c**	(*R*)-**2e-Lu**	5	25	49	0.41	75
58	**3c**	(*R*)-**2f-Y**	2	25	23.0	2.2	83
59	**3c**	(*R*)-**2f-Y**	2	60	1.4	39	82
60	**3c**	(*R*)-**2f-Lu**	2	60	3.0	15	88
61	**3c**	(*R*)-**2g-Y**	2	60	0.50	100	75
62	**3c**	(*R*)-**2g-Lu**	2	60	2.0	25	76
63	**3c**	(*R*)-**IIIa-Y**	2	25	24.0	2.6	70[d]
64	**3c**	(*R*)-**IIIa-Lu**	2	60	4	18	72[d]
65	**3c**	(*R*)-**IIIb-Lu**	5	22	16.5	1.7	90[d]

[a]General reaction conditions: 0.1 M (**3a**,**b**) and 0.25 M (**3c**), solution of substrate in C_6D_6, Ar atm. [b]Reaction time at which at least 95% NMR conversion relative to ferrocene internal standard was obtained. [c]Enantiomeric excess determined by ^{19}F NMR spectroscopy of the Mosher amides. [d]Taken from ref 9a.

Table 2. Asymmetric Intramolecular Hydroamination of 2,2-Dimethylpent-4-enylamine (3d) Catalyzed by Binaphtholate Rare-Earth-Metal Complexes[a]

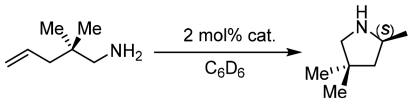

3d **4d**

entry	cat.	T (°C)	t (h)[b]	N_t (h^{-1})	ee (%)[c]
1	(*R*)-**2a-Y**	25	13.5	4	26
2	(*R*)-**2a-Lu**	25	17.0	3	60
3	(*R*)-**2b-Y**	25	3.75	13	59
4	(*R*)-**2b-Lu**	25	5.25	10	84
5	(*R*)-**2b-Lu**	40	0.67	75	87
6	(*R*)-**2b-Lu**	60	0.17	290	89
7	(*R*)-**2b-Lu**	110[d]	<0.025	>2000	90
8	(*R*)-**2c-Y**	25	2.5	20	50
9	(*R*)-**2c-Lu**	25	23.0	2.2	78
10	(*R*)-**2d-Y**	25	4.0	12.3	22
11	(*R*)-**2d-Lu**	25	10.0	4.8	39
12	(*R*)-**2e-Y**	25	7.0	7.0	59
13	(*R*)-**2e-Lu**	25	9.0	5.4	73
14	(*R*)-**2f-Y**	25	1.8	25	63
15	(*R*)-**2f-Y**	60	0.2	250	72
16	(*R*)-**2f-Y**	100[d]	<0.05	>1000	71
17	(*R*)-**2f-Lu**	25	2.9	20	76
18	(*R*)-**2f-Lu**	60	0.2	250	81
19	(*R*)-**2f-Lu**	100[d]	<0.05	>1000	77
20	(*R*)-**2g-Y**	25	2.75	17.5	30
21	(*R*)-**2g-Y**	60	0.2	250	49
22	(*R*)-**2g-Y**	100[d]	<0.05	>1000	53
23	(*R*)-**2g-Lu**	25	8.5	4.9	42
24	(*R*)-**2g-Lu**	60	0.2	250	55
25	(*R*)-**2g-Lu**	100[d]	<0.05	>1000	57
26	(*R*)-**2h-Y**	25	8.5	5.8	41
27	(*R*)-**2h-Lu**	25	20.5	2.4	59
28	(*R*)-**2i-Y**	25	2.75	19.7	70
29	(*R*)-**2i-Lu**	25	4.2	11.4	92
30	(*R*)-**IIIa-Y**[e]	60	0.07	480	65[f]
31	(*R*)-**IIIa-Lu**	22	27.5	2.4	69[f]

[a]General reaction conditions: 0.2 M solution of substrate **3d** in C_6D_6, Ar atmosphere. [b]Reaction time at which at least 95% NMR conversion relative to ferrocene internal standard was obtained. [c]Enantiomeric excess determined by ^{19}F NMR spectroscopy of the Mosher amides. [d]In toluene-d_8. [e]3 mol % cat. [f]Taken from ref 9a.

dependences of enantioselectivities were observed for the *gem*-dimethyl-substituted aminopentene **3d** (vide infra).

The cyclization of **3b** proceeded smoothly at room temperature with turnover rates as high as 1000 h^{-1}, generating pyrrolidine **4b** with moderate to excellent enantioselectivities (43−95% ee) (Figure 2, Table 1, entries 26−46) with lutetium complexes generally leading to significantly better selectivities in comparison to the larger yttrium. The highest enantioselectivities were observed for benzyldiphenylsilyl-substituted (*R*)-**2i-Lu** (95% ee), the cyclohexyldiphenylsilyl-substituted (*R*)-**2b-Lu** (89% ee), the diphenyl(*o*-tolyl)silyl-substituted (*R*)-**2f-Lu** (88% ee), and the dicyclohexylphenylsilyl-substituted (*R*)-**2e-Lu** (87% ee), exceeding selectivities observed for the triphenylsilyl-substituted (*R*)-**IIIa-Ln** (Ln = Sc (85% ee), Lu (83% ee))[9a] (compare Table 1, entries 29, 35, 38, and 44 with entries 45 and 46). The lowest selectivities were observed for the triisopropylsilyl-substituted (*R*)-**2d-Ln** (Ln = Lu (59% ee), Y (43% ee)), the tris(4-*tert*-butylphenyl)silyl-substituted complex (*R*)-**2g-Y** (45% ee), and the dibenzosilole-substituted (*R*)-**2a-Y** (49% ee) (Table 1, entries 26, 32, 33, and 39).

Cyclization of the unsubstituted aminopentene **3c** proceeds significantly more slowly at room temperature in comparison to the reaction of the *gem*-dialkyl-activated aminopentene derivatives **3a**,**b**,**d**. The slowest rates were observed for the triisopropylsilyl-substituted (*R*)-**2d-Ln** (Ln = Lu (0.07 h^{-1}, 46% ee), Y (0.22 h^{-1}, 31% ee)), which coincidentally afforded also the lowest selectivities in the formation of **4c**, while the highest rates were afforded by the diphenyl(*o*-tolyl)silyl-substituted (*R*)-**2f-Y** (2.2 h^{-1}) and the *tert*-butyldiphenylsilyl-substituted (*R*)-**2c-Y** (2.0 h^{-1}), which are comparable to that of the triphenylsilyl-substituted (*R*)-**IIIa-Y** (2.6 h^{-1}) (Table 1, entries 52, 54, 55, 58, and 63). More expedient rates of up to 100 h^{-1} (for the tris(4-*tert*-butylphenyl)silyl-substituted complex (*R*)-**2g-Y**, Table 1, entry 61) were observed at 60 °C.

The highest enantioselectivities in the cyclization of **3c** were observed for the diphenyl(*o*-tolyl)silyl-substituted (*R*)-**2f-Ln** (Ln = Lu (88% ee at 60 °C), Y (83% ee at 25 °C)) and the cyclohexyldiphenylsilyl-substituted (*R*)-**2b-Lu** (87% ee at 60 °C) (Table 1, entries 50, 58, and 60). Interestingly, (*R*)-**2b-Lu** formed pyrrolidine **4c** with a slightly lower selectivity of 83% ee at 25 °C (Table 1, entry 51). A similar temperature dependence of enantioselectivity has been observed in the cyclization of **3d** (vide infra).

The cyclization of the *gem*-dimethyl-substituted aminopentene **3d** proceeds smoothly at room temperature within a

DOI: 10.1021/acs.organomet.8b00510
Organometallics XXXX, XXX, XXX−XXX

Table 3. Asymmetric Intramolecular Hydroamination of Aminohexene 5 and Aminoheptene 7 Catalyzed by Binaphtholate Rare-Earth-Metal Complexes[a]

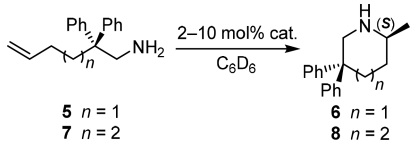

5 $n = 1$
7 $n = 2$

6 $n = 1$
8 $n = 2$

entry	subst	cat.	[cat.]/[subst] (%)	T (°C)	t (h)[b]	N_t (h^{-1})	% ee[c]
1	**5**	(*R*)-**2a-Y**	5	25	29.0	0.68	51
2	**5**	(*R*)-**2a-Lu**	5	25	36.2	0.55	21
3	**5**	(*R*)-**2b-Y**	2	25	7.5	6.5	46
4	**5**	(*R*)-**2b-Y**	2	60	0.58	85	43
5	**5**	(*R*)-**2b-Lu**	2	25	38.0	1.3	9
6	**5**	(*R*)-**2b-Lu**	2	60	1.17	41	5
7	**5**	(*R*)-**2c-Y**	5	25	25.0	0.78	36
8	**5**	(*R*)-**2c-Lu**	5	25	44.5	0.44	33
9	**5**	(*R*)-**2f-Y**	2	60	2.5	20	47
10	**5**	(*R*)-**2f-Lu**	2	60	1.2	42	48
11	**5**	(*R*)-**2g-Y**	2	25	0.8	62	13
12	**5**	(*R*)-**2g-Lu**	2	25	0.3	170	7
13	**5**	(*R*)-**2i-Y**	2	25	4.1	12	27
14	**5**	(*R*)-**2i-Lu**	2	25	27	1.7	16
15	**7**	(*R*)-**2a-Y**	10	80	169	0.06	44
16	**7**	(*R*)-**2b-Y**	5	80	116	0.17	50
17	**7**	(*R*)-**2b-Lu**	10	80	124	0.08	8
18	**7**	(*R*)-**2d-Y**	10	90	165	0.06	−8[d]
19	**7**	(*R*)-**IIIa-Lu**	4	80	72	0.35	55

[a]General reaction conditions: 0.1 M solution of substrate in C_6D_6, Ar atmosphere. [b]Reaction time at which at least 95% NMR conversion relative to ferrocene internal standard was obtained. [c]Enantiomeric excess determined by ^{19}F NMR spectroscopy of the Mosher amides. [d]Inverse configuration was observed.

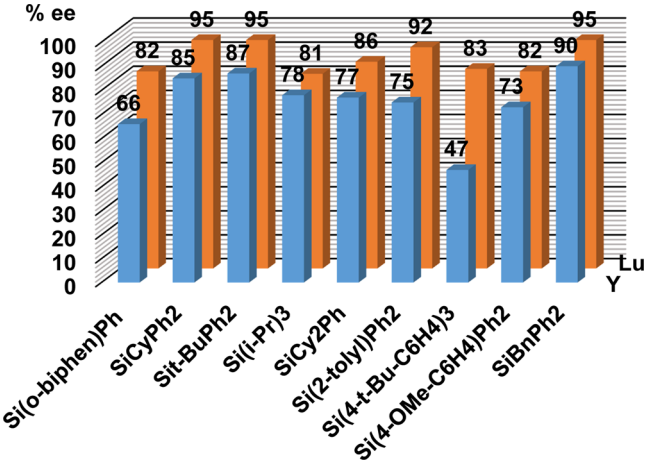

Figure 1. Enantioselectivity of complexes (*R*)-**2a−i** in the hydroamination of the *gem*-diphenyl-substituted aminopentene **3a** at 25 °C.

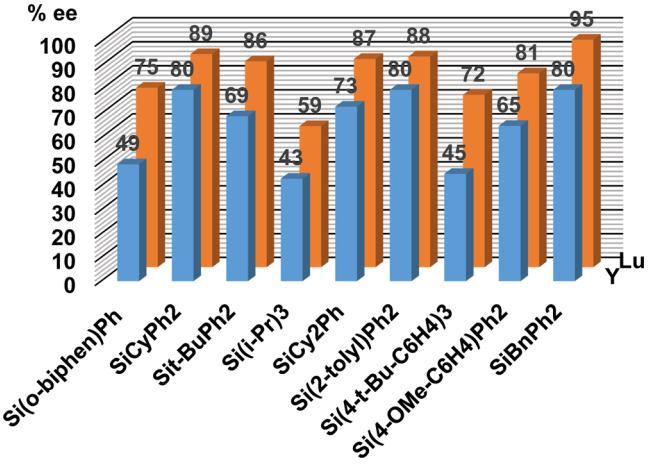

Figure 2. Enantioselectivity of complexes (*R*)-**2a−i** in the hydroamination of substrate **3b** at 25 °C.

reasonable period of time (Table 2). however, the rates of cyclization are substantially slower in comparison to the more activated substrates **3a**,**b**. For example, the rate of cyclization of **3a** (>1000 h^{-1}) and **3b** (330 h^{-1}) using (*R*)-**2f-Y** at room temperature (Table 1, entries 11 and 36) was much faster than the reaction rate of 25 h^{-1} observed for the cyclization of **3d** under the same catalytic reaction conditions (Table 2, entry 14). Overall, the rates of cyclization of **3d** fall in the range of 2.2−25 h^{-1} at room temperature.

The highest enantioselectivity in the formation of pyrrolidine **4d** at 25 °C was observed for the benzyldiphenylsilyl-substituted (*R*)-**2i-Lu** (92% ee at 25 °C) and the cyclohexyldiphenylsilyl-substituted (*R*)-**2b-Lu** (84% ee at 25 °C) (Table 2, entries 4 and 29), whereas the lowest selectivities at 25 °C were observed for the rigid dibenzosilole-substituted (*R*)-**2a-Y** (26% ee), the triisopropylsilyl-substituted (*R*)-**2d-Ln** (Ln = Lu (39% ee), Y (22% ee)), and the tris(4-*tert*-butylphenyl)silyl-substituted complex (*R*)-**2g-Y** (30% ee) (Table 2, entries 1, 10, 11, and 20).

It is noteworthy that enantioselectivities tend to increase for the formation of **4d** using (*R*)-**2b-Lu** and (*R*)-**2g-Ln** (Ln = Y, Lu) with increasing temperature, reaching the maximum enantioselectivity of 90% ee using (*R*)-**2b-Lu** at 110 °C (Figure 3, Table 2, entries 4−7 and 20−25). The selectivity for

DOI: 10.1021/acs.organomet.8b00510
Organometallics XXXX, XXX, XXX−XXX

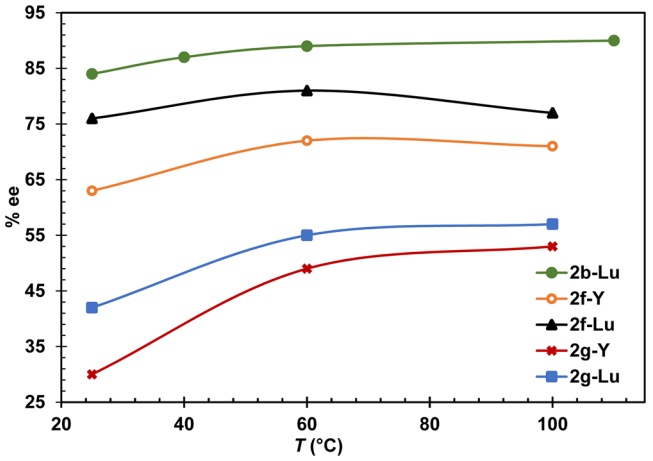

Figure 3. Temperature dependence of enantiomeric excess in the hydroamination/cyclization of **3d** ($[subst.]_0$ = 0.20 mol L^{-1}) with (*R*)-**2b-Lu**, (*R*)-**2f-Ln**, and (*R*)-**2g-Ln** ([cat.] = 0.004 mol L^{-1}) at variable temperatures in C_6D_6 (T = 25−60 °C) and toluene-d_8 (T = 100−110 °C), respectively. The lines are drawn as guides for the eye.

(*R*)-**2f-Ln** (Ln = Y, Lu) also increases from 25 to 60 °C but decreases slightly at 100 °C (Table 2, entries 14−19). This unusual behavior can be explained by an equilibrium between the two species **A** and **B**, as depicted in Scheme 3.[9a,25] While the lower coordinate species **A** is believed to be catalytically more active and more selective, the electronically more saturated species **B** is expected to be less active and presumably also less selective due to steric crowding.[9a] As the temperature increases, the equilibrium between species **A** and **B** is shifted toward the entropically favored lower coordinate species **A**, thus resulting in an increase in the observed selectivity.

Following the general trend that the rate of intramolecular hydroamination decreases with increasing ring size, cyclization of the *gem*-diphenyl-substituted aminohexene **5** (Table 3, entries 1−14) proceeded significantly more slowly with lower selectivity in comparison to the reaction of the *gem*-diphenyl-substituted aminopentene **3a**. While the rate of cyclization of **5** at 25 °C falls in the range of 0.44−12 h^{-1} for catalysts **2a−c,i**, the sterically highly shielded tris(4-*tert*-butylphenyl)silyl-substituted catalysts (*R*)-**2g-Ln** significantly excelled with rates of 62 h^{-1} (for Ln = Y) and 170 h^{-1} (for Ln = Lu), with the latter example also being one of the rare instances where the metal with a smaller ionic radius achieves a higher catalytic activity ($r(Lu^{3+})$ = 0.977 Å, $r(Y^{3+})$ = 1.019 Å).[26] The rigid dibenzosilole-substituted (*R*)-**2a-Y** afforded piperidine **6** with a moderate enantioselectivity of 51% ee at 25 °C, followed by the diphenyl(*o*-tolyl)silyl-substituted (*R*)-**2f-Ln** (Ln = Lu (48% ee), Y (47% ee). both at 60 °C) and the cyclohexyldiphenylsilyl-substituted complex (*R*)-**2b-Y** (46% ee at 25 °C) (see Table 3, entries 1, 3, 9, and 10). The enantiomeric excess of the hydroamination product **6** depended only slightly on the reaction temperature (see Table 3, entries 3−6). Interestingly, the enantioselectivity of the formation of piperidine **6** dropped markedly with decreasing ionic radius of the metal (e.g., Table 3, entry 1 vs entry 2 and entry 3 vs entry 5), except for complexes **2c,f**. This observation is in contrast with the general trend observed in the cyclization of aminopentenes **3a−d** (Tables 1 and 2).

Cyclization of the *gem*-diphenyl-substituted aminoheptene **7** required harsher reaction conditions. Prolonged heating to 80−90 °C and higher catalyst loadings were required to achieve complete cyclization of **7**. The highest selectivity was observed for the cyclohexyldiphenylsilyl-substituted complex (*R*)-**2b-Y** (50% ee), slightly below the selectivity observed for (*R*)-**IIIa-Lu** (55% ee) (Table 3, entries 16 and 19). The smaller lutetium catalyst (*R*)-**2b-Lu** produced the azepane **8** with significantly lower enantioselectivity in comparison to its yttrium congener (Table 3, entries 16 and 17). Also noteworthy seems to be the observation that the triisopropylsilyl-substituted binaphtholate complex (*R*)-**2d-Y** produced the azepane **8** with reversed absolute configuration, though the selectivity was very low (8% ee) (Table 3, entry 18).

In contrast to the reaction of terminal alkenes, the cyclization of the 1,2-disubstituted olefin **9** proceeds

Scheme 3. Catalytic Cycle of Intramolecular Hydroamination of Aminoalkenes

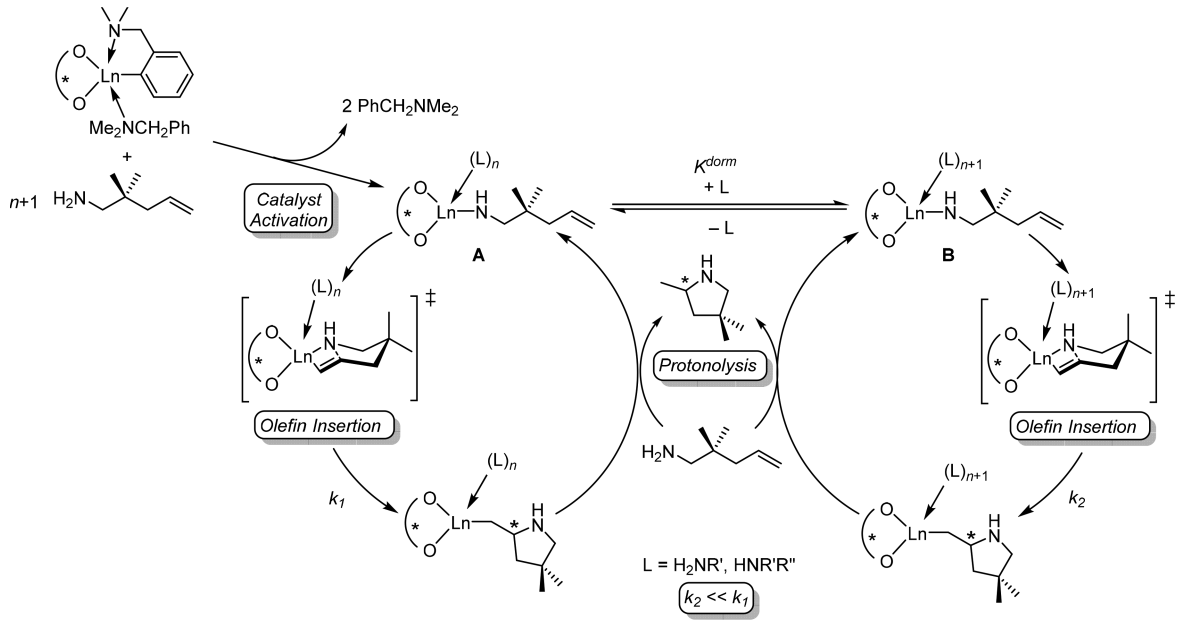

DOI: 10.1021/acs.organomet.8b00510
Organometallics XXXX, XXX, XXX−XXX

significantly more slowly than the reaction of the *gem*-diphenyl-substituted aminopentene **3a** (compare Table 1, entries 1−22, and Table 4). This observation is in agreement with the generally accepted mechanism of hydroamination/cyclization,[25] in which the rate of insertion of the sterically more hindered olefin is diminished by steric congestion. The binaphtholate rare-earth-metal complexes furnished the pyrrolidine product **10** with good to excellent enantioselectivities in the range of 75−96% ee (Table 4). Interestingly, ring closure of **9** generally proceeds with higher enantioselectivities in comparison to that of the corresponding terminal alkene analogue **3a**, with the exception of the cyclohexyldiphenylsilyl-substituted (*R*)-**2b-Ln** (Ln = Y, Lu) and the diphenyl(*o*-tolyl)silyl-substituted (*R*)-**2f-Lu** (compare Table 1, entries 3, 4, and 13, with Table 4, entries 3, 4, and 10).

Table 4. Asymmetric Intramolecular Hydroamination of the Internal Alkene 9 Catalyzed by Binaphtholate Rare-Earth-Metal Complexes[a]

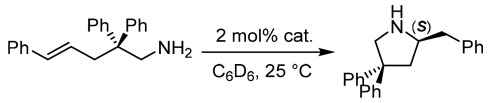

9 **10**

entry	cat.	t (h)[b]	N_t (h^{-1})	ee (%)[c]
1	(*R*)-**2a-Y**	3.0	17	93
2	(*R*)-**2a-Lu**	7.5	6.4	96
3	(*R*)-**2b-Y**	0.3	170	83
4	(*R*)-**2b-Lu**	0.75	67	88
5	(*R*)-**2c-Y**	1.0	50	92
6	(*R*)-**2c-Lu**	1.75	28	96
7	(*R*)-**2d-Y**	3.5	14.3	95
8	(*R*)-**2d-Lu**	7.75	6.4	91
9	(*R*)-**2f-Y**	0.67	75	93
10	(*R*)-**2f-Lu**	1.0	50	75
11	(*R*)-**2g-Y**	0.1	500	88
12	(*R*)-**2g-Lu**	0.15	330	91
13	(*R*)-**2i-Y**	0.75	67	95
14	(*R*)-**2i-Lu**	0.75	67	95

[a]General reaction conditions: 0.1 M solution of substrate in C_6D_6, Ar atm. [b]Reaction time at which at least 95% NMR conversion relative to ferrocene internal standard was obtained. [c]Determined by ^{19}F NMR spectroscopy of the Mosher amides.

Steric congestion around nitrogen, on the other hand, resulted in significantly increased rates of cyclization in case of the *N*-benzyl-substituted aminoalkene **11a** using the *tert*-butyldiphenylsilyl-substituted binaphtholate complexes (*R*)-**2c-Ln** in comparison to the primary aminoalkene analogue **3d** (Table 2, entries 8 and 9, vs Table 5, entries 1 and 2). While the cyclization of **11a** proceeded more selectively (71% ee) than that of **3d** (50% ee) using (*R*)-**2c-Y**, the opposite was true for the corresponding lutetium complex. A similar rate acceleration in the cyclization of a secondary amine in comparison to a primary amine analogue has been observed for neutral diamidobinaphthyl rare-earth-metal complexes.[27] On the basis of the proposed mechanism (Scheme 3), the rate acceleration can be explained by a shift in the equilibrium between the higher coordinate species **B** in favor of the lower coordinate and more catalytically active species **A**, facilitated by the bulkiness of the *N*-benzyl substituent.

However, the *N*-benzyl *gem*-diphenyl-substituted aminopentene **11b** is sterically more demanding than **11a**, leading to significantly more steric hindrance around the metal center. As a result, significantly lower activities and enantioselectivities were observed in the cyclization of the secondary amine **11b** (Table 5, entries 3−12) in comparison to those of the primary amine analogue **3a** and the secondary amine **11a**. Moreover, the hydroamination product **12b** was obtained with inverted *R* configuration using the *tert*-butyldiphenylsilyl-substituted binaphtholate complexes (*R*)-**2c-Ln** (Table 5, entries 6−9). Interestingly, the preferred enantiomer for product **12b**

Table 5. Asymmetric Intramolecular Hydroamination of Secondary Aminoalkenes Catalyzed by Binaphtholate Rare-Earth-Metal Complexes[a]

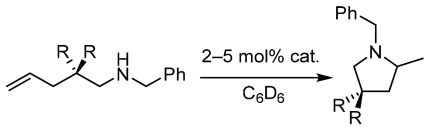

11a R = Me
11b R = Ph

12a R = Me
12b R = Ph

entry	subst	cat.	[cat.]/[subst] (%)	T (°C)	t (h)[b]	N_t (h^{-1})	ee (%)[c] (confign)
1	**11a**	(*R*)-**2c-Y**	2	25	0.33	148	71 (*S*)
2	**11a**	(*R*)-**2c-Lu**	2	25	0.33	148	69 (*S*)
3	**11b**	(*R*)-**2b-Y**	2	25	15.8	3.1	52 (*S*)
4	**11b**	(*R*)-**2b-Y**	2	60	5.5	8.9	50 (*S*)
5	**11b**	(*R*)-**2b-Lu**	2	25	2.2	22	77 (*S*)
6	**11b**	(*R*)-**2c-Y**	2	25	16.0	3.0	37 (*R*)
7	**11b**	(*R*)-**2c-Y**	2	60	6.5	7.5	13 (*R*)
8	**11b**	(*R*)-**2c-Lu**	2	25	6.0	3.0	3 (*R*)
9	**11b**	(*R*)-**2c-Lu**	2	60	2.0	24.5	16 (*S*)
10	**11b**	(*R*)-**2f-Y**	2	60	4.0	12.5	17 (*S*)
11	**11b**	(*R*)-**2g-Y**	2	60	3.5	14	48 (*S*)
12	**11b**	(*R*)-**2g-Lu**	2	60	3.5	14	68 (*S*)

[a]General reaction conditions: 0.1 mol L^{-1} solution of substrate in C_6D_6, Ar atmosphere. [b]Reaction time at which at least 95% NMR conversion relative to bis(trimethylsilyl)methane internal standard was obtained. [c]Determined by ^{19}F NMR spectroscopy of the Mosher amides after removal of *N*-benzyl group.

DOI: 10.1021/acs.organomet.8b00510
Organometallics XXXX, XXX, XXX−XXX

reversed back to *S* when the reaction was conducted with (*R*)-**2c**-**Lu** at 60 °C (Table 5, entry 8 vs entry 9). The other (*R*)-binaphtholate catalysts generally furnished the pyrrolidine products preferentially with *S* configuration.

Kinetics of the Intramolecular Hydroamination. A kinetic study was performed with the *gem*-dimethyl-substituted aminopentene **3d** and (*R*)-**2b**-**Y** at variable temperatures in the range of 25−60 °C (Figure 4), indicating an approximate zero-order rate dependence on substrate concentration. However, the plots representing the data for the hydroamination of **3d** at 25 and 32 °C show a slight curvature, indicating a slight rate acceleration during the catalytic reaction. A similar curvature was also observed for the diphenyl(*o*-tolyl)silyl-substituted (*R*)-**2f**-**Y** and tris(4-*tert*-butylphenyl)silyl-substituted catalyst (*R*)-**2g**-**Y** (see Figure S1 in the Supporting Information) for substrate **3d** and for the *gem*-diphenyl-substituted aminohexene **5** using (*R*)-**2f**-**Lu** as well (see Figure S4 in the Supporting Information). Similar catalytic behavior was previously reported for chiral lanthanocene complexes[28] and the triphenylsilyl-substituted binaphtholate complex (*R*)-**IIIa**-**Y**[9a] and can be rationalized to stem from a slight shift between the catalytically more active, lower coordinate species **A** and the less active, higher coordinate species **B** (Scheme 3). Species **A** is slightly more favored at higher conversion, because of weaker binding of the secondary amine hydroamination product in comparison to the sterically less hindered and stronger binding primary amine starting material.

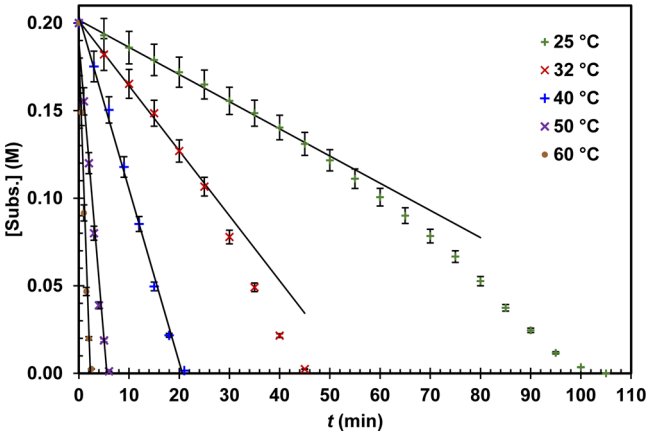

Figure 4. Time dependence of substrate concentration in the hydroamination/cyclization of aminopentene **3d** (0.2 M) using (*R*)-**2b**-**Y** ([cat.] = 0.004 M) at variable temperatures in C_6D_6. The lines through the data points represents the least-squares fits for the initial linear part of the data.

However, it should be mentioned that other catalytic reactions appear to be strictly zero order up to high conversions of 90% (see Figures S2−S5 in the Supporting Information).

The plot of the reaction rate versus catalyst concentration over an 8-fold range (4−32 mmol L^{-1}) (Figure 5) is a straight line, indicating that the rate of hydroamination/cyclization of **3d** using (*R*)-**2b**-**Y** is first order in catalyst concentration and that the catalytically active species is monomeric.

These findings are in agreement with our previous investigation using the triphenylsilyl-substituted binaphtholate complex (*R*)-**IIIa**-**Y**[9a] and the generally accepted mechanism of hydroamination, indicating that the cyclization of aminoalkenes proceeds via a rate-determining olefin insertion step.[25,29]

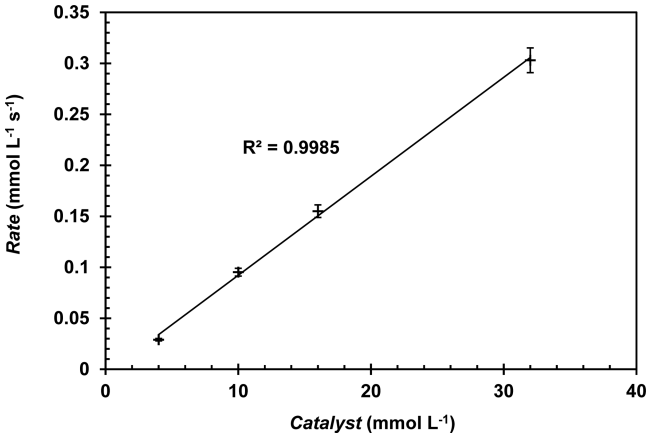

Figure 5. Rate versus catalyst concentration for the hydroamination of **3d** ($[subst]_0$ = 0.2 M) using (*R*)-**2b**-**Y** in C_6D_6 at 25 °C.

Unfortunately, attempts to observe species **A** and **B** by low-temperature NMR spectroscopy using stoichiometric amounts of 2-methylpyrrolidine (**4c**) or *n*-propylamine as substrate mimic have been unsuccessful so far and the NMR spectra remain broad and featureless over a large temperature range. No decoalescence to distinguishable species was observed down to −90 °C, indicating facile amine exchange even under those conditions. However, additional evidence on the effect of amine binding on catalytic activity can be inferred from the reaction of aminodiene **13**[30] using the triphenylsilyl-substituted binaphtholate complex (*R*)-**IIIa**-**Y** (Scheme 4). Cyclization of **13** initially leads to the 2,5-disubstituted pyrrolidine intermediate **14** and in a subsequent second cyclization step to the bicyclic pyrrolizidine **15**.[31]

Scheme 4. Catalytic Hydroamination/Bicyclization of Aminodiene 13 with (*R*)-IIIa

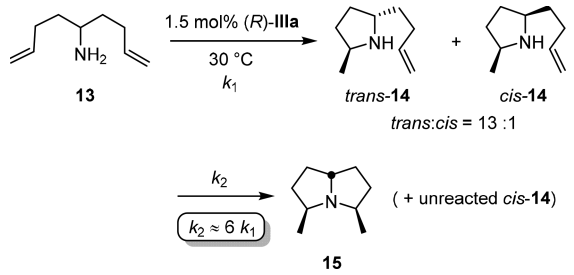

The reaction profile indicates that the formation of the bicyclic product sets in only after consumption of >90% of the aminodiene starting material with the first trace amounts of pyrrolizidine **15** becoming noticeable at 98% conversion of aminodiene **13** to pyrrolidine **14** (Figure 6; for an ^{1}H NMR stack plot of the various reaction stages see Figure S6 in the Supporting Information). Most intriguingly, the rate of the second cyclization step is approximately 6 times faster than the first cyclization event (k_1 = [6.70(8)] × 10^{-3} s^{-1}, k_2 = 0.041(4) s^{-1} at 30 °C). This observation contradicts previous studies on the cyclization of aminodiene **13**, in which elevated reaction temperatures were required to perform the bicyclization step.[30] For example, the reaction profile looks quite different when the simple tris-amido complex [Y{N(SiMe$_3$)$_2$}$_3$] was employed

DOI: 10.1021/acs.organomet.8b00510
Organometallics XXXX, XXX, XXX−XXX

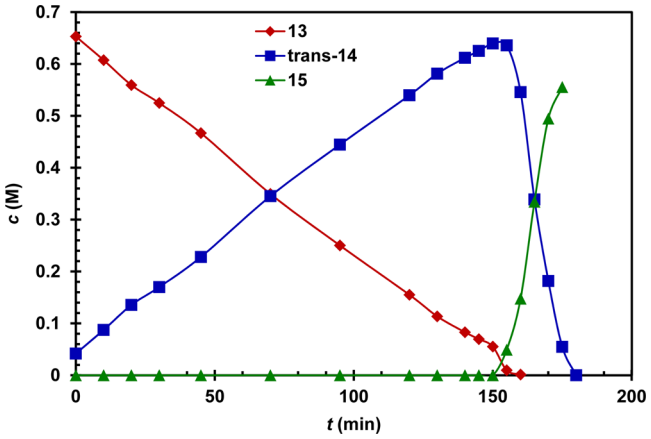

Figure 6. Kinetic profile for the hydroamination/cyclization of **13** ($[\mathbf{13}]_0$ = 0.67 M) with (*R*)-**IIIa-Y** (0.01 M, 1.5 mol %) at 30 °C in C_6D_6. The lines are drawn as guides for the eye.

(Figure 7). While the rate of the initial monocyclization step was quite rapid and formation of **14** was complete within 30

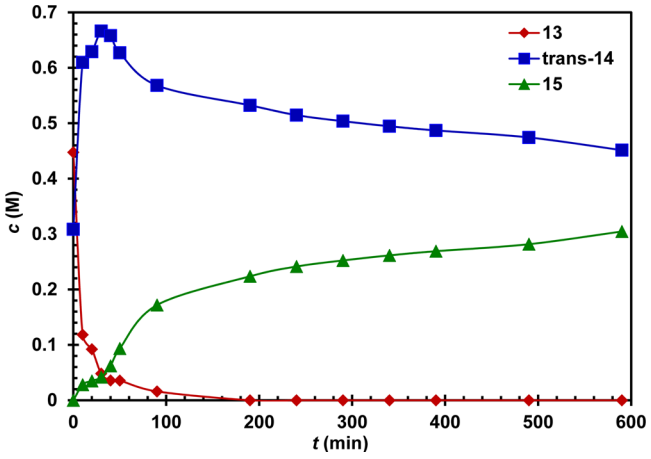

Figure 7. Kinetic profile for the hydroamination/cyclization of **13** ($[\mathbf{13}]_0$ = 0.67 M) with $[Y\{N(SiMe_3)_2\}_3]$ (0.02 M, 3 mol %) at 40 °C in C_6D_6. The lines are drawn as guides for the eye.

min, the second cyclization proceeded sluggishly (k_1:k_2 > 500:1 at 40 °C for the linear parts of the respective kinetic data), with the first traces of **15** becoming noticeable around 80% conversion of **13** to **14**. The obvious difference between (*R*)-**IIIa-Y** and $[Y\{N(SiMe_3)_2\}_3]$ is that the sterically demanding binaphtholate ligand in (*R*)-**IIIa-Y** limits binding of sterically hindered amines to the metal center, whereas amine binding to the sterically unshielded tris-amido complex presumably is unabated. Thus, it can be expected that only the sterically less hindered primary amine **13** binds to the metal center of the sterically shielded binaphtholate catalyst, while the pyrrolidine intermediate **14** does not bind or binds only very weakly. Upon consumption of the great majority of the aminodiene starting material, the equilibrium abruptly shifts in favor of the lower coordinate, significantly more active species **A** (Scheme 3), leading to a dramatic increase in the rate of the second cyclization step. In contrast, it can be assumed that **13** and **14** both bind to the sterically unprotected tris-amide $[Y\{N(SiMe_3)_2\}_3]$ with binding constants of comparable magnitude, taming its catalytic activity toward bicyclization. In order to test this hypothesis, we performed the cyclization of **13** in the presence of 10 equiv (relative to catalyst) of *n*-propylamine as a nonconsumable mimic of **13**. Indeed, no acceleration effect was observed, and the behavior of the binaphtholate catalyst (*R*)-**IIIa-Y** was similar to that of the tris-amide $[Y\{N(SiMe_3)_2\}_3]$ (see Figure S7 in the Supporting Information).

Asymmetric Intermolecular Hydroamination of Alkenes.[17] For the initial catalyst screening we chose the reaction of 1-heptene with benzylamine (Table 6, entries 1–12). The reactions proceeded smoothly in the presence of 5 mol % binaphtholate catalyst, generating exclusively the Markovnikov hydroamination product **16**. The enantiomeric excess of the intermolecular hydroamination product **16** was determined by ^{19}F NMR spectroscopy after the removal of the *N*-benzyl group. The absolute configuration of the intermolecular hydroamination product **16** using the *R*-configured binaphtholate complexes was found to be *R*, which is opposite to that observed for the intramolecular hydroamination of aminopentenes.

To achieve high conversions within a reasonable amount of time, the reactions were performed at a temperature as high as 150 °C and a 10–15-fold excess of alkene was used to accelerate the reaction. Reactions performed with (*R*)-**IIIa-Y** at 110 °C required significantly longer in order to achieve high conversion (Table 6, entry 2), leading to an improved enantioselectivity of 65% ee in comparison to 58% ee at 150 °C. The excess of alkene was necessary in order to counteract the poor binding ability of the alkene to the d^0 metal in comparison to the strongly binding amine.[32] A lower alkene/amine ratio resulted in lower conversion and longer reaction time (Table 6, entry 3), whereas a larger excess of the alkene significantly reduced the reaction time, concomitant with a slight reduction in the enantioselectivity (Table 6, entry 4).

The sterically more hindered cyclohexyldiphenylsilyl- and *tert*-butyldiphenylsilyl-substituted binaphtholate complexes (*R*)-**2b-Y** and (*R*)-**2c-Y**, respectively, exhibited comparable activity in the intramolecular hydroamination of aminopentenes in most cases (Tables 1 and 2); however, the rate of benzylamine addition to 1-heptene was about 3 times faster with (*R*)-**2b-Y** in comparison to (*R*)-**2c-Y** (Table 6, entries 7 and 8). The selectivities achieved with (*R*)-**2b-Y** and (*R*)-**2c-Y** of 47% and 46% ee, respectively, were slightly lower than that observed with (*R*)-**IIIa-Y** (Table 6, entries 7 and 8 vs entry 1).

High conversions were observed in most cases, except for complexes (*R*)-**2d-Y** and (*R*)-**2h-Y**, which gave lower conversions (Table 6, entries 9 and 11), and the rigid dibenzosilole-substituted complex (*R*)-**2a-Y**, which was completely inactive even when it was heated to 170 °C (Table 6, entry 6). The triisopropylsilyl-substituted binaphtholate complex (*R*)-**2d-Y** displayed not only low activity (60% conversion in 72 h) but also the lowest enantioselectivity of 38% ee (Table 6, entry 9). This result was expected because (*R*)-**2d-Y** was also the least efficient catalyst among the binaphtholate catalysts for the intramolecular hydroamination of aminoalkenes. The *p*-methoxyphenyl(diphenyl)silyl-substituted complex (*R*)-**2h-Y** displayed the highest enantioselectivity of up to 60% ee at 150 °C; however, only 45% conversion was observed due to catalyst decomposition under these conditions (Table 6, entry 11).

Further investigations were conducted with other terminal alkenes and primary amines (Table 6, entries 13–21). The dicyclohexylphenylsilyl-substituted binaphtholate complex (*R*)-**2e-Y** catalyzed the intermolecular hydroamination of 1-

DOI: 10.1021/acs.organomet.8b00510
Organometallics XXXX, XXX, XXX–XXX

Table 6. Asymmetric Intermolecular Hydroamination of Unactivated Alkenes with a Primary Amine Using Binaphtholate Catalysts[a]

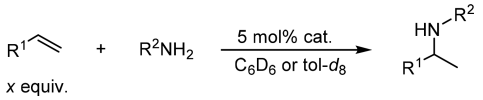

Entry	Alkene	Amine	Product	Cat.	x	T (°C)	t (h)	% conv.[b] (% yield)[c]	% ee[d] (config.)
1	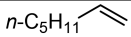	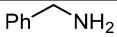	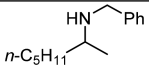 **16**	(*R*)-**IIIa-Y**	15	150	36	90 (65)	58 (*R*)
2				(*R*)-**IIIa-Y**	15	110	260	85 (51)	65 (*R*)
3				(*R*)-**IIIa-Y**	7	150	48	85 (57)	57 (*R*)
4				(*R*)-**IIIa-Y**[e]	50	150	18	95 (68)	54 (*R*)
5				(*R*)-**IIIa-Lu**	15	150	30	95 (62)	40 (*R*)
6				(*R*)-**2a-Y**	15	170	96	0	--
7				(*R*)-**2b-Y**	15	150	17	90	47 (*R*)
8				(*R*)-**2c-Y**	15	150	48	85 (59)	46 (*R*)
9				(*R*)-**2d-Y**	15	150	72	60 (44)	38 (*R*)
10				(*R*)-**2g-Y**	15	150	11	95 (72)	58 (*R*)
11				(*R*)-**2h-Y**	15	150	12	45	60 (*R*)
12				(*R*)-**2i-Y**	15	150	24	95 (64)	47 (*R*)
13	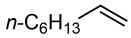	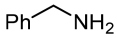	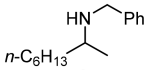 **17**	(*R*)-**IIIa-Y**	15	150	40	97 (72)	57 (*R*)
14				(*R*)-**2e-Y**	15	150	36	100 (56)	40 (*R*)
15	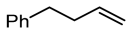	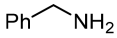	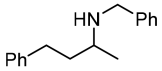 **18**	(*S*)-**IIIa-Y**[f]	10	150	11	100 (72)	56 (*S*)
16				(*R*)-**IIIa-Y**	15	110	212	68 (42)	66 (*R*)
17				(*R*)-**2e-Y**[f]	10	150	33	100 (65)	44 (*R*)
18				(*R*)-**2h-Y**	15	110	96	67 (40)	66 (*R*)
19	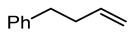	PMB-NH$_2$	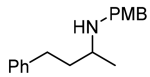 **19**	(*S*)-**IIIa-Y**	10	150	48	85 (66)	56 (*S*)
20				(*R*)-**2c-Y**	10	150	72	75 (61)	54 (*R*)
21				(*R*)-**2b-Y**	10	150	48	80	44 (*R*)

[a]General reaction conditions: 3.0 mmol of alkene, 0.2 mmol of amine, 10 μmol of cat. (0.1 mL of 0.1 M cat. solution in C_6D_6 or tol-d_8). [b]The conversion of amine was determined via ^{1}H NMR spectroscopy. [c]Isolated yield after column chromatography. [d]Determined by ^{19}F NMR spectroscopy of the Mosher amide after debenzylation. [e]8 mol % cat. was used. [f]4 mol % cat. was used.

octene with benzylamine at about the same rate as (*R*)-**IIIa-Y**; however, this occurred with significantly lower enantioselectivity (Table 6, entry 14).

The addition of benzylamine to 4-phenyl-1-butene was achieved with an alkene to amine ratio as low as 10:1. The *p*-methoxyphenyl(diphenyl)silyl-substituted binaphtholate complex (*R*)-**2h-Y** delivered the intermolecular hydroamination product **18** at 110 °C with the same 66% ee selectivity as (*R*)-**IIIa-Y** (Table 6, entries 16 and 18). A higher reaction rate was observed for (*R*)-**2h-Y** in comparison to (*R*)-**IIIa-Y**; however, again full conversion was not obtained with (*R*)-**2h-Y** due to significant decomposition of the catalyst even at the lower reaction temperature.

Hydroamination reactions with *p*-methoxybenzylamine proceeded significantly more slowly (Table 6, entries 19–21), presumably due to the presence of the coordinating

DOI: 10.1021/acs.organomet.8b00510
Organometallics XXXX, XXX, XXX−XXX

methoxy group that can compete for empty binding sites at the binaphtholate catalysts, resulting in longer reaction times and lower conversions.

While the binaphtholate complexes are efficient catalysts for intermolecular hydroaminations of unactivated alkenes with simple amines, the substrate scope is limited to primary amines and unbranched terminal alkenes. Attempts to perform the reactions involving disubstituted alkenes, such as cyclohexene and α-methylstyrene, or secondary amines, such as piperidine and pyrrolidine, were not successful. Moreover, the binaphtholate catalysts have a low functional group tolerance; thus, they are prone to deactivation under catalytic conditions, particularly in the presence of a methoxy group in the substrate or the catalyst. The reaction of 1,3-benzodioxol-5-ylmethylamine, a derivative of benzylamine, with 1-octene did not lead to any conversion, and significant decomposition of the catalyst was observed.

CONCLUSION

A variety of novel 3,3′-bis(trisarylsilyl)- and 3,3′-bis(arylalkylsilyl)-substituted binaphtholate rare-earth-metal complexes have been prepared and applied in the intramolecular hydroamination of aminoalkenes as well as the very challenging intermolecular hydroamination of nonactivated terminal alkenes with benzylamines. The complexes exhibit high catalytic activity and enantioselectivity in the hydroamination/cyclization of aminoalkenes, which is comparable to or even surpasses the acitivity and selectivity observed with the previous disclosed complexes (*R*)-**IIIa-Ln** and (*R*)-**IIIb-Ln**.[9a] The sterically demanding cyclohexyldiphenylsilyl-substituted complex (*R*)-**2b-Lu**, the *tert*-butyldiphenylsilyl-substituted complex (*R*)-**2c-Lu**, the diphenyl(*o*-tolyl)silyl-substituted complex (*R*)-**2f-Lu**, and the benzyldiphenylsilyl-substituted (*R*)-**2i-Lu** provide for most substrates the highest selectivities, while the rigid dibenzosilole-substituted complexes (*R*)-**2a-Ln** and the triisopropylsilyl-substituted complexes (*R*)-**2d-Ln** are often less selective and less active than the other complexes. However, as an exception, it should be noted that (*R*)-**2a-Lu** (as well as (*R*)-**2c-Lu**) provided pyrrolidine **10** with 96% ee, the highest selectivity observed in this series of complexes. While all new binaphtholate yttrium complexes, except (*R*)-**2a-Y** and (*R*)-**2d-Y**, exhibit catalytic activity comparable to or even greater than that of (*R*)-**IIIa-Y**[14b] in the intermolecular hydroamination, they show slightly lower selectivities, contrasting with the structure−selectivity motif observed in the intramolecular hydroamination. Only the *p*-methoxyphenyl(diphenyl)silyl-substituted complex (*R*)-**2h-Y** exhibited comparable selectivity; however, this system is plagued by catalyst decomposition. A plausible explanation for the differing selectivity patterns of intramolecular vs intermolecular hydroamination reactions may be construed out of the observation that the absolute configuration of the intermolecular hydroamination product is opposite to the configuration observed in the intramolecular reaction, thus implying that the stereodetermining olefin insertion steps in these two processes have different geometries.

EXPERIMENTAL SECTION

All reactions with air- or moisture-sensitive materials were performed with oven- (120 °C) and flame-dried glassware under an inert atmosphere of dry nitrogen or argon, employing standard Schlenk and glovebox techniques. (*R*)-3,3′-Dibromo-1,1′-binaphthalene-2,2′-diol,[18] (*R*)-3,3′-bis[*tert*-butyl(diphenyl)silyl]-1,1′-binaphthalene-2,2′-diol ((*R*)-**H_2BINOL-TBDPS**; **1c**),[18] 5-chloro-5-phenyldibenzosilole,[33] chloro(triisopropyl)silane,[34] bromotris(4-*tert*-butylphenyl)-silane,[35] chloro(4-methoxyphenyl)(diphenyl)silane,[36] benzylchlorodiphenylsilane,[37] [Ln(*o*-$C_6H_4CH_2NMe_2)_3$] (Ln = Y, Lu),[22] and (*R*)-**IIIa-Y**[9a] were synthesized according to literature procedures. Substrates 2,2-diphenylpent-4-enylamine (**3a**),[38a] C-(1-allylcyclohexyl)methylamine (**3b**),[38b] pent-4-enylamine (**3c**),[25] 2,2-dimethylpent-4-enylamine (**3d**),[38c] 2,2-diphenylhex-5-enylamine (**5**),[38d] 2,2-diphenylhept-6-enylamine (**7**),[38e] (4*E*)-2,2,5-triphenylpent-4-enylamine (**9**),[38f] *N*-benzyl-*N*-(2,2-dimethylpent-4-enyl)amine (**11a**),[38b] *N*-benzyl-*N*-(2,2-diphenylpent-4-enyl)amine (**11b**),[38b] and 5-amino-1,8-nonadiene (**13**)[30b] were synthesized as described in the literature. The substrates were distilled from finely powdered CaH_2 and stored over molecular sieves. All other chemicals were commercially available and were used as received unless otherwise stated. C_6D_6 and toluene-d_8 were distilled from sodium/benzophenone ketyl. (*S*)-Mosher acid was converted into the corresponding (*R*)-Mosher acid chloride according to the literature procedure.[39] The hydroamination products 2-methyl-4,4-diphenylpyrrolidine (**4a**),[38a] 3-methyl-2-azaspiro[4,5]decane (**4b**),[40a] 2-methylpyrrolidine (**4c**),[25] 2,4,4-trimethylpyrrolidine (**4d**),[25] 2-methyl-5,5-diphenylpiperidine (**6**),[38a] 2-methyl-6,6-diphenylazepane (**8**),[40b,c] 2-benzyl-4,4-diphenylpyrrolidine (**10**),[38e] 1-benzyl-2,4,4-trimethylpyrrolidine (**12a**),[38b] *N*-benzyl-2-methyl-4,4-diphenylpyrrolidine (**12b**),[38b] 2-(but-3-en-1-yl)-5-methylpyrrolidine (**14**),[30b] 3,5-dimethylhexahydro-1*H*-pyrrolizine (**15**),[30b] *N*-benzylheptan-2-amine (**16**),[14b,41a] *N*-benzyloctan-2-amine (**17**),[14b,41b] *N*-benzyl-4-phenylbutan-2-amine (**18**),[14b,41a] and *N*-(4-methoxybenzyl)-4-phenylbutan-2-amine (**19**)[14b,41c] are known compounds and were identified by comparison to the literature NMR spectroscopic data.

^{1}H, ^{13}C, and ^{19}F NMR spectra were recorded on Varian (400 and 500 MHz) spectrometers at 25 °C unless otherwise stated. The absolute configuration of the hydroamination products was determined by comparison of the ^{19}F NMR spectroscopic data of the Mosher amides with the assignments reported previously.[9a,14b] Silica gel (230−400 mesh, Sorbent Technologies) was used for column chromatography. Elemental analyses were performed by Robertson Microlit Laboratories, Inc., Ledgewood, NJ. Because the rare-earth-metal complexes **2a**−**i** retain trace amounts of free *N*,*N*-dimethylbenzylamine upon isolation, we have been unable to obtain correct elemental analyses for these compounds.

Chlorodicyclohexyl(phenyl)silane. To a suspension of finely cut lithium wire (1.60 g, 226.0 mmol) in pentane (100 mL) was added slowly chlorocyclohexane (19.2 g, 161.5 mmol) for 1 h with gentle heating. The resulting mixture was heated to refluxing temperature overnight. The violet mixture was chilled in an ice bath, and a solution of trichlorophenylsilane (7.04 g, 32.2 mmol) in pentane (10 mL) was added dropwise. The resulting mixture was warmed to room temperature and was stirred overnight. Precipitated lithium chloride salt and excessive lithium were filtered off. The filtrate was treated with ice-cold 4 M HCl solution (50 mL) to destroy the remaining cyclohexyllithium. The organic layer was separated, dried over anhydrous Na_2SO_4, and concentrated to give a yellow oil. The product was purified by vacuum distillation, giving two main fractions, 130−150 °C and above 150 °C at 0.5 Torr, which solidified in the refrigerator. Both fractions were shown to be identical and impure by NMR spectroscopy. An attempt to purify the desired product from dicyclohexyl(phenyl)silane through recrystallization in pentane did not improve the purity (ca. 77% purity). ^{1}H NMR (400 MHz, $CDCl_3$): δ 7.64−7.53 (m, 2H, aryl-H), 7.45−7.28 (m, 3H, aryl-H), 1.99−1.55 (m, 10H, cyclohexyl-H), 1.37−1.00 (m, 12H, cyclohexyl-H). ^{13}C{^{1}H} NMR (100 MHz, $CDCl_3$): δ 134.3, 129.9, 127.8 (aryl), 27.7, 27.6, 26.7, 26.6, 26.5, 25.2 (Cy).

Chlorodiphenyl(*o*-tolyl)silane. To a solution of 2-bromotoluene (5.13 g, 30 mmol) in Et_2O (30 mL) was added *n*-BuLi (12 mL, 2.5 M in hexanes, 30 mmol) slowly at room temperature. The mixture was stirred for 4 h, and to it was added dichlorodiphenylsilane (7.60 g, 30 mmol) at −10 °C. The reaction mixture was allowed to reach room temperature and stirred overnight. The precipitate was filtered off, and the filtrate was concentrated in vacuo. The product was extracted with

DOI: 10.1021/acs.organomet.8b00510
Organometallics XXXX, XXX, XXX−XXX

hexanes (70 mL), and the extract was then concentrated to a volume of about 15 mL and placed in a freezer to give white crystals (5.08 g, 55% yield). ^{1}H NMR (400 MHz, $CDCl_3$): δ 7.68−7.56 (m, 4H, aryl-H), 7.52−7.45 (m, 2H, aryl-H), 7.45−7.33 (m, 6H, aryl-H), 7.26−7.21 (m, 1H, aryl-H), 7.20−7.14 (m, 1H, aryl-H), 2.33 (s, 3H, aryl-CH_3). $^{13}C\{^1H\}$ NMR (100 MHz, $CDCl_3$): δ 145.2, 137.2, 135.2, 133.6, 131,4, 131.2, 130.71, 130.68, 128.3, 125.2 (aryl), 23.5 (aryl-CH_3).

3,3′-Bis(5-phenyl-5*H*-dibenzo[*b*,*d*]silyl-5-yl)-1,1′-binaphthalene-2,2′-diol ((*R*)-H$_2$BINOL-PDBS; 1a). To a solution of (*R*)-3,3′-dibromo-1,1′-binaphthalene-2,2′-diol (1.51 g, 3.40 mmol) in THF (65 mL) was added KH (409 mg, 10.2 mmol) in three portions. The resulting mixture was stirred for 30 min before a solution of 5-chloro-5-phenyldibenzosilole (2.17 g, 7.40 mmol) in THF (10 mL) was added at room temperature, to give a light orange reaction mixture which was then heated to 65 °C overnight. To the reaction mixture was added *t*-BuLi (9.1 mL, 13.6 mmol, 1.5 M in pentane) dropwise at −50 °C. The bright yellow mixture was warmed to room temperature slowly and was stirred for an additional 1 h. The solvent was evaporated in vacuo. The residue was dissolved in CH_2Cl_2 (50 mL), which was then treated with 1 M HCl (20 mL). The organic layer was separated, dried (Na_2SO_4), and concentrated. The product was purified using column chromatography on silica (hexanes/CH_2Cl_2 80/20) to afford a yellow solid (1.18 g, 43%) which was crystallized from pentane, giving the pure product **1a** as a white powder (0.91 g, 33% overall yield). ^{1}H NMR (500 MHz, C_6D_6): δ 8.53 (s, 2H, aryl-H), 8.05 (m, 2H, aryl-H), 7.94 (d, ^3J(H,H) = 6.85 Hz, 2H, aryl-H), 7.82 (m, 4H, aryl-H), 7.73 (dd, ^3J(H,H) = 7.95 Hz, ^4J(H,H) = 1.59 Hz, 4H, aryl-H), 7.48 (d, ^3J(H,H) = 7.83 Hz, 2H, aryl-H), 7.40 (m, 4H, aryl-H), 7.35 (m, 2H, aryl-H), 7.25 (t, ^3J(H,H) = 7.21 Hz, 2H, aryl-H), 7.16 (m, 6H, aryl-H overlapped with C_6D_5H), 7.1 (d, ^3J(H,H) = 8.31 Hz, 2H, aryl-H), 7.04 (m, 2H, aryl-H), 6.97 (m, 2H, aryl-H), 4.78 (s, 2H, OH). $^{13}C\{^1H\}$ NMR (125 MHz, C_6D_6): δ 156.9 (CO), 149.6, 149.1, 140.0, 136.97, 135.95, 135.6, 135.3, 135.1, 133.8, 131.0, 130.9, 129.8, 129.7, 129.0, 128.3, 128.3, 127.96, 127.94, 127.86, 127.81, 127.6, 124.2, 124.0, 123.0, 121.5, 121.4, 110.3 (aryl). Anal. Calcd for $C_{56}H_{38}O_2Si_2$: C, 84.17; H, 4.79. Found: C, 83.87; H, 4.80.

(*R*)-3,3′-Bis[cyclohexyl(diphenyl)silyl]-1,1′-binaphthalene-2,2′-diol ((*R*)-H$_2$BINOL-SiCyPh$_2$; 1b). This compound was prepared as reported previously[14b] with optimized reaction conditions. To a solution of (*R*)-3,3′-dibromo-1,1′-binaphthalene-2,2′-diol (1.50 g, 3.38 mmol) in DMF (11 mL) were added imidazole (1.39 g, 20.3 mmol) and chloro(cyclohexyl)diphenylsilane (4.07 g, 13.5 mmol). The resulting mixture was stirred at 90 °C overnight. The reaction was quenched by addition of saturated aqueous $NaHCO_3$ (5 mL) and was diluted with CH_2Cl_2 (150 mL). The organic layer was separated. The product was extracted with CH_2Cl_2 (3 × 30 mL). The combined organic layers were washed with water (3 × 15 mL), dried (Na_2SO_4) and concentrated in vacuo. The product was purified using column chromatography on silica (hexanes, then hexanes/CH_2Cl_2 9/1) to afford the crude bis(silyl ether) as a white powder (2.78 g, 84%), which was subjected to the next reaction without further purification. The crude bis(silyl ether) was dissolved in THF (50 mL), and a *t*-BuLi solution (7.2 mL, 11.4 mmol, 1.6 M in pentane) was added dropwise at −60 °C. The yellow solution was stirred for 5 min at −60 °C and was then allowed to reach room temperature slowly, after which it was stirred for an additional 1 h. The reaction was quenched with saturated aqueous NH_4Cl (5 mL), and the product was extracted with CH_2Cl_2 (3 × 40 mL). The combined organic layers were dried (Na_2SO_4) and concentrated, and the product was purified using column chromatography on silica (hexanes/CH_2Cl_2 8/2), to afford the pure product **1b** as a white powder (2.28 g, 82% overall yield): mp 263−265 °C. ^{1}H NMR (500 MHz, C_6D_6): δ 8.20 (s, 2H, aryl-H), 7.80−7.77 (m, 8H, aryl-H), 7.45−7.42 (m, 2H, aryl-H), 7.30−7.26 (m, 12H, aryl-H), 7.10−7.08 (m, 2H, aryl-H), 7.04−6.98 (m, 4H, aryl-H), 4.59 (s, 2H, OH), 2.09−2.02 (m, 4H, CH_2), 1.95−1.89 (m, 2H, CH_2), 1.78−1.71 (m, 6H, CH_2), 1.45−1.34 (m, 8H, CH_2), 1.23−1.16 (m, 2H, CH, Cy). $^{13}C\{^1H\}$ NMR (125 MHz, C_6D_6): δ 157.3 (CO), 141.4, 136.5, 135.2, 135.1, 135.0, 129.9, 124.2, 124.0, 110.3 (aryl), 29.2 (CH_2, Cy), 29.1 (CH_2, Cy), 28.84 (CH_2, Cy), 28.78 (CH_2, Cy), 27.4 (CH_2, Cy), 24.7 (CH, Cy). Anal. Calcd for $C_{56}H_{54}O_2Si_2$: C, 82.51; H, 6.68. Found: C, 82.31; H, 6.69.

((*R*)-3,3′-Bis(triisopropylsilyl)-1,1′-binaphthalene-2,2′-diol ((*R*)-H$_2$BINOL-TIPS; 1d). To a solution of (*R*)-3,3′-dibromo-1,1′-binaphthalene-2,2′-diol (1.50 g, 3.38 mmol) in DMF (20 mL) were added imidazole (0.70 g, 10.18 mmol) and chloro(triisopropyl)silane (1.63 g, 8.45 mmol). The resulting mixture was stirred at 90 °C overnight. The reaction was quenched by addition of saturated aqueous $NaHCO_3$ (10 mL), and the product was extracted with Et_2O (3 × 30 mL). The combined ether layers were washed with water (3 × 10 mL) and brine (10 mL) and dried ($MgSO_4$). The product was purified using column chromatography on silica (hexanes) to afford the crude bis(silyl ether) as a white powder (1.72 g, 67%) which was subjected to the next reaction without further purification. The crude bis(silyl ether) was dissolved in THF (25 mL), and *t*-BuLi (6.0 mL, 9.0 mmol, 1.5 M in pentane) was added dropwise at −50 °C. The yellow solution was warmed to room temperature slowly and was stirred for an additional 1 h. The reaction was quenched by addition of saturated aqueous NH_4Cl (10 mL), and the product was extracted with CH_2Cl_2 (3 × 20 mL). The combined organic layers were dried ($MgSO_4$). The product was purified using column chromatography on silica to afford the pure product **1d** as a light yellow powder (1.25 g, 63% overall yield). ^{1}H NMR (400 MHz, $CDCl_3$): δ 8.13 (s, 2H, aryl-H), 7.89 (d, ^3J(H,H) = 8.22 Hz, 2H, aryl-H), 7.38−7.23 (m, 4H, aryl-H), 7.10 (d, ^3J(H,H) = 8.22 Hz, 2H, aryl-H), 5.21 (s, 2H, OH), 1.64−1.51 (m, 6H, $CH(CH_3)_2$), 1.15−1.12 (m, 36H, $CH(CH_3)_2$). $^{13}C\{^1H\}$ NMR (125 MHz, $CDCl_3$): δ 157.2 (CO), 139.9, 134.1, 129.2, 128.6, 127.6, 124.5, 123.8, 123.6, 109.7 (aryl), 19.0 ($CH(CH_3)_2$), 11.7 ($CH(CH_3)_2$). Anal. Calcd for $C_{38}H_{54}O_2Si_2$: C, 76.19; H, 9.08. Found: C, 75.97; H, 9.14.

(*R*)-3,3′-Bis(dicyclohexylphenylsilyl)-1,1′-binaphtholene-2,2′-diol ((*R*)-H$_2$BINOL-SiCy$_2$Ph; 1e). To a solution of 3,3′-dibromo-1,1′-binaphthalene-2,2′-diol (500 mg, 1.13 mmol) in DMF (5 mL) was added imidazole (466 mg, 6.78 mmol) and chlorodicyclohexyl(phenyl)silane (1.50 g, ca. 77% purity, 3.67 mmol) at room temperature. The resulting mixture was stirred at 90 °C overnight. The reaction was quenched with a saturated aqueous $NaHCO_3$ solution (5 mL), and the product was extracted with CH_2Cl_2 (3 × 30 mL). The combined organic layers were dried ($NaSO_4$) and concentrated. The product was purified using column chromatography on silica (hexanes, then hexanes/CH_2Cl_2 9/1) to afford the crude bis(silyl ether) as a white powder (1.04 g, 94%), which was subjected to the next reaction without further purification. The bis(silyl ether) was dissolved in THF (30 mL), and *t*-BuLi (2.7 mL, 4.1 mmol, 1.6 M in pentane) was added dropwise at −60 °C. The bright yellow reaction mixture was warmed slowly to room temperature and was stirred for an additional 2 h. The reaction was quenched with a saturated aqueous NH_4Cl solution (5 mL) to obtain a clear solution. The organic layer was separated, and the product was extracted with CH_2Cl_2 (3 × 30 mL). The combined organic layers were dried (Na_2SO_4) and concentrated. The product was purified using column chromatography on silica (hexanes/ethyl acetate 95/5) to afford the pure product **1e** as a white powder (0.72 g, 80% overall yield). ^{1}H NMR (500 MHz, 25 °C, C_6D_6): δ 8.21 (s, 2H, aryl-H), 7.81 (d, ^3J(H,H) = 6.36 Hz, 4H, aryl-H), 7.54−7.46 (m, 2H, aryl-H), 7.46−7.29 (m, 6H, aryl-H), 7.22 (d, ^3J(H,H) = 7.83 Hz, 2H, aryl-H), 7.13−7.02 (m, 4H, aryl-H), 4.83 (s, 2H, OH), 2.16−1.90 (m, 8H, CH_2), 1.89−1.58 (m, 16H, CH_2), 1.55−1.27 (m, 12H, CH_2), 1.26−1.04 (m, 8H, CH_2 and CH). $^{13}C\{^1H\}$ NMR (125 MHz, 25 °C, C_6D_6): δ 157.5 (CO), 141.7, 136.2, 134.6, 134.5 129.6, 129.1, 129.0, 128.3, 128.1, 127.9, 127.8, 127.7, 123.9, 123.8, 123.6, 110.2 (aryl), 28.7 (CH_2), 28.6 (CH_2), 28.53 (CH_2), 28.50 (CH_2), 28.39 (CH_2), 28.33 (CH_2), 27.3 (CH_2), 27.2 (CH_2), 22.9 (CH, Cy), 22.6 (CH, Cy). Anal. Calcd for $C_{56}H_{66}O_2Si_2$: C, 81.30; H, 8.04. Found: C, 82.58; H, 8.29.

(*R*)-3,3′-Bis[diphenyl(*o*-tolyl)silyl]-1,1′-binaphthyl-2,2′-diol ((*R*)-H$_2$BINOL-DPTS; 1f). To a solution of (*R*)-3,3′-dibromo-2,2′-dihydroxy-1,1′-binaphthyl (2.11 g, 4.75 mmol) in THF (50 mL) was added KH (0.57 g, 14.2 mmol). The resulting mixture was stirred for

DOI: 10.1021/acs.organomet.8b00510
Organometallics XXXX, XXX, XXX−XXX

30 min at room temperature, and then chloro[diphenyl(*o*-tolyl)]silane (3.08 g, 10 mmol) was added. The reaction mixture was stirred for 4 days at 65 °C. To the reaction mixture was added *t*-BuLi (12 mL, 1.6 M in pentane, 19 mmol) dropwise at −60 °C over a period of 15 min, which was then allowed to slowly reach room temperature overnight. The solvent was removed in vacuo. The residue was dissolved in CH_2Cl_2 (70 mL), which was then treated with aqueous HCl solution (30 mL, 6 M). The organic layer was separated, dried over anhydrous Na_2SO_4, and evaporated. The product was purified using column chromatography on silica (hexanes/CH_2Cl_2 1/1) to afford pure product **1f** as a white powder (2.01 g, 51%). ^{1}H NMR (400 MHz, $CDCl_3$): δ 8.01 (s 2H, aryl-H), 7.77−7.69 (m, 2H, aryl-H), 7.68−7.58 (m, 8H, aryl-H), 7.43−7.35 (m, 8H, aryl-H), 7.34−7.28 (m, 10H, aryl-H), 7.24−7.18 (m, 4H, aryl-H), 7.15−7.06 (m, 2H, aryl-H), 5.25 (s, 2H, OH), 2.16 (s, 6H, aryl-CH_3). ^{13}C{^{1}H} NMR (100 MHz, $CDCl_3$): δ 156.6 (CO), 145.0, 141.5, 137.8, 136.5, 136.4, 134.87, 134.82, 134.7, 133.1, 130.3, 130.1, 129.51, 129.45, 129.2, 128.3, 128.00, 127.97, 125.3, 124.3, 124.05, 123.99, 110.9 (aryl), 24.2 (aryl-CH_3).

(*R*)-3,3′-Bis(tris(4-*tert*-butylphenyl)silyl)-1,1′-binaphthyl-2,2′-diol ((*R*)-H_2BINOL-TBPS; 1g). To a solution of (*R*)-3,3′-dibromo-2,2′-dihydroxy-1,1′-binaphthyl (0.74 g, 1.67 mmol) in THF (50 mL) was added KH (0.22 g, 5.5 mmol). The resulting mixture was stirred for 30 min at room temperature before bromotris(4-*tert*-butylphenyl)silane (2.12 g, 4.18 mmol) was added. The reaction mixture was heated for 5 days at 65 °C. The solvent was evaporated in vacuo. The residue was dissolved in CH_2Cl_2 (70 mL), which was then treated with aqueous HCl solution (30 mL, 6 M). The organic layer was separated, dried over anhydrous Na_2SO_4, and evaporated. The product was purified using column chromatography on silica (hexanes/CH_2Cl_2 8/1) to afford the crude bis(silyl ether) as a white powder (1.86 g, 86%), which was subjected to the next reaction without further purification. The bis(silyl ether) (1.01 g, 0.78 mmol) was dissolved in THF (40 mL), and *t*-BuLi (2 mL, 1.6 M in pentane, 3.2 mmol) was added dropwise at −60 °C. The reaction mixture was warmed to room temperature slowly and was stirred for an additional 5 h. The reaction was quenched with saturated aqueous NH_4Cl (5 mL) before the volatiles were removed in vacuo. The product was extracted with CH_2Cl_2 (5 × 20 mL). The organic layers were washed with brine (10 mL), dried over anhydrous Na_2SO_4, and evaporated. The product was purified using column chromatography on silica gel (hexanes/CH_2Cl_2 3/1) to afford the pure product **1g** (0.51 g, 50% overall yield). ^{1}H NMR (400 MHz, $CDCl_3$): δ 7.94 (s, 2H, aryl-H), 7.69 (d, ^3J(H,H) = 8 Hz, 2H, aryl-H), 7.59 (d, ^3J(H,H) = 8 Hz, 12H, aryl-H), 7.37 (d, ^3J(H,H) = 8 Hz, 12H, aryl-H), 7.32−7.21 (m, 6H, aryl-H), 5.32 (s, 2H, OH), 1.31 (s, 54H, C(CH_3)$_3$). ^{13}C{^{1}H} NMR (100 MHz, $CDCl_3$): δ 156.8 (CO), 152.2, 141.9, 136.2, 134.5, 131.0, 129.1, 129.0, 127.8, 124.7, 124.3, 124.0, 123.5, 110.9 (aryl), 34.7 (*C*(CH_3)$_3$), 31.3 (C(CH_3)$_3$). The data were in agreement with the literature.[35]

(*R*)-3,3′-Bis[4-methoxyphenyl(diphenyl)silyl]-2,2′-dihydroxy-1,1′-binaphthyl) ((*R*)-H_2BINOL-MPDPS; 1h). To a solution of (*R*)-3,3′-dibromo-1,1′-binaphthalene-2,2′-diol (400 mg, 0.90 mmol) in THF (20 mL) was added KH (80 mg, 2.0 mmol) with stirring. The mixture was stirred at room temperature for 30 min, and then chloro(4-methoxyphenyl)(diphenyl)silane (601 mg, 1.85 mmol) was added. The mixture was heated to 70 °C overnight. The reaction mixture was cooled to −78 °C, and to that was added dropwise *t*-BuLi (2.5 mL, 3.7 mmol, 1.5 M in pentane). The yellow solution was stirred for 5 min at −78 °C and was then allowed to reach room temperature slowly, after which it was stirred for an additional 1 h. The reaction was quenched with saturated aqueous NH_4Cl (50 mL), and the product was extracted with Et_2O (3 × 20 mL). The combined organic layers were dried (Na_2SO_4) and concentrated. The product was purified using column chromatography on silica (hexanes/CH_2Cl_2 70/30) to afford the pure product **1h** as a white powder (535 mg, 69% overall yield). ^{1}H NMR (400 MHz, $CDCl_3$): δ 7.97 (s, 2H, aryl-H), 7.76 (d, ^3J(H,H) = 7.8 Hz, 2H, aryl-H), 7.69 (d, ^3J(H,H) = 7.1 Hz, 8H, aryl-H), 7.63 (d, ^3J(H,H) = 8.6 Hz, 4H, aryl-H), 7.48−7.29 (m, 18H, aryl-H), 6.96 (d, ^3J(H,H) = 8.2 Hz, 4H, aryl-H), 5.36 (s, 2H, OH), 3.87 (s, 6H, OCH_3). ^{13}C{^{1}H} NMR (100 MHz, $CDCl_3$): δ 160.8 (CO), 156.5 (CO), 142.0, 137.9, 136.2, 134.7, 134.6, 129.4, 129.2, 129.0, 128.1, 127.8, 124.8, 123.93, 123.91, 123.8, 113.6, 110.7 (aryl), 55.0 (CH_3O).

(*R*)-3,3′-Bis(benzyldiphenylsilyl)-2,2′-dihydroxy-1,1′-binaphthyl ((*R*)-H_2BINOL-SiBnPh_2; 1i). This compound was prepared as reported previously.[37a] To a solution of (*R*)-3,3′-dibromo-2,2′-dihydroxy-1,1′-binaphthyl (0.800 g, 1.8 mmol) in THF (25 mL) was carefully added KH (0.148 g, 3.7 mmol) in two portions with stirring. The resulting yellow solution was stirred at room temperature for 30 min, and then benzylchlorodiphenylsilane (1.17 g, 3.8 mmol) was added. The mixture was stirred at room temperature for 16 h. Then cold H_2O (15 mL) was added carefully and the mixture stirred for 10 min. The organic layer was separated, and the aqueous layer was extracted with CH_2Cl_2. The combined organic layers were dried over Na_2SO_4. The solvent was removed by rotary evaporation, and the residue was flashed through a short Al_2O_3 pad. Removal of the solvent produced the silyl ether in quantitative yield (1.60 g), which was used without further purification. A solution of the silyl ether in THF (40 mL) was cooled to −80 °C, and *t*-BuLi (4.1 mL, 1.6 M in pentane, 6.56 mmol) was added dropwise over the course of 45 min. The reaction mixture was allowed to reach room temperature overnight. The reaction mixture was quenched with saturated aqueous NH_4Cl (30 mL) and stirred for 10 min. The organic layer was separated, and the aqueous layer was extracted with Et_2O. The combined organic layers were dried (Na_2SO_4) and concentrated. The product was purified using column chromatography on silica (hexanes/CH_2Cl_2 2/1) to afford the pure product **1i** as a white powder (0.70 g, 47%). ^{1}H NMR (400 MHz, 25 °C, C_6D_6): δ 8.11 (s, 2H, aryl-H), 7.71−7.59 (m, 8H, aryl-H), 7.38−7.32 (d, ^3J(H,H) = 7.9 Hz, 2H, aryl-H,), 7.31−6.90 (m, 28H, aryl-H), 4.83 (s, 2H, OH), 3.22 (d, ^2J(H,H) = 13.8 Hz, 2H, CH_2), 3.16 (d, ^2J(H,H) = 13.8 Hz, 2H, CH_2). ^{13}C{^{1}H} NMR (125 MHz, C_6D_6): δ 157.2 (CO), 142.0, 139.3, 136.40, 136.35, 135.3, 135.06, 135.01, 129.82, 129.78, 129.6, 129.4, 128.43, 128.38, 128.29, 128.14, 128.08, 124.9, 124.18, 124.14, 110.6 (aryl), 23.9 ($SiCH_2$). Anal. Calcd for $C_{58}H_{46}O_2Si_2$: C, 83.81; H, 5.58; Found: C, 83.71; H, 5.33.

(*R*)-[Y{BINOL-PDBS}(*o*-$C_6H_4CH_2NMe_2$)(Me_2NCH_2Ph)] ((*R*)-2a-Y). To a mixture of (*R*)-**H_2BINOL-PDBS** (**1a**; 24.0 mg, 0.03 mmol) and [Y(*o*-$C_6H_4CH_2NMe_2)_3$] (14.8 mg, 0.03 mmol) was added C_6D_6 (0.70 mL). The mixture was kept at room temperature for 1 h. ^{1}H and ^{13}C NMR spectra showed clean formation of (*R*)-**2a-Y**, which was used directly for catalytic experiments. ^{1}H NMR (500 MHz, 25 °C, C_6D_6): δ 8.56 (s, 2H, aryl-H), 8.37−8.24 (m, 2H, aryl-H), 7.98 (m, 2H, aryl-H), 7.92 (m, 2H, aryl-H), 7.82 (d, ^3J(H,H) = 7.83 Hz, 2H, aryl-H), 7.76 (d, ^3J(H,H) = 7.58 Hz, 1H, aryl-H), 7.71 (d, ^3J(H,H) = 7.83 Hz, 1H, aryl-H), 7.63 (d, ^3J(H,H) = 7.58 Hz, 1H, aryl-H), 7.57 (m, 1H, aryl-H), 7.48 (t, ^3J(H,H) = 7.58 Hz, 2H, aryl-H), 7.43−6.81 (m, 28H, aryl-H including free $PhCH_2NMe_2$), 6.76 (q, ^3J(H,H) = 7.42 Hz, 3H, aryl H), 6.50 (t, ^3J(H,H) = 7.21 Hz, 1H, aryl-H), 6.41 (d, ^3J(H,H) = 7.58 Hz, 2H, aryl-H), 3.80 (d, ^2J(H,H) = 14.43 Hz, 1H, *o*-$C_6H_4CH_2Me_2$), 3.23 (m, 4H, free and coordinated $PhCH_2NMe_2$), 2.05 (s, 6H, free $PhCH_2NMe_2$), 2.67 (d, ^2J(H,H) = 14.43 Hz, 1H, *o*-$C_6H_4CH_2NMe_2$), 1.48 (s, 3H, N(CH_3)$_2$), 1.42 (s, 3H, N(CH_3)$_2$), 1.23 (s, 3H, N(CH_3)$_2$), 1.15 (s, 3H, N(CH_3)$_2$). ^{13}C{^{1}H} NMR (125 MHz, 25 °C, C_6D_6): δ 182.2 (d, ^1J(Y,C) = 53.5 Hz), 162.3 (CO), 161.8 (CO), 149.30, 149.25, 149.1, 148.4, 140.6, 140.4, 140.0, 139.5, 139.4, 138.3, 138.0, 137.64, 137.61, 137.4, 135.8, 135.7, 135.6, 135.4, 135.2, 135.0, 134.3, 131.7, 131.0, 130.9, 130.0, 129.9, 129.5, 129.3, 129.10, 129.08, 129.0, 128.8, 128.7, 128.6, 128.53, 128.45, 128.4, 128.3, 127.7, 127.2, 126.4, 126.3, 125.7, 125.2, 122.93, 122.89, 122.7, 121.7, 121.3, 117.6, 116.3 (aryl), 67.9 (*o*-$C_6H_4CH_2NMe_2$), 64.5 (s, free $PhCH_2NMe_2$), 58.2 ($PhCH_2NMe_2$), 47.2 (N(CH_3)$_2$), 45.4 (s, free $PhCH_2NMe_2$), 44.1 (N(CH_3)$_2$), 40.51 ($PhCH_2NMe_2$), 40.45 ($PhCH_2NMe_2$).

(*R*)-[Lu{BINOL-PDBS}(*o*-$C_6H_4CH_2NMe_2$)(Me_2NCH_2Ph)] ((*R*)-2a-Lu). To a mixture of (*R*)-**H_2BINOL-PDBS** (**1a**; 25.5 mg, 0.032 mmol) and [Lu(*o*-$C_6H_4CH_2NMe_2)_3$] (18.4 mg, 0.032 mmol) was added C_6D_6 (0.80 mL). The mixture was kept at room temperature for 1 h. ^{1}H and ^{13}C NMR spectra showed clean formation of (*R*)-**2a-**

DOI: 10.1021/acs.organomet.8b00510
Organometallics XXXX, XXX, XXX−XXX

Lu, which was used directly for catalytic experiments. ^{1}H NMR (400 MHz, 25 °C, C_6D_6): δ 8.63 (s, 1H, aryl-H), 8.61 (s, 1H, aryl-H), 8.33 (d, ^3J(H,H) = 7.04 Hz, 1H), 8.26 (d, ^3J(H,H) = 7.04 Hz, 1H), 8.05 (m, 2H, aryl-H), 7.99 (d, ^3J(H,H) = 6.65 Hz, 1H, aryl-H), 7.91 (m, 2H, aryl-H), 7.80 (m, 5H, aryl-H), 7.69 (d, ^3J(H,H) = 7.43 Hz, 1H, aryl-H), 7.63 (m, 1H, aryl-H), 7.54 (m, 2H, aryl-H), 7.48 (t, ^3J(H,H) = 7.04 Hz, 1H, aryl-H), 7.44−6.84 (m, 24H, aryl-H including free $PhCH_2NMe_2$), 6.80 (m, 4H), 6.54 (t, ^3J(H,H) = 7.24 Hz, 1H, aryl-H), 6.44 (d, ^3J(H,H) = 7.04 Hz, 2H, aryl-H), 3.81 (d, ^2J(H,H) = 14.48 Hz, 1H, o-$C_6H_4CH_2NMe_2$), 3.36 (s, 2H, $PhCH_2NMe_2$), 3.27 (s, 2H, free $PhCH_2NMe_2$), 2.67 (d, ^2J(H,H) = 14.48 Hz, 1H, o-$C_6H_4CH_2NMe_2$), 2.09 (s, 6H, CH_3 of free $PhCH_2NMe_2$), 1.49 (s, 3H, $N(CH_3)_2$), 1.43 (s, 3H, $N(CH_3)_2$), 1.30 (s, 3H, $N(CH_3)_2$), 1.24 (s, 3H, $N(CH_3)_2$). ^{13}C{^{1}H} NMR (100 MHz, 25 °C, C_6D_6): δ 191.3 (C-Lu), 162.7 (CO), 162.2 (CO), 149.4, 149.3, 149.2, 148.8, 140.2, 139.9, 139.6, 139.4, 137.7, 137.3, 135.9, 135.7, 135.5, 135.2, 135.1, 131.8, 130.9, 129.9, 129.5, 129.1, 128.9, 128.7, 128.5, 127.6, 127.5, 127.2, 126.62, 126.59, 126.0, 125.7, 125.0, 122.8, 122.7, 121.7, 121.5, 121.3, 117.3, 116.3 (aryl), 67.3 (o-$C_6H_4CH_2NMe_2$), 64.5 (s, free $PhCH_2NMe_2$), 58.4 ($PhCH_2NMe_2$), 47.8 ($N(CH_3)_2$), 46.2 ($N(CH_3)_2$), 45.4 (s, free $PhCH_2NMe_2$), 44.5 ($N(CH_3)_2$), 40.84 ($PhCH_2NMe_2$), 40.78 ($PhCH_2NMe_2$).

(*R*)-[Y{BINOL-SiCyPh$_2$}(o-C$_6$H$_4$CH$_2$NMe$_2$)(Me$_2$NCH$_2$Ph)] ((*R*)-2b-Y). This complex was prepared as reported previously.[14b] To a mixture of (*R*)-**H$_2$BINOL-SiCyPh$_2$** (**1b**; 48.9 mg, 0.06 mmol) and [Y(o-$C_6H_4CH_2NMe_2)_3$] (29.3 mg, 0.06 mmol) was added C_6D_6 (0.55 mL). The mixture was kept at room temperature for 1 h. ^{1}H and ^{13}C NMR showed clean formation of (*R*)-**2b-Y**, which was used directly for catalytic experiments. ^{1}H NMR (500 MHz, 25 °C, C_6D_6): δ 8.48 (s, 1H, aryl-H), 8.47 (s, 1H, aryl-H), 7.94−7.91 (m, 2H, aryl-H), 7.29−7.87 (m, 4H, aryl-H), 7.87−7.82 (m, 2H, aryl-H), 7.70−7.68 (m, 1H, aryl-H), 7.65 (d, ^3J(H,H) = 6.9 Hz, 1H, aryl-H), 7.60 (d, ^3J(H,H) = 8.0 Hz, 1H, aryl-H), 7.55 (m, 2H, aryl-H), 7.34−6.94 (m, 26H, aryl-H including free $PhCH_2NMe_2$), 6.80 (d, ^3J(H,H) = 7.3 Hz, 1H, aryl-H), 6.67 (m, 2H, aryl-H), 3.25 (s, 2H, free $PhCH_2NMe_2$), 3.13 (d, ^2J(H,H) = 13.9 Hz, 1H, o-$C_6H_4CH_2NMe_2$), 2.99 (d, ^2J(H,H) = 13.2 Hz, 1H, $PhCH_2NMe_2$), 2.93 (d, ^2J(H,H) = 13.2 Hz, 1H, $PhCH_2NMe_2$), 2.33 (d, ^2J(H,H) = 13.9 Hz, 1H, o-$C_6H_4CH_2NMe_2$), 2.28−2.12 (m, 6H), 2.09 (s, 6H, free $PhCH_2NMe_2$), 1.76−1.60 (m, 10H), 1.44−1.26 (m, 12H), 1.06−0.97 (m, 6H). ^{13}C{^{1}H} NMR (125 MHz, 25 °C, C_6D_6): δ 181.5 (d, ^1J(Y,C) = 53.5 Hz), 163.5 (CO), 162.5 (CO), 148.8, 140.1, 140.0, 139.2, 139.1, 138.3, 136.9, 136.7, 136.2, 135.72, 135.67, 135.57, 135.46, 131.8, 130.3, 129.3, 129.2, 129.1, 128.8, 128.7, 128.51, 128.45, 128.38, 128.29, 127.9, 127.2, 126.0, 125.8, 125.6, 125.5, 124.8, 122.54, 122.48, 116.93, 116.85 (aryl), 67.6 (CH_2), 64.5 (s, free $PhCH_2NMe_2$), 57.9 ($PhCH_2NMe_2$), 46.1 ($N(CH_3)_2$), 45.4 (s, free $PhCH_2NMe_2$), 43.6 ($N(CH_3)_2$), 40.5 ($PhCH_2NMe_2$), 40.2 ($PhCH_2NMe_2$), 29.0 (CH_2, Cy), 28.9 (CH_2, Cy), 28.8 (CH_2, Cy), 28.6 (2C, CH_2, Cy), 28.5 (CH_2, Cy), 27.9 (CH_2, Cy), 27.8 (CH_2, Cy), 27.21 (CH_2, Cy), 27.20 (CH_2, Cy), 23.7 (CH, Cy), 23.4 (CH, Cy).

(*R*)-[Lu{BINOL-SiCyPh$_2$}(o-C$_6$H$_4$CH$_2$NMe$_2$)(Me$_2$NCH$_2$Ph)] ((*R*)-2b-Lu). To a mixture of (*R*)-**H$_2$BINOL-SiCyPh$_2$** (**1b**; 24.9 mg, 0.031 mmol) and [Lu(o-$C_6H_4CH_2NMe_2)_3$] (17.6 mg, 0.031 mmol) was added C_6D_6 (0.50 mL). The mixture was kept at room temperature for 1.5 h. ^{1}H and ^{13}C NMR spectra showed clean formation of (*R*)-**2b-Lu**, which was used directly for catalytic experiments. ^{1}H NMR (500 MHz, 25 °C, C_6D_6): δ 8.51 (s, 1H, aryl-H), 8.50 (s, 1H, aryl-H), 8.06−7.80 (m, 8H, aryl-H), 7.66 (dd, ^3J(H,H) = 6.11 Hz, ^4J(H,H) = 3.18 Hz, 1H, aryl-H), 7.47−7.30 (m, 3H, aryl-H), 7.30−6.90 (m, 27H, aryl-H including free $PhCH_2NMe_2$), 6.85 (d, ^3J(H,H) = 7.34 Hz, 1H, aryl-H), 6.68 (dd, ^3J(H,H) = 7.34 Hz, ^4J(H,H) = 1.96 Hz, 2H, aryl-H), 3.27 (s, 2H, free $PhCH_2NMe_2$), 3.08 (d, ^2J(H,H) = 14.2 Hz, 1H, o-$C_6H_4CH_2Me_2$), 2.99 (d, ^2J(H,H) = 13.2 Hz, 1H, $PhCH_2NMe_2$), 2.94 (d, ^2J(H,H) = 13.2 Hz, 1H, $PhCH_2NMe_2$), 2.21 (d, ^2J(H,H) = 13.9 Hz, 1H, o-$C_6H_4CH_2NMe_2$), 2.20−2.08 (m, 6H), 2.09 (s, 6H, free $PhCH_2NMe_2$), 1.80−1.55 (m, 10H), 1.52−1.25 (m, 12H), 1.11−0.85 (m, 6H). ^{13}C{^{1}H} NMR (125 MHz, 25 °C, C_6D_6): δ 191.0 (C-Lu), 164.0 (CO), 163.0 (CO), 149.3, 140.0, 139.6, 139.5, 139.37, 139.33, 139.2, 136.9, 136.7, 136.2, 135.6, 135.5, 131.9, 130.1, 129.3, 129.2, 129.1, 128.9, 128.7, 128.6, 128.53, 128.48, 128.4, 128.3, 128.2, 127.2, 127.1, 127.0, 126.2, 125.9, 125.8, 125.2, 122.4, 122.3, 116.8, 115.9 (aryl), 66.9 (CH_2), 64.5 (s, free $PhCH_2NMe_2$), 57.7 ($PhCH_2NMe_2$), 46.4 ($N(CH_3)_2$), 45.4 (s, free $PhCH_2NMe_2$), 43.8 ($N(CH_3)_2$), 40.9 ($PhCH_2NMe_2$), 40.3 ($PhCH_2NMe_2$), 29.0 (CH_2, Cy), 28.9 (CH_2, Cy), 28.8 (CH_2, Cy), 28.6 (3C, CH_2, Cy), 27.9 (CH_2, Cy), 27.8 (CH_2, Cy), 27.2 (2C, CH_2, Cy), 23.6 (CH, Cy), 23.4 (CH, Cy).

(*R*)-[Y{BINOL-TBDPS}(o-C$_6$H$_4$CH$_2$NMe$_2$)(Me$_2$NCH$_2$Ph)] ((*R*)-2c-Y). This complex was prepared as reported previously.[14b] To a mixture of (*R*)-**BINOL-TBDPS** (**1c**; 45.6 mg, 0.06 mmol) and [Y(o-$C_6H_4CH_2NMe_2)_3$] (29.3 mg, 0.06 mmol) was added toluene-d_8 (0.55 mL). The mixture was kept at room temperature for 1 h. ^{1}H and ^{13}C NMR showed clean formation of (*R*)-**2c-Y**, which was used directly for catalytic experiments. ^{1}H NMR (125 MHz, 0 °C, toluene-d_8): δ 8.55 (s, 1H, aryl-H), 8.52 (s, 1H, aryl-H), 8.07 (d, ^3J(H,H) = 8.1 Hz, 2H, aryl-H), 7.95 (m, 1H, aryl-H), 7.93 (m, 1H, aryl-H), 7.89−7.84 (m, 4H, aryl-H), 7.57 (d, ^3J(H,H) = 6.9 Hz, 1H, aryl-H), 7.55 (d, ^3J(H,H) = 8.1 Hz, 1H, aryl-H), 7.48−7.46 (m, 1H, aryl-H), 7.34−6.94 (m, 28H, aryl-H, including 5H from free $PhCH_2NMe_2$), 6.77 (d, ^3J(H,H) = 7.6 Hz, 1H, aryl-H), 6.62 (d, ^3J(H,H) = 6.9 Hz, 2H, aryl-H), 3.44 (d, ^2J(H,H) = 13.9 Hz, 1H, o-$C_6H_4CH_2NMe_2$), 3.20 (s, 2H, free $PhCH_2NMe_2$), 3.09 (br s, 2H, $PhCH_2NMe_2$), 2.52 (d, ^2J(H,H) = 13.2 Hz, 1H, o-$C_6H_4CH_2NMe_2$), 2.05 (s, 6H, free $PhCH_2NMe_2$), 1.44 (s, 9H, *t*-Bu), 1.41 (s, 3H, o-$C_6H_4CH_2NMe_2$), 1.39 (s, 9H, *t*-Bu), 1.29 (s, 3H, $PhCH_2NMe_2$), 1.24 (s, 3H, $PhCH_2NMe_2$), 1.19 (s, 3H, o-$C_6H_4CH_2NMe_2$). ^{13}C{^{1}H} NMR (125 MHz, 0 °C, toluene-d_8): δ 181.9 (d, ^1J (Y,C) = 52.6 Hz), 163.4 (CO), 162.8 (CO), 148.3, 141.4, 141.2, 139.3, 138.9, 138.3, 137.18, 137.15, 136.83, 136.75, 136.71, 136.68, 136.5, 131.9, 130.0, 129.7, 129.3, 129.24, 129.23, 128.82, 128.76, 128.6, 128.4, 128.3, 128.2, 128.1, 127.7, 127.5, 127.4, 127.2, 126.0, 125.8, 125.6, 125.5, 122.6, 122.4, 117.18, 117.15 (aryl), 68.0 (o-$C_6H_4CH_2NMe_2$), 64.5 (s, free $PhCH_2NMe_2$), 58.0 ($PhCH_2NMe_2$), 46.8 ($N(CH_3)_2$), 45.4 (s, free $PhCH_2NMe_2$), 44.2 ($N(CH_3)_2$), 40.4 ($PhCH_2NMe_2$), 40.3 ($PhCH_2NMe_2$), 29.7 ($C(CH_3)_3$), 29.4 ($C(CH_3)_3$), 19.7 ($C(CH_3)_3$), 19.6 ($C(CH_3)_3$).

(*R*)-[Lu{BINOL-TBDPS}(o-C$_6$H$_4$CH$_2$NMe$_2$)(Me$_2$NCH$_2$Ph)] ((*R*)-2c-Lu). To a mixture of (*R*)-**H$_2$BINOL-TBDPS** (**1c**; 22.9 mg, 0.030 mmol) and [Lu(o-$C_6H_4CH_2NMe_2)_3$] (17.3 mg, 0.030 mmol) was added C_6D_6 (0.50 mL). The mixture was kept at room temperature for 1.5 h. ^{1}H and ^{13}C NMR spectra showed clean formation of (*R*)-**2c-Lu**, which was used directly for catalytic experiments. ^{1}H NMR (400 MHz, 25 °C, C_6D_6): δ 8.63 (s, 2H, aryl-H), 8.12 (d, ^3J(H,H) = 6.65 Hz, 2H, aryl-H), 8.04 (d, ^3J(H,H) = 6.26 Hz, 2H, aryl-H), 7.98−7.89 (m, 4H, aryl-H), 7.76−7.62 (m, 2H, aryl-H), 7.56 (d, ^3J(H,H) = 7.04 Hz, 1H, aryl-H), 7.41−7.28 (m, 3H, aryl-H), 7.06 (m, 25H, aryl-H including free $PhCH_2NMe_3$), 6.86 (d, ^3J(H,H) = 7.43 Hz, 1H, aryl-H), 6.68 (d, ^3J(H,H) = 6.65 Hz, 2H, aryl-H), 3.36 (d, ^2J(H,H) = 14.09 Hz, 1H, o-$C_6H_4CH_2NMe_2$), 3.27 (s, 2H, free $PhCH_2NMe_2$), 3.20 (d, ^2J(H,H) = 13.7 Hz, 1H, $PhCH_2NMe_2$), 3.13 (d, ^2J(H,H) = 13.3 Hz, 1H, $PhCH_2NMe_2$), 2.50 (d, ^2J(H,H) = 14.09 Hz, 1H, o-$C_6H_4CH_2NMe_2$), 2.09 (s, 6H, free $PhCH_2NMe_2$), 1.47 (s, 9H, *t*-Bu), 1.44 (s, 3H, o-$C_6H_4CH_2NMe_2$), 1.42 (s, 9H, *t*-Bu), 1.35 (s, 3H, $PhCH_2NMe_2$), 1.28 (s, 3H, $PhCH_2NMe_2$), 1.21 (s, 3H, o-$C_6H_4CH_2NMe_2$). ^{13}C{^{1}H} NMR (100 MHz, 25 °C, C_6D_6): δ 191.4 (C-Lu), 163.7 (CO), 163.5 (CO), 148.8, 140.79, 140.76, 140.65, 140.62, 140.0, 139.67, 139.63, 139.4, 139.2, 137.3, 137.2, 136.9 136.8 136.64, 136.55, 132.0, 129.9, 129.1, 128.9, 128.8, 128.7, 128.5, 128.37, 128.32, 127.5, 127.4, 127.3, 127.2, 126.1, 125.9, 125.2, 122.3, 117.4, 116.9 (aryl), 67.3 (o-$C_6H_4CH_2Me_2$), 64.5 (s, free $PhCH_2NMe_2$), 58.0 ($PhCH_2Me_2$), 46.9 ($N(CH_3)_2$), 45.4 (s, free $PhCH_2NMe_2$), 44.3 ($N(CH_3)_2$), 40.7 ($PhCH_2NMe_2$), 29.5 ($C(CH_3)_3$), 29.4 ($C(CH_3)_3$), 19.6 ($C(CH_3)_3$), 19.5 ($C(CH_3)_3$).

(*R*)-[Y{BINOL-TIPS}(o-C$_6$H$_4$CH$_2$NMe$_2$)(Me$_2$NCH$_2$Ph)] ((*R*)-2d-Y). To a mixture of (*R*)-**H$_2$BINOL-TIPS** (**1d**; 16.2 mg, 0.027 mmol) and [Y(o-$C_6H_4CH_2NMe_2)_3$] (13.3 mg, 0.027 mmol) was added C_6D_6 (0.50 mL). The mixture was kept at room temperature for 1 h. ^{1}H and ^{13}C NMR spectra showed clean formation of (*R*)-**2d-Y**, which was used directly for catalytic experiments. ^{1}H NMR (400 MHz, 25 °C, C_6D_6): δ 8.42 (s, 1H, aryl-H), 8.39 (s, 1H, aryl-H), 8.10

DOI: 10.1021/acs.organomet.8b00510
Organometallics XXXX, XXX, XXX−XXX

(d, ^3J(H,H) = 6.60 Hz, 1H, aryl-H), 8.02−7.78 (m, 3H, aryl-H), 7.66−6.94 (m, 18H, aryl-H including free $PhCH_2NMe_3$), 4.28−4.01 (br m, 3H), 3.69−3.36 (br m, 3H), 2.48−2.14 (m, 9H), 2.14−2.07 (s, 4H), 2.07−1.90 (m, 6H, $CH(CH_3)_2$), 1.89−1.80 (m, 2H), 1.77 (s, 3 H, $N(CH_3)_2$), 1.71−0.90 (m, 36H, $CH(CH_3)_2$). $^{13}C\{^1H\}$ NMR (100 MHz, 25 °C, C_6D_6): δ 181.5 (d, ^1J(Y,C) = 53.1 Hz), 163.9 (CO), 163.3 (CO), 148.2, 140.8, 140.5, 138.9, 138.5, 138.2, 131,7, 130.5, 129.5, 129.1, 128.7, 128.6, 127.24, 127.19, 126.3, 125.7, 125.6, 125.4, 125.2, 122.8, 122.6, 117.0, 116.6 (aryl), 68.5 (o-$C_6H_4CH_2NMe_2$), 64.5 (s, free $PhCH_2NMe_2$), 59.7 ($PhCH_2NMe_2$), 47.0 ($N(CH_3)_2$), 45.4 (s, free $PhCH_2NMe_2$), 44.7 ($N(CH_3)_2$), 41.9 ($PhCH_2NMe_2$), 19.9 (3C, $CH(CH_3)_2$), 19.8 (3C, $CH(CH_3)_2$), 19.7 (6C, $CH(CH_3)_2$), 12.8 (3C, $CH(CH_3)_2$), 12.7 (3C, $CH(CH_3)_2$).

(*R*)-[Lu{BINOL-TIPS}(o-$C_6H_4CH_2NMe_2$)(Me_2NCH_2Ph)] ((*R*)-2d-Lu). To a mixture of (*R*)-**H_2BINOL-TIPS** (**1d**; 15.0 mg, 0.025 mmol) and [Lu(o-$C_6H_4CH_2NMe_2)_3$] (14.4 mg, 0.025 mmol) was added C_6D_6 (0.50 mL). The mixture was kept at room temperature for 1 h. ^1H and ^{13}C NMR spectra showed clean formation of (*R*)-**2d-Lu**, which was used directly for catalytic experiments. ^1H NMR (400 MHz, 25 °C, C_6D_6): δ 8.45 (s, 1H, aryl-H), 8.43 (s, 1H, aryl-H), 8.21 (d, ^3J(H,H) = 6.26 Hz, 1H, aryl-H), 8.13−7.83 (m, 2H, aryl-H), 7.82−6.78 (m, 19H, aryl-H including free $PhCH_2NMe_3$), 4.24 (br s, 2H), 4.08 (d, ^2J(H,H) = 13.7 Hz, 1H, o-$C_6H_4CH_2NMe_2$), 3.51 (br m, 3H including free $PhCH_2NMe_2$), 2.32 (s, 6H), 2.20 (s, 3H), 2.10 (s, 6H, free $PhCH_2NMe_2$), 2.07−1.94 (m, 6H, $CH(CH_3)_2$), 1.85 (s, 3H, $N(CH_3)_2$), 1.80−1.02 (m, 36H, $CH(CH_3)_2$). $^{13}C\{^1H\}$ NMR (100 MHz, 25 °C, C_6D_6): δ 190.2 (C-Lu), 163.9 (CO), 163.3 (CO), 148.3, 139.8, 139.7, 139.4, 138.8, 138.5, 131.6, 129.6, 128.9, 128.4, 128.2, 126.9, 126.84, 126.80, 126.2, 125.8, 125.6, 125.5, 125.3, 122.3, 122.1, 116.5, 116.4 (aryl), 67.5 (o-$C_6H_4CH_2NMe_2$), 64.3 (s, free $PhCH_2NMe_2$), 59.4 ($PhCH_2NMe_2$), 47.0 ($N(CH_3)_2$), 45.1 (s, free $PhCH_2NMe_2$), 44.7 ($N(CH_3)_2$), 41.8 ($PhCH_2NMe_2$), 19.6 ($CH(CH_3)_2$), 19.51 ($CH(CH_3)_2$), 19.46 ($CH(CH_3)_2$), 19.45 ($CH(CH_3)_2$), 12.7 ($CH(CH_3)_2$), 12.6 ($CH(CH_3)_2$).

(*R*)-[Y{BINOL-SiCy$_2$Ph}(o-$C_6H_4CH_2NMe_2$)(Me_2NCH_2Ph)] ((*R*)-2e-Y). To a mixture of (*R*)-**H_2BINOL-SiCy$_2$Ph** (**1e**; 51.0 mg, 0.061 mmol) and [Y(o-$C_6H_4CH_2NMe_2)_3$] (29.9 mg, 0.061 mmol) was added C_6D_6 (0.60 mL). The mixture was kept at room temperature for 1 h. ^1H and ^{13}C NMR spectra showed clean formation of (*R*)-**2e-Y**, which was used directly for catalytic experiments. ^1H NMR (500 MHz, 6 °C, C_6D_6): δ 8.29 (s, 2H, aryl-H), 7.83 (d, ^3J(H,H) = 6.85 Hz, 2H, aryl-H), 7.75 (d, ^3J(H,H) = 6.85 Hz, 2H, aryl-H), 7.58 (d, ^3J(H,H) = 7.34 Hz, 2H, aryl-H), 7.38−7.27 (m, 4H, aryl-H), 7.26−6.89 (m, 20H, aryl-H including free $PhCH_2NMe_2$), 6.87−6.76 (m, 2H, aryl-H), 3.86 (d, ^2J(H,H) = 13.94 Hz, 1H, o-$C_6H_4CH_2NMe_2$), 3.49 (d, ^2J(H,H) = 13.45 Hz, 1H, $PhCH_2NMe_2$), 3.32 (d, ^2J(H,H) = 13.45 Hz, 1H, $PhCH_2NMe_2$), 3.23 (s, 2H, free $PhCH_2NMe_2$), 3.08 (d, ^2J(H,H) = 13.94 Hz, 1H, o-$C_6H_4CH_2NMe_2$), 2.42−2.25 (m, 4H, Cy), 2.22−2.08 (m, 6H, Cy), 2.05 (s, 6H, free $PhCH_2NMe_2$), 2.01−1.08 (m, 50H, Cy and $N(CH_3)_2$). $^{13}C\{^1H\}$ NMR (125 MHz, 6 °C, C_6D_6): δ 181.5 (d, ^1J(Y,C) = 53.5 Hz), 163.1 (CO), 162.8 (CO), 148.3, 141.2, 140.00, 139.97, 139.0, 138.6, 138.4, 137.7, 136.3, 135.7, 131.8, 130.3, 129.4, 129.3, 129.1, 128.8, 128.6, 128.5, 128.3, 127.9, 127.8, 127.3, 126.2, 125.8, 125.5, 125.3, 125.2, 122.8, 122.6, 116.6, 116.4 (aryl), 68.2 (o-$C_6H_4CH_2NMe_2$), 64.5 (s, free $PhCH_2NMe_2$), 58.2 ($PhCH_2NMe_2$), 47.0 ($N(CH_3)_2$), 45.4 (s, free $PhCH_2NMe_2$), 44.7 ($N(CH_3)_2$), 40.9, 40.7 ($PhCH_2NMe_2$), 29.6, 29.29, 29.25, 29.22, 29.14, 29.05, 28.95, 28.88, 28.84, 28.72, 28.65, 28.62, 28.3, 27.7, 27.5, 27.4, 27.3 (CH_2, Cy), 24.4, 24.1, 23.9, 23.0 (CH, Cy).

(*R*)-[Lu{BINOL-SiCy$_2$Ph}(o-$C_6H_4CH_2NMe_2$)(Me_2NCH_2Ph)] ((*R*)-2e-Lu). To a mixture of (*R*)-**H_2BINOL-SiCy$_2$Ph** (**1e**; 25.9 mg, 0.031 mmol) and [Lu(o-$C_6H_4CH_2NMe_2)_3$] (18.1 mg, 0.031 mmol) was added C_6D_6 (0.50 mL). The mixture was kept at room temperature for 1 h. ^1H and ^{13}C NMR spectra showed clean formation of (*R*)-**2e-Lu**, which was used directly for catalytic experiments. ^1H NMR (500 MHz, 7 °C, C_6D_6): δ 8.34 (s, 1H, aryl-H), 8.32 (s, 1H, aryl-H), 7.93 (d, ^3J(H,H) = 6.60 Hz, 2H, aryl-H), 7.85 (d, ^3J(H,H) = 7.09 Hz, 2H, aryl-H), 7.79 (d, ^3J(H,H) = 7.09 Hz, 2H, aryl-H), 7.68−7.60 (m, 6H, aryl-H), 7.46−6.92 (m, 18H, aryl-H including free $PhCH_2NMe_2$), 6.91−6.81 (m, 2H, aryl-H), 3.79 (d, ^2J(H,H) = 13.94 Hz, 1H, o-$C_6H_4CH_2NMe_2$), 3.52 (d, ^2J(H,H) = 13.21 Hz, 1H, $PhCH_2NMe_2$), 3.33 (d, ^2J(H,H) = 13.45 Hz, 1H, $PhCH_2NMe_2$), 3.25 (s, 2H, free $PhCH_2NMe_2$), 3.01 (d, ^2J(H,H) = 13.94 Hz, 1H, o-$C_6H_4CH_2NMe_2$), 2.45−2.29 (m, 2H), 2.29−2.09 (m, 10H), 2.07 (s, 6H, free $PhCH_2NMe_2$), 2.04−1.03 (m, 43H, Cy and $N(CH_3)_2$). $^{13}C\{^1H\}$ NMR (125 MHz, 7 °C, C_6D_6): δ 190.6 (C-Lu), 163.5 (CO), 163.3 (CO), 148.7, 140.3, 139.9, 139.1, 138.8, 136.8, 136.4, 135.8, 132.0, 130.1, 129.1, 128.8, 128.7, 128.5, 127.2, 127.1, 126.4, 126.1, 125.8, 125.7, 116.5, 116.3 (aryl), 67.4 (o-$C_6H_4CH_2NMe_2$), 64.5 (s, free $PhCH_2NMe_2$), 58.1 ($PhCH_2NMe_2$), 47.3, 46.1 ($N(CH_3)_2$), 45.4 (s, free $PhCH_2NMe_2$), 44.8, 41.2, 40.9 ($N(CH_3)_2$), 29.7, 29.5, 29.3, 29.1, 29.0, 28.9, 28.81, 28.76, 28.6, 28.4, 27.7, 27.51, 27.45, 27.3 (CH_2, Cy), 24.4, 24.3, 24.1, 23.3 (CH, Cy).

(*R*)-[Y-{BINOL-DPTS}(o-$C_6H_4CH_2NMe_2$)(Me_2NCH_2Ph)] ((*R*)-2f-Y). To a mixture of (*R*)-**H_2BINOL-DPTS** (**1f**; 24.9 mg, 0.03 mmol) and [Y(o-$C_6H_4CH_2NMe_2)_3$] (14.7 mg, 0.03 mmol) was added C_6D_6 (0.50 mL). The mixture was kept at room temperature for 1 h. ^1H and ^{13}C NMR spectra showed clean formation of (*R*)-**2f-Y**, which was used directly for catalytic experiments. ^1H NMR (400 MHz, 25 °C, C_6D_6): δ 8.41 (br s, 2H, aryl-H), 8.10−7.91 (br m, 6H, aryl-H), 7.60−6.57 (br m, 44H, aryl-H including free $PhCH_2NMe_2$), 3.27, (br s, 4H, free and coordinate $PhCH_2NMe_2$), 3.21 (d, partially overlapped by other signal, 1H, o-$C_6H_4CH_2NMe_2$), 2.59 (d, ^2J(H,H) = 14.1 Hz, 1H, o-$C_6H_4CH_2NMe_2$), 2.34 (br s 6H, aryl−CH_3), 2.07 (s, 6H, free $PhCH_2NMe_2$), 1.59 (s, 3H, $N(CH_3)_2$), 1.40 (br s, 6H, $PhCH_2NMe_2$), 1.29 (br s, 3H, $N(CH_3)_2$). $^{13}C\{^1H\}$ NMR (100 MHz, 25 °C, C_6D_6): δ 181.6 (d, ^1J (Y,C) = 52.3 Hz), 163.3 (CO), 160.0 (CO), 148.5, 145.0, 144.8, 141.6, 140.0 (br s), 139.6, 139.5, 138.4, 138.3, 137.0, 136.8, 136.6, 136.3, 136.1, 135.8, 134.3, 134.1, 131.9 (br s), 130.7, 130.0, 129.5, 129.3, 128.9, 128.8, 127.4, 127.5, 127.3, 126.0, 125.73, 125.65, 124.8, 122.5, 117.3, 116.8 (aryl), 67.9, 64.6 (br s, free $PhCH_2NMe_2$), 58.4 (br s, $PhCH_2NMe_2$), 46.5 ($N(CH_3)_2$), 45.4 (br s, free $PhCH_2NMe_2$), 44.5 ($N(CH_3)_2$), 40.6 (br s, $PhCH_2NMe_2$), 24.6 (aryl-CH_3), 24.4 (aryl-CH_3).

(*R*)-[Lu-{BINOL-DPTS}(o-$C_6H_4CH_2NMe_2$)(Me_2NCH_2Ph)] ((*R*)-2f-Lu). To a mixture of (*R*)-**H_2BINOL-DPTS** (**1f**; 24.9 mg, 0.03 mmol) and [Lu(o-$C_6H_4CH_2NMe_2)_3$] (17.3 mg, 0.03 mmol) was added C_6D_6 (0.50 mL). The mixture was kept at room temperature for 1 h. ^1H and ^{13}C NMR spectra showed clean formation of (*R*)-**2f-Lu**, which was used directly for catalytic experiments. ^1H NMR (300 MHz, 25 °C, C_6D_6): δ 8.42 (br s, partially overlapped by other signal, 1H, aryl-H), 8.38 (br s, partially overlapped by other signal, 1H, aryl-H), 8.20−7.82 (br m, 6H, aryl-H), 7.75−7.65 (br d, ^3J(H,H) = 7.70 Hz, 2H, aryl-H), 7.57−7.50 (br d, ^3J(H,H) = 7.53 Hz, 2H, aryl-H), 7.50−7.40 (br d, ^3J(H,H) = 7.45 Hz, 2H, aryl-H), 7.50−6.85 (m, 34H, aryl-H including free $PhCH_2NMe_2$), 6.85−6.72 (br d, ^3J(H,H) = 6.79 Hz, 2H, aryl-H), 6.72−6.52 (br d, ^3J(H,H) = 6.63 Hz, 2H, aryl-H), 3.26 (br s, 2H, free $PhCH_2NMe_2$), 3.12 (d, ^2J(H,H) = 14.0 Hz, 1H, o-$C_6H_4CH_2NMe_2$), 2.46 (d, ^2J(H,H) = 14.7 Hz, 1H, o-$C_6H_4CH_2NMe_2$), 2.35 (s, 2H, $PhCH_2NMe_2$), 2.08 (s, 12H, aryl−CH_3 and free $PhCH_2NMe_2$), 1.55 (br s, 3H $N(CH_3)_2$), 1.38 (br s, partially overlapped by other signal, 3H, $N(CH_3)_2$), 1.38 (br s, partially overlapped by other signal, 3H, NCH_3), 1.25 (br s, 3H, NCH_3). $^{13}C\{^1H\}$ NMR (100 MHz, 25 °C, C_6D_6): δ 191.1 (C-Lu), 163.8, 163.4 (CO), 148.9, 147.3, 144.9, 144.8, 141.2, 141.0, 139.9, 139.68, 139.63, 139.57, 138.4, 138.3, 137.3, 137.1, 136.8, 136.6, 136.5, 136,2, 135.8, 134.3, 134.1, 132.0, 130.6, 130.0, 129.93, 129.87, 129.4, 129.3, 129.2, 129.1, 128.9, 128.8, 128.76, 128.72, 128,71, 128.6, 128.53, 128.45, 128.1, 127.3, 127.2, 126.1, 126.0, 125.9, 125.7, 125.5, 125.4, 125.1, 125.0, 122.3, 117.1, 116.6 (aryl), 67.2 (o-$C_6H_4CH_2NMe_2$), 64.5 (free $PhCH_2NMe_2$), 58.2 ($PhCH_2NMe_2$), 46.7 ($N(CH_3)_2$), 46.2 ($N(CH_3)_2$), 45.3 (free $PhCH_2NMe_2$), 44.5 ($N(CH_3)_2$), 40.7 ($N(CH_3)_2$), 24.5 (aryl-CH_3), 24.3 (aryl-CH_3).

(*R*)-[Y-{BINOL-TBPS}(o-$C_6H_4CH_2NMe_2$)(Me_2NCH_2Ph)] ((*R*)-2g-Y). To a mixture of (*R*)-**H_2BINOL-TBPS** (**1g**; 34.9 mg, 0.03 mmol) and [Y(o-$C_6H_4CH_2NMe_2)_3$] (14.7 mg, 0.03 mmol) was added C_6D_6 (0.50 mL). The mixture was kept at room temperature for 2 h. ^1H and ^{13}C NMR spectra showed clean formation of (*R*)-**2g-Y**, which was used directly for catalytic experiments. ^1H NMR (400 MHz, 25 °C,

DOI: 10.1021/acs.organomet.8b00510
Organometallics XXXX, XXX, XXX−XXX

C_6D_6): δ 8.59 (s, 1H, aryl-H), 8.51 (s, 1H, aryl-H), 8.01 (br d, ^3J(H,H) = 7.8 Hz, 6H, aryl-H), 7.95 (br d, ^3J(H,H) = 8.2 Hz, 6H, aryl-H), 7.62 (br d, ^3J(H,H) = 6.7 Hz, 1H, aryl-H), 7.40 (pt, ^3J(H,H) = 7.6 Hz, 2H, aryl-H), 7.25 (pt, ^3J(H,H) = 7.1 Hz, 4H, aryl-H), 7.19 (d, ^3J(H,H) = 6.7 Hz, 8H, aryl-H), 7.15−7.05 (m, 12H, aryl-H including free $PhCH_2NMe_2$), 7.03 (pt, ^3J(H,H) = 7.4 Hz, 2H, aryl-H), 6.98−6.87 (m, 4H, aryl-H including free $PhCH_2NMe_2$), 6.83 (pt, ^3J(H,H) = 7.4 Hz, 1H, aryl-H), 6.75 (d, ^3J(H,H) = 7.1 Hz, 1H, aryl-H), 6.68 (br d, 1H, aryl-H), 3.77 (br d, ^2J(H,H) = 14.1 Hz, 1H, *o*-$C_6H_4CH_2NMe_2$), 3.21 (br d, partially overlapped by other signal, 1H, $PhCH_2NMe_2$), 3.19 (br s, 2H, free $PhCH_2NMe_2$), 2.84 (br d, ^2J(H,H) = 13.3 Hz, 1H, $PhCH_2NMe_2$), 2.68 (d, ^2J(H,H) = 14.1 Hz, 1H, *o*-$C_6H_4CH_2NMe_2$), 2.01 (br s, 6H, free $PhCH_2NMe_2$), 1.47 (br s, 3H, $N(CH_3)_2$), 1.33 (br s, 3H, $N(CH_3)_2$), 1.31 (br s, 3H, $N(CH_3)_2$), 1.23 (br s, 3H, $N(CH_3)_2$), 1.08 (br s, 54H, $C(CH_3)_3$). $^{13}C\{^1H\}$ NMR (100 MHz, 25 °C, C_6D_6): δ 182.2 (d, ^1J(Y,C) = 52.4 Hz), 163.5 (CO), 162.6 (CO), 151.9, 151.8, 148.1, 141.6, 141.2, 140.0, 139.7, 139.3, 138.3, 137.1, 137.0, 133.3, 133.2, 131.9, 130.3, 130.0, 129.3, 129.1, 128.9, 128.8, 128.7, 128.5, 127.5, 127.3, 127.2, 126.07, 126.00, 125.7 (s), 125.3, 125.2, 125.1, 122.4, 122.3, 117.1, 116.7 (aryl), 67.9 (*o*-$C_6H_4CH_2NMe_2$), 64.5 (free $PhCH_2NMe_2$), 58.0 ($PhCH_2NMe_2$), 47.4 ($N(CH_3)_2$), 45.4 (free $PhCH_2NMe_2$), 43.5 ($N(CH_3)_2$), 40.6 ($N(CH_3)_2$), 40.3 ($N(CH_3)_2$), 34.6 ($C(CH_3)_3$), 31.3 ($C(CH_3)_3$).

(*R*)-[Lu-{BINOL-TBPS}(*o*-$C_6H_4CH_2NMe_2$)(Me_2NCH_2Ph)] ((*R*)-2g-Lu). To a mixture of (*R*)-**H_2BINOL-TBPS** (**1g**; 34.9 mg, 0.03 mmol) and [Lu(*o*-$C_6H_4CH_2NMe_2)_3$] (17.3 mg, 0.03 mmol) was added C_6D_6 (0.50 mL). The mixture was kept at room temperature for 1 h. ^{1}H and ^{13}C NMR spectra showed clean formation of (*R*)-**2g-Lu**, which was used directly for catalytic experiments. ^{1}H NMR (400 MHz, 25 °C, C_6D_6): δ 8.68 (br s, 1H, aryl-H), 8.62 (br s, 1H, aryl-H), 8.24−7.86 (br m, 12H, aryl-H), 7.81−7.73 (br s, 1H, aryl-H), 7.56−7.44 (m, 2H, aryl-H), 7.44−7.08 (m, 24H, aryl-H including free $PhCH_2NMe_2$), 7.06−6.92 (br s, 4H, aryl-H including free $PhCH_2NMe_2$), 6.92−6.88 (br m, 1H, aryl-H), 6.87−6.80 (br m, 1H, aryl-H), 6.80−6.71 (br s, 1H, aryl-H), 3.75 (d, ^2J(H,H) = 14.1 Hz, 1H, *o*-$C_6H_4CH_2NMe_2$), 3.30 (br d, partially overlapped by other signal, 1H, $PhCH_2NMe_2$), 3.26 (br s, 2H, free $PhCH_2NMe_2$), 2.86 (br d, ^2J(H,H) = 13.3 Hz, 1H, $PhCH_2NMe_2$), 2.62 (br d, ^2J(H,H) = 14.1 Hz, 1H, *o*-$C_6H_4CH_2NMe_2$), 2.07 (br s, 6H, free $PhCH_2NMe_2$) 1.54 (br s, 3H, $N(CH_3)_2$), 1.40 (br s, 3H, $N(CH_3)_2$), 1.37 (br s, 3H, $N(CH_3)_2$), 1.21 (br s, partially overlapped by other signal, 3H, $N(CH_3)_2$), 1.14 (s, 54H, CH_3 of $C(CH_3)_3$). $^{13}C\{^1H\}$ NMR (100 MHz, 25 °C, C_6D_6): δ 192.0 (C-Lu), 164.0 (CO), 163.1 (CO), 151.84, 151.77, 148.5, 141.0 140.8, 139.7, 139.61, 139.57, 137.1, 137.0, 133.3, 133.2, 130.1, 129.1, 129.0, 128.86, 128.81, 128.7, 128.5, 128.4, 127.2, 127.12, 127.09, 126.2, 126.0, 125.7, 125.2, 125.0, 122.2, 122.1, 116.71, 116.69 (aryl), 67.2 (*o*-$C_6H_4CH_2NMe_2$), 64.5 (free $PhCH_2NMe_2$), 57.9 ($PhCH_2Me_2$), 48.0 ($N(CH_3)_2$), 45.3 (free $PhCH_2NMe_2$), 43.3 ($N(CH_3)_2$), 41.0 ($N(CH_3)_2$), 40.3 ($N(CH_3)_3$), 34.57 ($C(CH_3)_3$), 34.54 ($C(CH_3)_3$), 31.3 ($C(CH_3)_3$).

(*R*)-[Y{BINOL-MPDPS}(*o*-$C_6H_4CH_2NMe_2$)(Me_2NCH_2Ph)] ((*R*)-2h-Y). To a mixture of (*R*)-**H_2BINOL-MPDPS** (**1h**; 33.0 mg, 0.039 mmol) and [Y(*o*-$C_6H_4CH_2NMe_2)_3$] (19.3 mg, 0.039 mmol) was added toluene-d_8 (0.55 mL). The mixture was kept at room temperature for 0.5 h. ^{1}H and ^{13}C NMR spectra showed clean formation of (*R*)-**2h-Y**, which was used directly for catalytic experiments. ^{1}H NMR (500 MHz, 0 °C, toluene-d_8): δ 8.46 (s, 1H, aryl-H), 8.43 (s, 1H, aryl-H), 8.07−7.96 (br m, 4H, aryl-H), 7.96−7.90 (br m, 6H, aryl-H), 7.85 (d, ^3J(H,H) = 8.3 Hz, 2H, aryl-H), 7.55 (d, ^3J(H,H) = 6.8 Hz, 1H, aryl-H), 7.52 (d, ^3J(H,H) = 7.6 Hz, 1H, aryl-H),), 7.43 (d, ^3J(H,H) = 7.8 Hz, 1H, aryl-H), 7.28 (d, ^3J(H,H) = 7.3 Hz, 3H, aryl-H), 7.25−6.84 (m, 30H, aryl-H including free $PhCH_2NMe_2$ and C_7D_7H), 6.70 (d, ^3J(H,H) = 7.6 Hz, 1H, aryl-H), 6.66−6.54 (m, 6H, aryl-H), 3.23 (d, ^2J(H,H) = 13.9 Hz, partially overlapped by other signal, 1H, CH_2), 3.20 (s, 3H, CH_2 and free $PhCH_2NMe_2$), 3.19 (s, 3H, OCH_3), 3.18 (s, 3H, OCH_3), 3.09 (d, ^2J(H,H) = 13.5 Hz, 1H, $PhCH_2NMe_2$), 2.45 (d, ^2J(H,H) = 14.4 Hz, 1H, *o*-$C_6H_4CH_2NMe_2$), 2.05 (s, 6H, free $PhCH_2NMe_2$), 1.49 (s, 3H, *o*-$C_6H_4CH_2NMe_2$), 1.33 (s, 3H, $PhCH_2NMe_2$), 1.28 (s, 3H, $PhCH_2NMe_2$), 1.19 (s, 3H, *o*-$C_6H_4CH_2NMe_2$). $^{13}C\{^1H\}$ NMR (125 MHz, 0 °C, toluene-d_8): δ 182.4 (d, ^1J (Y,C) = 53.0 Hz), 163.4 (CO), 163.1 (CO), 161.41 (CO), 161.36 (CO), 148.9, 141.9, 140.4, 139.81, 139.75, 139.0, 138.8, 138.5, 137.4, 137.3, 137.2, 136.93, 136.88, 136.81, 136.7, 132.3, 130.3, 129.7, 129.5, 129.2, 128.8, 128.7, 127.7, 127.5, 126.6, 126.5, 126.2, 126.0, 122.8, 117.6, 116.9, 114.6, 114.4 (aryl), 68.1 (*o*-$C_6H_4CH_2NMe_2$), 64.9 (free $PhCH_2NMe_2$), 58.4 ($PhCH_2NMe_2$), 54.75 (OCH_3), 54.69 (OCH_3), 46.9 ($N(CH_3)_2$), 45.8 (free $PhCH_2NMe_2$) 44.5 ($N(CH_3)_2$), 40.6 ($N(CH_3)_2$).

(*R*)-[Lu{BINOL-MPDPS}(*o*-$C_6H_4CH_2NMe_2$)(Me_2NCH_2Ph)] ((*R*)-2h-Lu). To a mixture of (*R*)-**H_2BINOL-MPDPS** (**1h**; 31.3 mg, 0.036 mmol) and [Lu(*o*-$C_6H_4CH_2NMe_2)_3$] (20.8 mg, 0.036 mmol) was added toluene-d_8 (0.60 mL). The mixture was kept at room temperature for 1 h. ^{1}H and ^{13}C NMR spectra showed clean formation of (*R*)-**2h-Lu**, which was used directly for catalytic experiments. ^{1}H NMR (500 MHz, 0 °C, toluene-d_8): δ 8.49 (s, 1H, aryl-H), 8.45 (s, 1H, aryl-H), 8.06−7.98 (m, 4H, aryl-H), 7.97−7.91(m, 6H, aryl-H), 7.86 (d, ^3J(H,H) = 8.6 Hz, 2H, aryl-H), 7.67 (d, ^3J(H,H) = 6.9 Hz, 1H, aryl-H), 7.55 (m, 1H, aryl-H), 7.46 (d, ^3J(H,H) = 7.6 Hz, 1H, aryl-H), 7.28 (d, ^3J(H,H) = 7.3 Hz, 2H, aryl-H), 7.25−6.84 (m, 33H, aryl-H including free $PhCH_2NMe_2$ and C_7D_7H), 6.72 (d, ^3J(H,H) = 7.3 Hz, 1H, aryl-H), 6.67−6.54 (m, 6H, aryl-H), 3.24 (d, ^2J(H,H) = 13.5 Hz, partially overlapped by other signal, 1H, $PhCH_2NMe_2$), 3.20 (s, 6H, OCH_3), 3.18 (s, 2H, free $PhCH_2NMe_2$), 3.15 (d, ^2J(H,H) = 14.2 Hz, 1H, *o*-$C_6H_4CH_2NMe_2$), 3.09 (d, ^2J(H,H) = 13.5 Hz, 1H, $PhCH_2NMe_2$), 2.34 (d, ^2J(H,H) = 14.2 Hz, 1H, *o*-$C_6H_4CH_2NMe_2$), 2.05 (s, 6H, free $PhCH_2NMe_2$), 1.46 (s, 3H, *o*-$C_6H_4CH_2NMe_2$), 1.32 (s, 3H, $PhCH_2NMe_2$), 1.28 (s, 3H, $PhCH_2NMe_2$), 1.16 (s, 3H, *o*-$C_6H_4CH_2NMe_2$). $^{13}C\{^1H\}$ NMR (125 MHz, 0 °C, toluene-d_8): δ 192.0 (C-Lu), 164.0 (CO), 163.6 (CO), 161.4 (CO), 161.3 (CO), 149.4, 141.5, 141.3, 140.3, 139.9, 139.8, 139.0, 138.8, 137.4, 137.3, 137.2, 137.0, 136.8, 136.7, 132.4, 130.2, 129.1, 128.95, 128.94, 128.8, 128.4, 127.6, 126.6, 126.5, 126.3, 122.7, 117.4, 116.7, 114.6, 114.3 (aryl), 67.4 (*o*-$C_6H_4CH_2NMe_2$), 64.8 (free $PhCH_2NMe_2$), 58.3 ($PhCH_2NMe_2$), 54.73 (OCH_3), 54,67 (OCH_3), 47.3 ($N(CH_3)_2$), 45.8 (free $PhCH_2NMe_2$), 44.5 ($N(CH_3)_2$), 40.80 ($PhCH_2NMe_2$), 40.78 ($PhCH_2NMe_2$).

(*R*)-[Y(BINOL-$SiBnPh_2$)(*o*-$C_6H_4CH_2NMe_2$)(Me_2NCH_2Ph)] ((*R*)-2i-Y). In the glovebox, a screw-cap NMR tube was charged with (*R*)-**H_2BINOL-$SiBnPh_2$** (**1i**; 53.3 mg, 0.064 mmol) and [Y(*o*-$C_6H_4CH_2NMe_2)_3$] (31.5 mg, 0.064 mmol), and then C_6D_6 (0.60 mL) was added. The mixture was kept at room temperature for 0.5 h. ^{1}H and ^{13}C NMR spectra showed clean formation of (*R*)-**2i-Y**, which was used directly for catalytic experiments. ^{1}H NMR (400 MHz, 25 °C, C_6D_6): δ 8.41 (s, 1H, aryl-H), 8.38 (s, 1H, aryl-H), 7.80−7.58 (m, 6H, aryl-H), 7.40−6.71 (m, 46H, aryl-H including free $PhCH_2NMe_2$), 3.81 (d, ^2J(H,H) = 12.9 Hz, 1H, $SiCH_2$), 3.73 (d, ^2J(H,H) = 13.3 Hz, 1H, $SiCH_2$), 3.26 (br s, 5H, free $PhCH_2NMe_2$ and $SiCH_2$), 3.01 (d, ^2J(H,H) = 14.1 Hz, 1H, *o*-$C_6H_4CH_2NMe_2$), 2.85 (d, ^2J(H,H) = 13.3 Hz, 1H, $PhCH_2NMe_2$), 2.82 (d, ^2J(H,H) = 13.3 Hz, 1H, $PhCH_2NMe_2$), 2.47 (d, ^2J(H,H) = 14.1 Hz, 1H, *o*-$C_6H_4CH_2NMe_2$), 2.09 (br s, 6H, free $PhCH_2NMe_2$), 1.85 (s, 3H, *o*-$C_6H_4CH_2NMe_2$), 1.35 (br s, 6H, $PhCH_2NMe_2$), 1.22 (s, partially overlapped by other signal, 3H, *o*-$C_6H_4CH_2NMe_2$). $^{13}C\{^1H\}$ NMR (100 MHz, 25 °C, C_6D_6): δ 181.3 (d, ^1J(Y,C) = 52.4 Hz), 163.9 (CO), 162.2 (CO), 148.7, 140.7, 140.4, 140.0, 139.5, 139.4, 139.2, 138.3, 136.9, 136.8, 136.5, 136.1, 135.8, 135.6, 135.2, 129.8, 129.6, 129.5, 129.4, 129.3, 129.1, 128.9, 128.8, 128.63, 128.59, 128.54, 128.48, 128.3, 128.2, 128.1, 127.8, 127.5, 127.4, 127.3, 127.0, 126.19, 126.15, 126.07, 125.6, 124.84, 124.82, 124.6, 122.6, 122.5, 118.0, 116.5 (aryl), 67.4 (*o*-$C_6H_4CH_2NMe_2$), 64.5 (free $PhCH_2NMe_2$), 58.4 ($PhCH_2NMe_2$), 45.8 ($N(CH_3)_2$), 45.3 (free $PhCH_2NMe_2$)), 44.5 ($N(CH_3)_2$), 40.6 ($N(CH_3)_2$), 24.0 ($SiCH_2$).

(*R*)-[Lu(Binol-$SiBnPh_2$)(*o*-$C_6H_4CH_2NMe_2$)(Me_2NCH_2Ph)] ((*R*)-2i-Lu). In the glovebox, a screw-cap NMR tube was charged with (*R*)-**H_2BINOL-$SiBnPh_2$** (**1i**; 42.5 mg, 0.051 mmol) and [Lu(*o*-$C_6H_4CH_2NMe_2)_3$] (29.5 mg, 0.051 mmol), and then C_6D_6 (0.50 mL) was added. The mixture was kept at room temperature for 0.5 h. ^{1}H and ^{13}C NMR spectra showed clean formation of (*R*)-**2i-Lu**, which was used directly for catalytic experiments. ^{1}H NMR (500 MHz, 25 °C, C_6D_6): δ 8.42 (s, 1H, aryl-H), 8.38 (s, 1H, aryl-H), 7.77−7.59 (m,

DOI: 10.1021/acs.organomet.8b00510
Organometallics XXXX, XXX, XXX−XXX

6H, aryl-H), 7.34−6.84 (m, 46H, aryl-H), 6.65−6.50 (m, 3H, aryl-H), 3.80 (d, ^2J(H,H) = 13.2 Hz, 1H, $SiCH_2$), 3.71 (d, ^2J(H,H) = 13.2 Hz, 1H, $SiCH_2$), 3.27 (s, 2H, free $PhCH_2NMe_2$), 3.16 (d, ^2J(H,H) = 13.4 Hz, 1H, $SiCH_2$), 3.10 (d, ^2J(H,H) = 13.4 Hz, 1H, $SiCH_2$), 2.97 (d, ^2J(H,H) = 14.0 Hz, 1H, CH_2), 2.83 (d, ^2J(H,H) = 14.0 Hz, 1H, CH_2), 2.82 (d, ^2J(H,H) = 14.2 Hz, 1H, CH_2), 2.38 (d, ^2J(H,H) = 14.2 Hz, 1H, CH_2), 2.09 (s, 6H, free $PhCH_2NMe_2$), 1.77 (s, 3H, *o*-$C_6H_4CH_2NMe_2$) 1.35 (s, 3H, $PhCH_2NMe_2$), 1.31 (s, 3H, $PhCH_2NMe_2$), 1.20 (s, 3H, *o*-$C_6H_4CH_2NMe_2$). $^{13}C\{^1H\}$ NMR (125 MHz, 11 °C, C_6D_6): δ 190.7 (C-Lu), 164.2 (CO), 162.6 (CO), 149.2, 140.3, 140.0, 139.9, 139.7, 139.5, 139.29, 139.26, 139.16, 137.0, 136.8, 136.3, 136.1, 135.9, 135.7, 135.5, 135.1, 135.0, 131.8, 129.9, 129.63, 129.58, 129.54, 129.48, 129.41, 129.3, 129.1, 128.8, 128.64, 128.59, 128.54, 128.46, 128.40, 128.34, 128.29, 128.26, 128.14, 128.08, 127.9, 127.3, 127.2, 126.5, 126.4, 126.2, 126.0, 125.2, 124.6, 122.5, 122.4, 117.6, 116.4 (aryl), 66.6 (*o*-$C_6H_4CH_2NMe_2$), 64.4 (free $PhCH_2NMe_2$), 58.2 ($PhCH_2NMe_2$), 46.0 ($N(CH_3)_2$), 45.4 (free $PhCH_2NMe_2$), 44.6 ($N(CH_3)_2$), 40.59 ($N(CH_3)_2$), 40.58 ($N(CH_3)_2$), 23.9 ($SiCH_2$).

General Procedure for Catalytic Asymmetric Hydroamination/Cyclization of Aminoalkenes. In a glovebox, a screw-cap NMR tube was charged with aminoalkene (0.03−0.10 mmol), ferrocene (3.0 mg, 16.1 μmol), C_6D_6 (to give a total volume of 0.50 mL), and catalysts (0.60−3.0 μmol, 0.060 M in C_6D_6). The NMR tube was capped, immediately removed from the glovebox, and shaken well to dissolve ferrocene. The progress of cyclization was monitored by ^{1}H NMR spectroscopy by following the disappearance of the olefinic signals of the substrate relative to the internal standard ferrocene. The NMR tube was heated in a thermostated oil bath, if required. The time was recorded after a conversion of at least 95% was achieved.

General Procedure for Preparing Mosher Amides. The amine (0.01−0.03 mmol) was dissolved in $CDCl_3$, C_6D_6, or toluene-d_8 (0.50 mL) in a NMR tube. Hünig's base (2.5 equiv with respect to amine and (*R*)-Mosher acid chloride (1.5 equiv with respect to amine) were added. The enantiomeric excess was determined by ^{19}F NMR spectroscopy at 60−110 °C.

General Procedure for Determining Enantiomeric Excess of *N*-Benzyl Hydroamination Product via Debenzylation/Mosher Amide Formation Sequence. A completed reaction mixture containing *N*-benzyl hydroamination product (0.07 mmol) was transferred to a 25 mL round-bottom flask, and the volatiles were evaporated. The residue was dissolved in absolute ethanol (2 mL), and to that were added ammonium formate (40 mg, 0.62 mmol) and 10% palladium on charcoal (20 mg, 0.019 mmol). The contents were stirred at reflux for 30 min. The solid was filtered off, and the filtrate was treated with 4 M HCl (1 mL). The volatiles were removed in vacuo, and the residue was dissolved in distilled water (5 mL), which was then evaporated under reduced pressure. The residue was dissolved in $CDCl_3$ or C_6D_6 (0.60 mL) which was allowed to pass through a short pad of Celite. The Mosher amide was prepared by the procedure described above, and the enantiomeric excess was determined by ^{19}F NMR spectroscopy at 60−80 °C.

General Procedure for Kinetic Catalytic Hydroamination/Cyclization Reactions. In a glovebox, a screw cap NMR tube was charged with the aminoalkene (0.10 mmol), ferrocene (3.0 mg), C_6D_6 (to give a total volume of 500 μL), and catalyst (2−16 mol %, 2−16 μmol, 33−267 μL of a 0.060 M stock solution in C_6D_6). The tube was placed in either a 400 or 500 MHz NMR thermostatic probe with the temperature set to 25−60 °C and an arrayed experiment was set up to record ^{1}H NMR spectra automatically in time intervals (30 s., 1 min, 3 min, 5 min, 10 min.). The conversion was determined based on the disappearance of the olefinic signals of the substrate relative to the internal standard ferrocene. The linear part of the data was fitted by least-square analysis and k_{obs} was determined from the slope α of a plot of concentration of amine (M) versus time (min.).

General Procedure for NMR-Scale Intermolecular Hydroamination Reactions. In the glovebox, a screw-cap NMR tube was charged with the appropriate amine (0.2 mmol), an alkene (3 mmol), and a solution of catalyst (0.1 M in C_6D_6 or toluene-d_8, 0.1 mL, 10.0 μmol, 5 mol %). The tube was then sealed, removed from the glovebox, and placed into the thermostated oil bath. The progress of the reaction was monitored by ^{1}H NMR spectroscopy. After completion of the reaction, the mixture was concentrated in vacuo and purified by column chromatography on a 3 cm height pad of silica or alumina.

■ ASSOCIATED CONTENT

Supporting Information

The Supporting Information is available free of charge on the ACS Publications website at DOI: 10.1021/acs.organomet.8b00510.

Additional kinetic data and NMR spectra of ligands, complexes, and Mosher amides (PDF)

■ AUTHOR INFORMATION

Corresponding Author

*E-mail for K.C.H.: kai.hultzsch@univie.ac.at.

ORCID

Bernd Schmidt: 0000-0002-0224-6069

Kai C. Hultzsch: 0000-0002-5298-035X

Notes

The authors declare no competing financial interest.

■ ACKNOWLEDGMENTS

This work was supported by the National Science Foundation through a NSF CAREER Award (CHE 0956021). S.A. thanks the Deutscher Akademischer Austauschdienst (DAAD) for an overseas exchange award.

■ REFERENCES

(1) (a) Ricci, A. *Modern Amination Methods*; Wiley-VCH, 2000. (b) Ricci, A. *Amino Group Chemistry: From Synthesis to the Life Sciences*; Wiley-VCH: 2008.

(2) General reviews on hydroamination: (a) Müller, T. E.; Beller, M. Metal-Initiated Amination of Alkenes and Alkynes. *Chem. Rev.* **1998**, *98*, 675−704. (b) Brunet, J. J.; Neibecker, D. Catalytic Hydroamination of Unsaturated Carbon-Carbon Bonds. In *Catalytic Heterofunctionalization from Hydroamination to Hydrozirconation*; Togni, A., Grützmacher, H., Eds.; Wiley-VCH: Weinheim, Germany, 2001; pp 91−141. (c) Müller, T. E.; Hultzsch, K. C.; Yus, M.; Foubelo, F.; Tada, M. Hydroamination: Direct Addition of Amines to Alkenes and Alkynes. *Chem. Rev.* **2008**, *108*, 3795−3892. (d) Doye, S. Hydroamination. In *Science of Synthesis*; Enders, D., Ed.; Thieme: Stuttgart, Germany, 2009; Vol. *40a*, pp 241−304. (e) Reznichenko, A. L.; Hultzsch, K. C. Early Transition Metal (Group 3−5, Lanthanides and Actinides) and Main Group Metal (Group 1, 2, and 13) Catalyzed Hydroamination. *Top. Organomet. Chem.* **2011**, *43*, 51−114. (f) Nishina, N.; Yamamoto, Y. Late Transition Metal-Catalyzed Hydroamination. *Top. Organomet. Chem.* **2012**, *43*, 115−143. (g) Reznichenko, A. L.; Hultzsch, K. C. Hydroamination of Alkenes. In *Organic Reactions*; Denmark, S. E., Charette, A., Eds.; Wiley: Hoboken, NJ, 2016; pp 1−554.

(3) Reviews on rare-earth-metal-catalyzed hydroaminations: (a) Hong, S.; Marks, T. J. Organolanthanide-Catalyzed Hydroamination. *Acc. Chem. Res.* **2004**, *37*, 673−686. (b) Reznichenko, A. L.; Hultzsch, K. C. Catalytic σ-bond Metathesis. *Struct. Bonding (Berlin, Ger.)* **2010**, *137*, 1−48.

(4) Reviews on group 4 and actinide-catalyzed hydroaminations: (a) Bytschkov, I.; Doye, S. Group-IV Metal Complexes as Hydroamination Catalysts. *Eur. J. Org. Chem.* **2003**, *2003*, 935−946. (b) Pohlki, F.; Doye, S. The catalytic hydroamination of alkynes. *Chem. Soc. Rev.* **2003**, *32*, 104−114. (c) Doye, S. Development of the Ti-catalyzed Intermolecular Hydroamination of Alkynes. *Synlett* **2004**, 1653−1672. (d) Odom, A. L. New C−N and C−C bond forming

DOI: 10.1021/acs.organomet.8b00510
Organometallics XXXX, XXX, XXX−XXX

reactions catalyzed by titanium complexes. *Dalton Trans.* **2005**, 225−233. (e) Severin, R.; Doye, S. The catalytic hydroamination of alkynes. *Chem. Soc. Rev.* **2007**, *36*, 1407−1420. (f) Lee, A. V.; Schafer, L. L. Modular N,O-Chelating Ligands: Group-4 Amidate Complexes for Catalytic Hydroamination. *Eur. J. Inorg. Chem.* **2007**, *2007*, 2245−2255. (g) Eisenberger, P.; Schafer, L. L. Catalytic synthesis of amines and N-containing heterocycles: Amidate complexes for selective C−N and C−C bond-forming reactions. *Pure Appl. Chem.* **2010**, *82*, 1503−1515.

(5) Review on alkali-metal- and alkaline-earth-metal-catalyzed hydroaminations: (a) Seayad, J.; Tillack, A.; Hartung, C. G.; Beller, M. Base-Catalyzed Hydroamination of Olefins: An Environmentally Friendly Route to Amines. *Adv. Synth. Catal.* **2002**, *344*, 795−813. (b) Harder, S. From Limestone to Catalysis: Application of Calcium Compounds as Homogeneous Catalysts. *Chem. Rev.* **2010**, *110*, 3852−3876. (c) Barrett, A. G. M.; Crimmin, M. R.; Hill, M. S.; Procopiou, P. A. Heterofunctionalization catalysis with organometallic complexes of calcium, strontium and barium. *Proc. R. Soc. London, Ser. A* **2010**, *466*, 927−963. (d) Crimmin, M. R.; Hill, M. S. Homogeneous Catalysis with Organometallic Complexes of Group 2. *Top. Organomet. Chem.* **2013**, *45*, 191−241.

(6) Reviews on late-transition-metal-based catalysts: (a) Beller, M.; Breindl, C.; Eichberger, M.; Hartung, C. G.; Seayad, J.; Thiel, O. R.; Tillack, A.; Trauthwein, H. Advances and Adventures in Amination Reactions of Olefins and Alkynes. *Synlett* **2002**, 1579−1594. (b) Hartwig, J. F. Development of catalysts for the hydroamination of olefins. *Pure Appl. Chem.* **2004**, *76*, 507−516. (c) Widenhoefer, R. A.; Han, X. Gold(I)-Catalyzed Hydroamination of C-C Multiple Bonds. *Eur. J. Org. Chem.* **2006**, *2006*, 4555−4563. (d) Brunet, J. J.; Chu, N. C.; Rodriguez-Zubiri, M. Platinum-Catalyzed Intermolecular Hydroamination of Alkenes: Halide-Anion-Promoted Catalysis. *Eur. J. Inorg. Chem.* **2007**, *2007*, 4711−4722. (e) Hesp, K. D.; Stradiotto, M. Rhodium- and Iridium-Catalyzed Hydroamination of Alkenes. *ChemCatChem* **2010**, *2*, 1192−1207. (f) Jenter, J.; Lühl, A.; Roesky, P. W.; Blechert, S. Aminotroponiminate zinc complexes as catalysts for the intramolecular hydroamination. *J. Organomet. Chem.* **2011**, *696*, 406−418. (g) Rodriguez-Ruiz, V.; Carlino, R.; Bezzenine-Lafollee, S.; Gil, R.; Prim, D.; Schulz, E.; Hannedouche, J. Recent developments in alkene hydro-functionalisation promoted by homogeneous catalysts based on earth abundant elements: formation of C-N, C-O and C-P bond. *Dalton Trans.* **2015**, *44*, 12029−12059. (h) Huang, L.; Arndt, M.; Gooßen, K.; Heydt, H.; Gooßen, L. J. Late transition metal-catalyzed hydroamination and hydroamidation. *Chem. Rev.* **2015**, *115*, 2596−2697.

(7) For reviews on photocatalytic hydroaminations see: (a) Margrey, K. A.; Nicewicz, D. A. A General Approach to Catalytic Alkene Anti-Markovnikov Hydrofunctionalization Reactions via Acridinium Photoredox Catalysis. *Acc. Chem. Res.* **2016**, *49*, 1997−2006. (b) Menigaux, D.; Belmont, P.; Brachet, E. Light on Unsaturated Hydrocarbons - "Gotta Heterofunctionalize Them All". *Eur. J. Org. Chem.* **2017**, *2017*, 2008−2055.

(8) For reviews on asymmetric hydroamination see: (a) Roesky, P. W.; Müller, T. E. Enantioselective Catalytic Hydroamination of Alkenes. *Angew. Chem., Int. Ed.* **2003**, *42*, 2708−2710. (b) Hultzsch, K. C. Transition Metal-Catalyzed Asymmetric Hydroamination of Alkenes (AHA). *Adv. Synth. Catal.* **2005**, *347*, 367−391. (c) Hultzsch, K. C. Catalytic asymmetric hydroamination of non-activated olefins. *Org. Biomol. Chem.* **2005**, *3*, 1819−1824. (d) Hultzsch, K. C.; Gribkov, D. V.; Hampel, F. Non-Metallocene Rare Earth Metal Catalysts for the Diastereoselective and Enantioselective Hydroamination of Aminoalkenes. *J. Organomet. Chem.* **2005**, *690*, 4441−4452. (e) Aillaud, I.; Collin, J.; Hannedouche, J.; Schulz, E. Asymmetric hydroamination of non-activated carbon−carbon multiple bonds. *Dalton Trans.* **2007**, 5105−5118. (f) Zi, G. Asymmetric hydroamination/cyclization catalyzed by organolanthanide complexes with chiral biaryl-based ligands. *Dalton Trans.* **2009**, 9101−9109. (g) Chemler, S. R. The enantioselective intramolecular aminative functionalization of unactivated alkenes, dienes, allenes and alkynes for the synthesis of chiral nitrogen heterocycles. *Org. Biomol. Chem.* **2009**, *7*, 3009−3019. (h) Reznichenko, A. L.; Hultzsch, K. C. Hydroamination of Alkenes. In *Chiral Amine Synthesis: Methods, Developments and Applications*; Nugent, T., Ed.; Wiley-VCH: Weinheim, Germany, 2010; pp 341−375. (i) Zi, G. Asymmetric hydroamination/cyclization catalyzed by group 4 metal complexes with chiral biaryl-based ligands. *J. Organomet. Chem.* **2011**, *696*, 68−75. (j) Hannedouche, J.; Collin, J.; Trifonov, A.; Schulz, E. Intramolecular enantioselective hydroamination catalyzed by rare earth binaphthylamides. *J. Organomet. Chem.* **2011**, *696*, 255−262. (k) Hannedouche, J.; Schulz, E. Asymmetric Hydroamination: A Survey of the Most Recent Developments. *Chem. - Eur. J.* **2013**, *19*, 4972−4985. (l) Reznichenko, A. L.; Nawara-Hultzsch, A. J.; Hultzsch, K. C. Hydroamination of Alkenes. *Top. Curr. Chem.* **2013**, *343*, 191−260. (m) Michon, C.; Abadie, M. A.; Medina, F.; Agbossou-Niedercorn, F. Recent metal-catalysed asymmetric hydroaminations of alkenes. *J. Organomet. Chem.* **2017**, *847*, 13−27. (n) For a review on the asymmetric formal hydroamination of alkenes using copper hydride catalysts see: Pirnot, M. T.; Wang, Y. M.; Buchwald, S. L. Copper Hydride Catalyzed Hydroamination of Alkenes and Alkynes. *Angew. Chem., Int. Ed.* **2016**, *55*, 48−57.

(9) (a) Gribkov, D. V.; Hultzsch, K. C.; Hampel, F. 3,3′-Bis(trisarylsilyl)-Substituted Binaphtholate Rare Earth Metal Catalysts for Asymmetric Hydroamination. *J. Am. Chem. Soc.* **2006**, *128*, 3748−3759. (b) Zhang, X.; Emge, T. J.; Hultzsch, K. C. A Chiral Phenoxyamine Magnesium Catalyst for the Enantioselective Hydroamination/Cyclization of Aminoalkenes and Intermolecular Hydroamination of Vinyl Arenes. *Angew. Chem., Int. Ed.* **2012**, *51*, 394−398.

(10) (a) Wood, M. C.; Leitch, D. C.; Yeung, C. S.; Kozak, J. A.; Schafer, L. L. Chiral Neutral Zirconium Amidate Complexes for the Asymmetric Hydroamination of Alkenes. *Angew. Chem., Int. Ed.* **2007**, *46*, 354−358. (b) Gott, A. L.; Clarke, A. J.; Clarkson, G. J.; Scott, P. Structure-Activity Relationships for Group 4 Biaryl Amidate Complexes in Catalytic Hydroamination/Cyclization of Aminoalkenes. *Organometallics* **2007**, *26*, 1729−1737. (c) Ogata, T.; Ujihara, A.; Tsuchida, S.; Shimizu, T.; Kaneshige, A.; Tomioka, K. Catalytic asymmetric intramolecular hydroamination of aminoalkenes. *Tetrahedron Lett.* **2007**, *48*, 6648−6650. (d) Zi, G.; Zhang, F.; Xiang, L.; Chen, Y.; Fang, W.; Song, H. Synthesis and characterization of group 4 metal amides with new C_2-symmetric binaphthyldiamine-based ligands and their use as catalysts for asymmetric hydroamination/cyclization. *Dalton Trans.* **2010**, *39*, 4048−4061. (e) Manna, K.; Xu, S.; Sadow, A. D. Highly Enantioselective Zirconium Catalyst for Intramolecular Alkene Hydroamination: Significant Isotope Effects on Rate and Stereoselectivity. *Angew. Chem., Int. Ed.* **2011**, *50*, 1865−1868. (f) Shen, X.; Buchwald, S. L. Rhodium-Catalyzed Asymmetric Intramolecular Hydroamination of Unactivated Alkenes. *Angew. Chem., Int. Ed.* **2010**, *49*, 564−567. (g) Manna, K.; Kruse, M. L.; Sadow, A. D. Concerted C-N/C-H Bond Formation in Highly Enantioselective Yttrium(III)-Catalyzed Hydroamination. *ACS Catal.* **2011**, *1*, 1637−1642. (h) Zhang, Y.; Yao, W.; Li, H.; Mu, Y. Rare-Earth-Metal Complexes Supported by New Chiral Tetra-Azane Chelating Ligands: Synthesis, Characterization, and Catalytic Properties for Intramolecular Asymmetric Hydroamination. *Organometallics* **2012**, *31*, 4670−4679. (i) Manna, K.; Everett, W. C.; Schoendorff, G.; Ellern, A.; Windus, T. L.; Sadow, A. D. Highly Enantioselective Zirconium-Catalyzed Cyclization of Aminoalkenes. *J. Am. Chem. Soc.* **2013**, *135*, 7235−7250. (j) Chai, Z.; Hua, D.; Li, K.; Chu, J.; Yang, G. A novel chiral yttrium complex with a tridentate linked amido-indenyl ligand for intramolecular hydroamination. *Chem. Commun.* **2014**, *50*, 177−179. (k) Hussein, L.; Purkait, N.; Biyikal, M.; Tausch, E.; Roesky, P. W.; Blechert, S. Highly enantioselective hydroamination to six-membered rings by hetero-bimetallic catalysts. *Chem. Commun.* **2014**, *50*, 3862−3864. (l) Zhou, X.; Wei, B.; Sun, X. L.; Tang, Y.; Xie, Z. Asymmetric hydroamination catalyzed by a new chiral zirconium system: reaction scope and mechanism. *Chem. Commun.* **2015**, *51*, 5751−5753. (m) Manna, K.; Eedugurala, N.; Sadow, A. D. Zirconium-catalyzed desymmetrization of aminodialkenes and aminodialkynes through enantioselective hydroamination. *J. Am. Chem. Soc.* **2015**, *137*, 425−435.

DOI: 10.1021/acs.organomet.8b00510
Organometallics XXXX, XXX, XXX−XXX

(11) For highly enantioselective intramolecular hydroamination reactions of aminodienes and aminoallenes see: (a) LaLonde, R. L.; Sherry, B. D.; Kang, E. J.; Toste, F. D. Gold(I)-Catalyzed Enantioselective Intramolecular Hydroamination of Allenes. *J. Am. Chem. Soc.* **2007**, *129*, 2452−2453. (b) Hamilton, G. L.; Kang, E. J.; Mba, M.; Toste, F. D. A powerful chiral counterion strategy for asymmetric transition metal catalysis. *Science* **2007**, *317*, 496−499. (c) Zhang, Z.; Bender, C. F.; Widenhoefer, R. A. Gold(I)-Catalyzed Dynamic Kinetic Enantioselective Intramolecular Hydroamination of Allenes. *J. Am. Chem. Soc.* **2007**, *129*, 14148−14149. (d) Zhang, Z.; Bender, C. F.; Widenhoefer, R. A. Gold(I)-Catalyzed Enantioselective Hydroamination of N-Allenyl Carbamates. *Org. Lett.* **2007**, *9*, 2887−2889. (e) LaLonde, R. L.; Wang, Z. J.; Mba, M.; Lackner, A. D.; Toste, F. D. Gold(I)-Catalyzed Enantioselective Synthesis of Pyrazolidines, Isoxazolidines, and Tetrahydrooxazines. *Angew. Chem., Int. Ed.* **2010**, *49*, 598−601. (f) Shapiro, N. D.; Rauniyar, V.; Hamilton, G. L.; Wu, J.; Toste, F. D. Asymmetric additions to dienes catalysed by a dithiophosphoric acid. *Nature* **2011**, *470*, 245−249. (g) Li, H.; Lee, D. L.; Widenhoefer, R. A. Gold(I)-catalyzed enantioselective intramolecular hydroamination of allenes with ureas. *J. Organomet. Chem.* **2011**, *696*, 316−320. (h) Kanno, O.; Kuriyama, W.; Wang, Z. J.; Toste, F. D. Regio- and Enantioselective Hydroamination of Dienes by Gold(I)/Menthol Cooperative Catalysis. *Angew. Chem., Int. Ed.* **2011**, *50*, 9919−9922. (i) Teller, H.; Corbet, M.; Mantilli, L.; Gopakumar, G.; Goddard, R.; Thiel, W.; Fürstner, A. One-Point Binding Ligands for Asymmetric Gold Catalysis: Phosphoramidites with a TADDOL-Related but Acyclic Backbone. *J. Am. Chem. Soc.* **2012**, *134*, 15331−15342.

(12) Trifonov, A. A.; Basalov, I. V.; Kissel, A. A. Use of organolanthanides in the catalytic intermolecular hydrophosphination and hydroamination of multiple C-C bonds. *Dalton Trans* **2016**, *45*, 19172−19193.

(13) Selected examples of asymmetric intermolecular hydroamination involving activated alkenes: (a) Dorta, R.; Egli, P.; Zürcher, F.; Togni, A. The $[IrCl(Diphosphine)]_2$/Fluoride System. Developing Catalytic Asymmetric Olefin Hydroamination. *J. Am. Chem. Soc.* **1997**, *119*, 10857−10858. (b) Kawatsura, M.; Hartwig, J. F. Palladium-catalyzed intermolecular hydroamination of vinylarenes using arylamines. *J. Am. Chem. Soc.* **2000**, *122*, 9546−9547. (c) Löber, O.; Kawatsura, M.; Hartwig, J. F. Palladium-catalyzed hydroamination of 1,3-dienes: a colorimetric assay and enantioselective additions. *J. Am. Chem. Soc.* **2001**, *123*, 4366−4367. (d) Utsunomiya, M.; Hartwig, J. F. Intermolecular, Markovnikov Hydroamination of Vinylarenes with Alkylamines. *J. Am. Chem. Soc.* **2003**, *125*, 14286−14287. (e) Hu, A.; Ogasawara, M.; Sakamoto, T.; Okada, A.; Nakajima, K.; Takahashi, T.; Lin, W. Palladium-catalyzed intermolecular asymmetric hydroamination with 4,4′-disubstituted BINAP and SEGPHOS. *Adv. Synth. Catal.* **2006**, *348*, 2051−2056. (f) Zhou, J.; Hartwig, J. F. Intermolecular, Catalytic Asymmetric Hydroamination of Bicyclic Alkenes and Dienes in High Yield and Enantioselectivity. *J. Am. Chem. Soc.* **2008**, *130*, 12220−12221. (g) Pan, S.; Endo, K.; Shibata, T. Ir(I)-Catalyzed Intermolecular Regio- and Enantioselective Hydroamination of Alkenes with Heteroaromatic Amines. *Org. Lett.* **2012**, *14*, 780−783. (h) Butler, K. L.; Tragni, M.; Widenhoefer, R. A. Gold(I)-Catalyzed Stereoconvergent, Intermolecular Enantioselective Hydroamination of Allenes. *Angew. Chem., Int. Ed.* **2012**, *51*, 5175−5178. (i) Cooke, M. L.; Xu, K.; Breit, B. Enantioselective Rhodium-Catalyzed Synthesis of Branched Allylic Amines by Intermolecular Hydroamination of Terminal Allenes. *Angew. Chem., Int. Ed.* **2012**, *51*, 10876−10879. (j) Xu, K.; Wang, Y. H.; Khakyzadeh, V.; Breit, B. Asymmetric synthesis of allylic amines via hydroamination of allenes with benzophenone imine. *Chem. Sci.* **2016**, *7*, 3313−3316. (k) Haydl, A. M.; Hilpert, L. J.; Breit, B. Regioconvergent and Enantioselective Rhodium-Catalyzed Hydroamination of Internal and Terminal Alkynes: A Highly Flexible Access to Chiral Pyrazoles. *Chem. - Eur. J.* **2016**, *22*, 6547−6551. (l) Teng, H. L.; Luo, Y.; Wang, B.; Zhang, L.; Nishiura, M.; Hou, Z. Synthesis of Chiral Aminocyclopropanes by Rare-Earth-Metal-Catalyzed Cyclopropene Hydroamination. *Angew. Chem., Int. Ed.* **2016**, *55*, 15406−15410. (m) Yang, X. H.; Dong, V. M. Rhodium-Catalyzed Hydrofunctionalization: Enantioselective Coupling of Indolines and 1,3-Dienes. *J. Am. Chem. Soc.* **2017**, *139*, 1774−1777.

(14) Asymmetric intermolecular hydroamination of unactivated alkenes: (a) Zhang, Z.; Lee, S. D.; Widenhoefer, R. A. Intermolecular Hydroamination of Ethylene and 1-Alkenes with Cyclic Ureas Catalyzed by Achiral and Chiral Gold(I) Complexes. *J. Am. Chem. Soc.* **2009**, *131*, 5372−5373. (b) Reznichenko, A. L.; Nguyen, H. N.; Hultzsch, K. C. Asymmetric Intermolecular Hydroamination of Unactivated Alkenes with Simple Amines. *Angew. Chem., Int. Ed.* **2010**, *49*, 8984−8987. (c) Sevov, C. S.; Zhou, J.; Hartwig, J. F. Iridium-Catalyzed Intermolecular Hydroamination of Unactivated Aliphatic Alkenes with Amides and Sulfonamides. *J. Am. Chem. Soc.* **2012**, *134*, 11960−11963.

(15) For selected examples of nonstereoselective intermolecular hydroaminations of unactivated alkenes see: (a) Li, Y.; Marks, T. J. Diverse Mechanistic Pathways and Selectivities in Organo-f-Element-Catalyzed Hydroamination. Intermolecular Organolanthanide-Catalyzed Alkyne and Alkene Hydroamination. *Organometallics* **1996**, *15*, 3770−3772. (b) Ryu, J.-S.; Li, G. Y.; Marks, T. J. Organolanthanide-Catalyzed Regioselective Intermolecular Hydroamination of Alkenes, Alkynes, Vinylarenes. Scope and Mechanistic Comparison to Intramolecular Cyclohydroaminations. *J. Am. Chem. Soc.* **2003**, *125*, 12584−12605. (c) Brunet, J.-J.; Chu, N. C.; Diallo, O. Intermolecular Highly Regioselective Hydroamination of Alkenes with Ligandless Platinum(II) Catalysts in Ionic Solvents: Activation Role of n-Bu_4PBr. *Organometallics* **2005**, *24*, 3104−3110. (d) Khedkar, V.; Tillack, A.; Benisch, C.; Melder, J.-P.; Beller, M. Base-catalyzed hydroamination of ethylene with diethylamine. *J. Mol. Catal. A: Chem.* **2005**, *241*, 175−183. (e) Baudequin, C.; Brunet, J. J.; Rodriguez-Zubiri, M. Rhodium-Catalyzed Hydroamination of Ethylene. Highly Promoting Effect of Iodide Ions. *Organometallics* **2007**, *26*, 5264−5266. (f) Rodriguez-Zubiri, M.; Baudequin, C.; Béthegnies, A.; Brunet, J.-J. Intermolecular Rhodium-Catalysed Hydroamination of Non-Activated Olefins: Effect of Olefin, Amine, Phosphine and Phosphonium Salt. *ChemPlusChem* **2012**, *77*, 445−454. (g) Sevov, C. S.; Zhou, J. S.; Hartwig, J. F. Iridium-catalyzed, intermolecular hydroamination of unactivated alkenes with indoles. *J. Am. Chem. Soc.* **2014**, *136*, 3200−3207. (h) Motolko, K. S. A.; Emslie, D. J. H.; Jenkins, H. A. Yttrium and Aluminum Alkyl Complexes of a Rigid Bis-Anilido NON-Donor Ligand: Synthesis and Hydroamination Catalysis. *Organometallics* **2017**, *36*, 1601−1608.

(16) (a) Gribkov, D. V.; Hultzsch, K. C.; Hampel, F. Synthesis and Characterization of New Biphenolate and Binaphtholate Rare Earth Metal Amido Complexes. Catalysts for Asymmetric Olefin Hydroamination/Cyclization. *Chem. - Eur. J.* **2003**, *9*, 4796−4810. (b) Gribkov, D. V.; Hultzsch, K. C. Kinetic resolution of chiral aminoalkenes via asymmetric hydroamination/cyclisation using binaphtholate yttrium complexes. *Chem. Commun.* **2004**, 730−731. (c) Gribkov, D. V.; Hampel, F.; Hultzsch, K. C. Synthesis and Characterization of Alkyllanthanum Biphenolate Complexes as Catalysts for Hydroamination/Cyclization and Hydrosilylation. *Eur. J. Inorg. Chem.* **2004**, *2004*, 4091−4101. (d) Reznichenko, A. L.; Hampel, F.; Hultzsch, K. C. Kinetic Resolution of Aminoalkenes by Asymmetric Hydroamination: A Mechanistic Study. *Chem. - Eur. J.* **2009**, *15*, 12819−12827. (e) Reznichenko, A. L.; Hultzsch, K. C. C_1-Symmetric Rare-Earth-Metal Aminodiolate Complexes for Intra- and Intermolecular Asymmetric Hydroamination of Alkenes. *Organometallics* **2013**, *32*, 1394−1408. See also: (f) Yu, X.; Marks, T. J. Organophosphine Oxide/Sulfide-Substituted Lanthanide Binaphtholate Catalysts for Enantioselective Hydroamination/Cyclization. *Organometallics* **2007**, *26*, 365−376.

(17) The synthesis of complexes (*R*)-**2b**-**Y** and (*R*)-**2c**-**Y** and their catalytic application in the intermolecular hydroamination was communicated in ref 14b.

(18) Maruoka, K.; Itoh, T.; Araki, Y.; Shirasaka, T.; Yamamoto, H. Efficient Synthesis of Sterically Hindered Chiral Binaphthol Derivatives. *Bull. Chem. Soc. Jpn.* **1988**, *61*, 2975−2976.

DOI: 10.1021/acs.organomet.8b00510
Organometallics XXXX, XXX, XXX−XXX

(19) (a) Gong, L.-Z.; Pu, L. The asymmetric hetero-Diels−Alder reaction of enamide aldehydes with Danishefsky's diene and an efficient synthesis of chiral binaphthyl ligands. *Tetrahedron Lett.* **2000**, *41*, 2327−2331. (b) Cox, P. J.; Wang, W.; Snieckus, V. Expedient route to 3- and 3,3′-substituted 1,1′-bi-2-naphthols by directed ortho metalation and Suzuki cross coupling methods. *Tetrahedron Lett.* **1992**, *33*, 2253−2256.

(20) Incomplete and reversible catalyst activation of rare-earth-metal silylamido complexes resulting from lower basicity of their Ln−amido bond can significantly diminish catalytic activity in hydroamination reactions; see: (a) O'Shaughnessy, P. N.; Scott, P. Biaryl amine ligands for lanthanide catalysed enantioselective hydroamination/cyclisation of aminoalkenes. *Tetrahedron: Asymmetry* **2003**, *14*, 1979−1983. (b) Hultzsch, K. C.; Hampel, F.; Wagner, T. New Yttrium Complexes Bearing Diamidoamine Ligands as Efficient and Diastereoselective Catalysts for the Intramolecular Hydroamination of Alkenes and Alkynes. *Organometallics* **2004**, *23*, 2601−2612.

(21) Hitchcock, P. B.; Lappert, M. F.; Smith, R. G.; Bartlett, R. A.; Power, P. P. Synthesis and Structural Characterization of the First Neutral Homoleptic Lanthanide Metal(III)Alkyls: [LnR_3] Ln = La, Sm, R = $CHTMS_2$. *J. Chem. Soc., Chem. Commun.* **1988**, 1007−1009.

(22) (a) Ln = Y: Booij, M.; Kiers, N. H.; Heeres, H. J.; Teuben, J. H. On the synthesis of monopentamethylcyclopentadienyl derivatives of yttrium, lanthanum, and cerium. *J. Organomet. Chem.* **1989**, *364*, 79−86. (b) Ln = Lu: Wayda, A. L.; Rogers, R. D. Synthesis, X-Ray Crystal Structures, and Reaction Chemistry of Homoleptic and Heteroleptic Organolanthanoid Complexes Incorporating the [(Dimethylamino)methyl]phenyl Ligand. *Organometallics* **1985**, *4*, 1440−1444.

(23) Frozen stock solutions of complexes **2a−i** in C_6D_6 can be stored at −30 °C under argon for extended periods of time.

(24) Jung, M. E.; Piizzi, G. gem-Disubstituent-Effect: Theoretical Basis and Synthetic Applications. *Chem. Rev.* **2005**, *105*, 1735−1766.

(25) Gagné, M. R.; Stern, C. L.; Marks, T. J. Organolanthanide-Catalyzed Hydroamination. A Kinetic, Mechanistic, and Diastereoselectivity Study of the Cyclization of N-Unprotected Amino-Olefins. *J. Am. Chem. Soc.* **1992**, *114*, 275−294.

(26) For eight-coordinate effective ionic radii of trivalent rare-earth metals, see: Shannon, R. D. Revised effective ionic radii and systematic studies of interatomic distances in halides and chalcogenides. *Acta Crystallogr., Sect. A: Cryst. Phys., Diffr., Theor. Gen. Crystallogr.* **1976**, *32*, 751−767.

(27) Queffelec, C.; Boeda, F.; Pouilhés, A.; Meddour, A.; Kouklovsky, C.; Hannedouche, J.; Collin, J.; Schulz, E. Enantioselective Intramolecular Hydroamination of Secondary Amines Catalyzed by Easily Accessible Ate and Neutral Rare-Earth Complexes. *ChemCatChem* **2011**, *3*, 122−126.

(28) Giardello, M. A.; Conticello, V. P.; Brard, L.; Gagné, M. R.; Marks, T. J. Chiral Organolanthanides Designed for Asymmetric Catalysis. A Kinetic and Mechanistic Study of Enantioselective Olefin Hydroamination/Cyclization and Hydrogenation. *J. Am. Chem. Soc.* **1994**, *116*, 10241−10254.

(29) Motta, A.; Lanza, G.; Fragalà, I. L.; Marks, T. J. Energetics and Mechanism of Organolanthanide-Mediated Aminoalkene Hydroamination/Cyclization. A Density Functional Theory Analysis. *Organometallics* **2004**, *23*, 4097−4104.

(30) For studies on the cyclization of **13** and related aminodienes, see: (a) Kim, Y. K.; Livinghouse, T.; Bercaw, J. E. Intramolecular alkene hydroaminations catalyzed by simple amido derivatives of the group 3 metals. *Tetrahedron Lett.* **2001**, *42*, 2933−2935. (b) Kim, J. Y.; Livinghouse, T. Chelating Diamide Based Rate Enhancement of Intramolecular Alkene Hydroaminations Catalyzed by a Neutral Sc(III) Complex. *Org. Lett.* **2005**, *7*, 4391−4393. (c) Jiang, T.; Livinghouse, T. A Stereocontrolled Synthesis of (±)-Xenovenine via a Scandium(III)-Catalyzed Internal Aminodiene Bicyclization Terminated by a 2-(5-Ethyl-2-thienyl)ethenyl Group. *Org. Lett.* **2010**, *12*, 4271−4273. (d) Jiang, T.; Livinghouse, T.; Lovick, H. M. On the stereoselective bicyclization of aminodienes catalyzed by chelating diamide complexes of the group 3 metals. A direct comparison of Sc(III) and Y(III) bis(amide)s with an application to the synthesis of alkaloid 195F. *Chem. Commun.* **2011**, *47*, 12861−12863. (e) For an example of the reaction of a related aminoallene-alkene see: Arredondo, V. M.; Tian, S.; McDonald, F. E.; Marks, T. J. Organolanthanide-Catalyzed Hydroamination/Cyclization. Efficient Allene-Based Transformations for the Syntheses of Naturally Occuring Alkaloids. *J. Am. Chem. Soc.* **1999**, *121*, 3633−3639.

(31) The first cyclization proceeded with an approximate 13:1 trans:cis diastereomeric ratio. Only *trans*-**14** underwent bicyclization, while *cis*-**14** remained unchanged because the relative stereochemistry disfavors the second cyclization.

(32) Marks and co-workers reported the addition of *n*-propylamine to 1-pentene with an >70-fold excess of the alkene using the *ansa*-lanthanocene $Me_2Si(C_5H_4)_2NdCH(SiMe_3)_2$ as catalyst; see refs 15a and b.

(33) Gilman, H.; Gorsich, R. D. Cyclic Organosilicon Compounds. I. Synthesis of Compounds Containing the Dibenzosilole Nucleus. *J. Am. Chem. Soc.* **1958**, *80*, 1883−1886.

(34) (a) Masaoka, S.; Banno, T.; Ishikawa, M. Versatile method for introduction of bulky substituents to alkoxychlorosilanes. *J. Organomet. Chem.* **2006**, *691*, 182−192. (b) Masaoka, S.; Banno, T.; Ishikawa, M. The synthesis of chlorosilanes from alkoxysilanes, silanols, and hydrosilanes with bulky substituents. *J. Organomet. Chem.* **2006**, *691*, 174−181.

(35) Akiyama, T.; Suzuki, T.; Mori, K. Enantioselective Aza-Darzens Reaction Catalyzed by A Chiral Phosphoric Acid. *Org. Lett.* **2009**, *11*, 2445−2447.

(36) Gilman, H.; Dunn, G. E. The Effects of Substituents on the Rate of Hydrolysis of Triarylsilanes in Wet Piperidine. *J. Am. Chem. Soc.* **1951**, *73*, 3404−3407.

(37) (a) Reznichenko, A. L.; Emge, T. J.; Audörsch, S.; Klauber, E. G.; Hultzsch, K. C.; Schmidt, B. Group 5 Metal Binaphtholate Complexes for the Catalytic Asymmetric Hydroaminoalkylation and Hydroamination/Cyclization. *Organometallics* **2011**, *30*, 921−924. (b) Lyčka, A.; Šnobl, D.; Handlír, K.; Holeček, J.; Nádvorník, M. ^{29}Si and ^{13}C NMR spectra of some alkyldiphenylchlorosilanes, alkyldiphenylsilanoles and bis(alkyldiphenylsilyl)chromates. *Collect. Czech. Chem. Commun.* **1982**, *47*, 603−612.

(38) (a) Hong, S.; Tian, S.; Metz, M. V.; Marks, T. J. C_2-symmetric Bis(oxazolinato)lanthanide Catalysts for Enantioselective Intramolecular Hydroamination/Cyclization. *J. Am. Chem. Soc.* **2003**, *125*, 14768−14783. (b) Bender, C. F.; Widenhoefer, R. A. Platinum-Catalyzed Intramolecular Hydroamination of Unactivated Olefins with Secondary Alkylamines. *J. Am. Chem. Soc.* **2005**, *127*, 1070−1071. (c) Tamaru, Y.; Hojo, M.; Higashimura, H.; Yoshida, Z. Urea as the most reactive and versatile nitrogen nucleophile for the Palladium(2+)-catalyzed cyclization of unsaturated Amines. *J. Am. Chem. Soc.* **1988**, *110*, 3994−4002. (d) Kondo, T.; Okada, T.; Mitsudo, T.-a. Ruthenium-Catalyzed Intramolecular Oxidative Amination of Aminoalkenes Enables Rapid Synthesis of Cyclic Imines. *J. Am. Chem. Soc.* **2002**, *124*, 186−187. (e) Bexrud, J. A.; Beard, J. D.; Leitch, D. C.; Schafer, L. L. Intramolecular Hydroamination of Unactivated Olefins with $Ti(NMe_2)_4$ as a Precatalyst. *Org. Lett.* **2005**, *7*, 1959−1962. (f) Black, D. S. C.; Doyle, J. E. The limited scope of azabicyclohexane synthesis from δ,ε-unsaturated amines. *Aust. J. Chem.* **1978**, *31*, 2247−2257.

(39) Smith, P. M.; Thomas, E. J. Approaches to a synthesis of galbonolide B. *J. Chem. Soc., Perkin Trans. 1* **1998**, 3541−3556.

(40) (a) Collin, J.; Daran, J.-D.; Jacquet, O.; Schulz, E.; Trifonov, A. Lanthanide Complexes Coordinated by N-Substituted (R)-1,1′-binaphthyl-2,2′-diamido Ligands in the Catalysis of Enantioselective Intramolecular Hydroamination. *Chem. - Eur. J.* **2005**, *11*, 3455−3462. (b) Bexrud, J. A.; Eisenberger, P.; Leitch, D. C.; Payne, P. R.; Schafer, L. L. Selective C-H Activation α to Primary Amines. Bridging Metallaaziridines for Catalytic, Intramolecular α-Alkylation. *J. Am. Chem. Soc.* **2009**, *131*, 2116−2118. (c) Reznichenko, A. L.; Hultzsch, K. C. C_2-Symmetric Zirconium Bis(Amidate) Complexes with Enhanced Reactivity in Aminoalkene Hydroamination. *Organometallics* **2010**, *29*, 24−27.

DOI: 10.1021/acs.organomet.8b00510
Organometallics XXXX, XXX, XXX−XXX

(41) (a) Peterson, M. A.; Bowman, A.; Morgan, S. Efficient Preparation of N-Benzyl Secondary Amines via Benzylamine−Borane Mediated Reductive Amination. *Synth. Commun.* **2002**, *32*, 443−448. (b) Lopez, R. M.; Fu, G. C. A mild, convenient, and inexpensive method for converting imines into amines: Tin-catalyzed reduction with polymethylhydrosiloxane (PMHS). *Tetrahedron* **1997**, *53*, 16349−16354. (c) Miyamura, H.; Morita, M.; Inasaki, T.; Kobayashi, S. Aerobic Oxidation of Amines Catalyzed by Polymer-Incarcerated Au Nanoclusters: Effect of Cluster Size and Cooperative Functional Groups in the Polymer. *Bull. Chem. Soc. Jpn.* **2011**, *84*, 588−599.

DOI: 10.1021/acs.organomet.8b00510
Organometallics XXXX, XXX, XXX−XXX